QUANTIFYING GROUNDWATER-SURFACE WATER EXCHANGE: DEVELOPMENT AND TESTING OF SHELBY TUBES AND SEEPAGE BLANKETS AS DISCHARGE MEASUREMENT AND SAMPLE COLLECTION DEVICES

by

John Edward Eberly Solder

A thesis submitted to the faculty of
The University of Utah
in partial fulfillment of the requirements for the degree of

Master of Science

in

Geology

Department of Geology and Geophysics

The University of Utah

August 2014

The University of Utah Graduate School

STATEMENT OF THESIS APPROVAL

The thesis of **John Edward Eberly Solder**

has been approved by the following supervisory committee members:

D. Kip Solomon	, Chair	**10/10/13** Date Approved
Paul W. Jewell	, Member	**10/10/13** Date Approved
Victor M. Heilweil	, Member	**10/10/13** Date Approved

and by **John M. Bartley** , Chair of the Department of **Geology and Geophysics**

and by **David B. Kieda** , Dean of the Graduate School.

ABSTRACT

Quantification of groundwater-surface water exchange and the role of hyporheic flow in this exchange is increasingly of interest to a wide range of disciplines (e.g., hydrogeology, geochemistry, biology, ecology). The most direct method to quantify groundwater-surface water exchange is a seepage meter, first developed in the 1940s. Widespread use of the traditional 1970s-era 55-gallon half-barrel seepage meter has shown that the method is subject to potential errors, particularly in flowing waters (e.g., streams, rivers, tidal zones). This study presents two new direct seepage measurement devices, the Shelby tube and the seepage blanket, designed to minimize potential measurement errors associated with flowing surface waters. The objective of the study is to develop and test the new methods by comparing results (specific discharge, hydraulic conductivity, and dissolved constituent concentration) to established methods. Results from both laboratory and field testing suggest that the new devices have utility in quantifying the water and dissolved constituent exchange between surface water and groundwater.

TABLE OF CONTENTS

ABSTRACT iii

ACKNOWLEDGEMENTS vii

THESIS INTRODUCTION 1

Chapters

I DEVELOPMENT AND TESTING OF SHELBY TUBES AS AN IN-SITU SPECIFIC DISCHARGE AND HYDRAULIC CONDUCTIVITY MEASUREMENT DEVICE 4

- Abstract 4
- Introduction 5
- Methods 6
  - Device Description 6
  - Theory of Device 7
  - Measurement Method 9
  - Discharge Analysis 11
  - Hydraulic Conductivity Analysis 12
  - Sampling Device 13
- Empirical Testing 13
  - University of Utah Seepage Drum 13
  - USGS Denver Federal Center 14
- Lab Results 14
  - Discharge Measurement Efficiency of Shelby Tube from University of Utah 15
  - Discharge Measurement Efficiency of Shelby Tube from USGS Denver Federal Center 15
  - Hydraulic Conductivity Measurements with Shelby Tube 16
  - Amplification Factor Calibration 16
- Field Testing 17
  - Comparison of Amplified to Unamplified Shelby Measurements 18
  - Shelby Versus Darcian Method 20
  - Hvorslev K Analysis of Shelby Data 20
- Discussion 21
- Conclusion 23
- References 24

II SEEPAGE BLANKETS: A NOVEL STREAM-BOTTOM SEEPAGE COLLECTION DEVICE 39

Abstract 39
Introduction 40
Methods 41
Blanket Construction 41
Dilution Flow Meters 42
Blanket Performance Evaluation 45
Empirical Testing in USGS Seepage Tank 45
Field Implementation of Seepage Blankets at West Bear Creek, NC 47
Darcian Measurement Method 48
Reach Mass Balance 48
Field Sample Suite Collected from Blankets and Points 49
Results 51
July 2012 51
March 2013 54
Discussion 59
Conclusion 64
References 65

THESIS CONCLUSION 82

Appendices

A: DERIVATION OF DISCHARGE AND HYDRAULIC CONDUCTIVITY EQUATIONS 85

B: RESULTS FROM LAB TESTING OF THE SHELBY TUBE 91

C: FIELD RESULTS FOR SHELBY TUBE COMPARISON TO DARCIAN METHOD 99

D: MIXING CHAMBER VOLUME CALIBRATION AND TESTING FOR DILUTION FLOW METERS 107

E: EXAMPLE DILUTION FLOW METER CALCULATION AND PLOTS 114

F: USGS DENVER FEDERAL CENTER SEEPAGE BLANKET TESTING 116

G: REACH MASS BALANCE FOR WEST BEAR CREEK IN JULY 2012 125

H: JULY 2012 RESULTS FROM BLANKETS AND POINTS AT WEST BEAR CREEK, NC 131

I: MARCH 2013 RESULTS FROM BLANKETS AT WEST BEAR CREEK, NC 142

J: MEASUREMENT STATISTICS AND UNCERTAINTY FOR BLANKET DISCHARGE FIELD MEASUREMENTS 146

ACKNOWLEDGEMENTS

Heartfelt thanks to my advisor Kip Solomon for his patience and the invaluable discussions, David Genereux and Troy Gilmore for their extensive efforts in the field and pivotal roles in this work, Donald Rosenberry for access to DFC testing facilities and insightful discussion, Alan Rigby for his assistance in the lab and dear friendship, Olivia Miller for help running field samples, Wil Mace for his availability and assistance on a wide range of issues, Paul Jewell and Vic Heilweil, members of my thesis committee, for providing valuable edits, my fellow graduate students for moral and intellectual support, the Department of Geology and Geophysics for providing this opportunity and critical support along the way, my family for their love and steadfast belief in me, and my beautiful girlfriend Britt Espinosa for seeing me through some difficult times with a smile. I am indebted to all of you. Thank you.

THESIS INTRODUCTION

Quantification of groundwater-surface water exchange has become increasingly important as the physical, chemical, and biological process understanding of the hyporheic zone has advanced. The most direct method to measure this water exchange, a seepage meter, was developed by Israelsen and Reeve [1944] and first used to measure groundwater inflow by Lee [1977]. These original seepage meters were cut-off 55-gallon drums, fitted with a port and flexible bag, and inserted into the sediment so that naturally discharging water is captured in the bag. More current half-barrel seepage meters [e.g., Rosenberry and LaBaugh, 2008] are designed with a large areal footprint to integrate spatial heterogeneities and make low specific discharge (~1–30 cm day^{-1}) measurements feasible, large diameter ports and tubing to limit hydraulic head loss, and collection bag isolation containers to minimize stream flow influence on measured discharge. The benefit of seepage meters, other than being the only established direct discharge measurement device, is the spatial integration of discharge heterogeneity and the potential to collect flow-weighted spatially integrated samples from the devices. The basic design of the half-barrel seepage meter has been widely used to measure groundwater discharge in lakes and ponds [e.g., Lee, 1977; Shaw and Prepas, 1990b; Boyle, 1994; Rosenberry, 2000], streams and rivers [e.g., Libelo and MacIntyre, 1994; Landon et al., 2001; Rosenberry, 2008] and near-shore submarine settings [e.g., Cable et al., 1997; Burnett et al., 2001]. Decades of use and testing has revealed that half-barrel

seepage meters are subject to numerous potential errors such as flow constriction, resistance to filling of collection bags, stream effects on exposed bags, etc. [Murdoch and Kelly, 2003; Rosenberry and LaBaugh, 2008], although careful design, installation, measurement technique, and meter calibration [e.g., Rosenberry and Menheer, 2006] can provide reliable field results. This study presents two new methods for use in flowing surface water, the Shelby tube and the seepage blanket, designed to minimize potential errors and expand available techniques used in quantification of groundwater-surface water exchange. The two chapters presented here are to be published as separate stand-alone articles, thus some information in this introduction will be repeated in the respective sections.

The Shelby tube (a.k.a. thin-walled soil sampler) has been used since the 1940s as an undisturbed soil core collection device [Hvorslev, 1949]. In this study Shelby Tubes have been repurposed to measure specific discharge (q) and hydraulic conductivity (K) and can be configured as a self-purging groundwater sampling device. The device consists of a short section (~1 m) of Shelby tubing that has two openings drilled in the sides and a differential pressure transducer with data logger. The benefits of the Shelby tube measurement device are a) direct measure of specific discharge, b) measurement of hydraulic conductivity in the same sediment as measured q, c) a smaller cross-sectional footprint and obstruction to stream flow than half-barrel seepage meters, d) ease of construction and installation, and e) high temporal resolution. The length of time needed to complete a measurement with the Shelby tube can be reduced by use of an amplifier, which reduces the interior cross-sectional area and thus the volume of water to change the head within the standpipe. Testing of the Shelby tube was completed in a laboratory

setting (University of Utah and USGS Denver Federal Center) and in the field (West Bear Creek, NC). Performance was evaluated by comparing Shelby tube derived q and K to established methods.

The seepage blankets are designed for use in flowing water with the objective of advancing seepage meters design in this setting by minimizing potential sources of error [Murdoch and Kelly, 2003; Rosenberry and LaBaugh, 2008]. The seepage blanket design addresses the potential errors by a) using a semi-automated flow meter, b) reducing the perimeter to area ratio, c) minimizing the profile and obstruction to flowing water, d) using inserted metal stock to cut off shallow hyporheic flow, and e) providing a flexible medium across which pressure differences are minimized. A set of five low profile seepage blankets was constructed for installation across the width of a stream. The blankets were constructed from rubberized cloth (Hypalon©), and shallow hyporheic flow paths are blocked (and blanket retained) by short sections of stainless steel bar stock and aluminum L. The five blankets were designed to be placed end to end and cover a 71-cm wide transect across the stream. A semi-automated dilution flow meter was designed and developed for use with the seepage blanket at the University of Utah following the design of Sholkovitz et al. [2003]. The primary objective of the blankets was to isolate groundwater from streamwater, providing a representative sample of the exchange across the sediment-water interface and secondly to measure discharge. Testing was conducted in a laboratory setting (USGS Denver Federal Center) and in a low-gradient sandy-bottom stream (West Bear Creek, NC). The performance of the seepage blankets was evaluated by comparing seepage blanket measured discharge and samples to results from established methods.

CHAPTER I

DEVELOPMENT AND TESTING OF SHELBY TUBES AS AN IN-SITU SPECIFIC DISCHARGE AND HYDRAULIC CONDUCTIVITY MEASUREMENT DEVICE

Abstract

The Shelby tube (a.k.a. thin-walled soil sampler) has been used since the 1940s as an undisturbed soil core collection device. In this study, a Shelby tube was repurposed to measure specific discharge (q) and hydraulic conductivity (K) in shallow surface waters. Data needed to determine q and K was the head as a function of time inside the Shelby tube (H(t)), and the stream head outside the Shelby tube (H_s). Laboratory testing of the Shelby tube was conducted in seepage tanks at the University of Utah and the USGS Denver Federal Center. Utah tests were conducted in fine glass beads and coarse irregular sand. For both the beads and sand the Shelby tube discharge matched the bucket-gauged pumping rate (R^2 = 0.95, m = 0.96, n = 10, q = 1 to 0.6 m day^{-1}; R^2 = 0.998, m = 1.07, n = 38, q = 50 to -50 m day^{-1}, respectively. m = slope, n = measurement number).

Denver tests were conducted in a medium sand and Shelby measured discharge agreed with controlled seepage rates (R^2 = 0.994, m =1.06, n = 13, -0.47 to 0.6 m day^{-1}). K comparisons made at Utah indicated that the Shelby calculated hydraulic conductivity (K_S) agreed well with falling head permeameter tests (K_F) for the beads (K_S =

16 m day^{-1}, SD = 2.7, n = 10; K_F = 14.2 m day^{-1}, SD = 0.2, n = 5) and sand (K_S = 228 m day^{-1}, SD = 52, n = 38; K_F = 158 m day^{-1}, SD = 10.4, n = 5). Mean field results for the Shelby tube agreed with Darcian methods for q (0.43 to 0.54 m day^{-1}, respectively) and K (12.6 and 5.4 m day^{-1}, respectively). Lab and field comparisons suggest the Shelby tube is a robust measurement device for specific discharge and hydraulic conductivity.

Introduction

The Shelby tube (a.k.a. thin-walled soil sampler) has been used since the 1940's as an undisturbed soil core collection device. Harry A. Mohr originally conceived the use of thin-walled tubing for sample collection in 1936 while working with Prof. Arthur Casagrande, who requested a larger and less disturbed soil sample than current methods allowed [Hvorslev, 1949]. The samples were collected for geotechnical purposes and would be extruded from the tubing for testing. The method was found to be most successful in high clay content material that was more cohesive and less prone to falling out of the sampling device during retrieval. The name "Shelby tubing" is derived from the trade name for hard-drawn seamless steel tubing originally manufactured by the National Tube Company [Hvorslev, 1949].

In this study, Shelby tubes were repurposed to measure specific discharge (q) and hydraulic conductivity (K). Additionally the Shelby tube can function as a self-purging groundwater sampling device. The benefits of such a device are direct measure of specific discharge, measurement of hydraulic conductivity in the same sediment, smaller cross-sectional footprint and obstruction to stream flow than traditional seepage meters,

ease of installation, and high temporal resolution.

Traditional direct specific discharge measurement methods (half barrel seepage meters in the work of Rosenberry and LaBaugh, [2008]) have been designed with a large areal footprint to both integrate spatial heterogeneities and to capture enough flow to make low specific discharge (~1–30 cm day^{-1}) measurements feasible (length of test and measurement technique precision). Importantly, seepage meters are inherently inefficient requiring calibration and an efficiency correction factor be applied to field measurements (D. Rosenberry, personal communication, 2013). In a setting where water is flowing over the device the disruption of the surface water flow field can possibly alter the discharge rates being measured by the seepage meter [Lieblo and MacIntyre, 1994; Shinn et al., 2002; Murdoch and Kelly, 2003; Cable et al., 2006]. Additionally, the larger devices are more involved logistically with regards to manufacture, calibration, installation and measurement. The smaller diameter Shelby tube was easier to install and less disruptive to stream flow and sediment. The time to complete a measurement with the Shelby tube can be reduced by constricting the tube interior diameter above the sediment water interface.

Methods

Device Description

The tubing used in this study was 7-cm inner diameter thin-walled steel tubing, commonly known as Shelby tubing. Although the method will work for any tubing, the thin-walled metal tubing was chosen based on strength, weight, ease of insertion, and minimization of sediment disturbance. The tubing was cut into short lengths (< 1 m), and

two holes were drilled opposite each other at the desired insertion depth (Fig. 1.1). Other items needed were a differential pressure transducer and data logger, rubber stopper, syringe, and amplifier. The Shelby tube amplifier was used to reduce the time to complete a test by constricting the interior cross-sectional area and can be easily constructed with a few considerations. The amplifier should be securely attached to the Shelby tube to avoid changing the pressure of the interior during the test, be designed to not capture air, and have a consistent interior cross-sectional area. For areas of low q (<10 cm day^{-1}) with an unamplified Shelby tube, the measurement may take in excess of 30 minutes. While in the same location with an amplifier (such that A/a = 50), the head inside the standpipe could be fully recovered in less than 5 minutes. An amplifier designed for use in the field was constructed with solid PVC 3" round. The lower interior of the amplifier was machined into a cone to gradually reduce the diameter of the standpipe and to insure that no air was captured. A thin walled ½" PVC pipe was affixed to the top of the cone to provide a standpipe (Fig. 1.2). The physical amplification factor (ratio of the cross-sectional areas of the Shelby to the amplifier standpipe) for this configuration was 17.6. A modified Shelby tube was designed for use with the amplifier (Fig. 1.3). The various attachments (unamplified Shelby tube, amplifier, cap) were secured to the Shelby tube with a no-hub neoprene coupling.

Theory of Device

The specific discharge and the hydraulic conductivity of the sediment inside the Shelby tube were calculated with the following equations. The derivation of these equations is found in Appendix A.

The equation for specific discharge (q) is

$$q = \left.\frac{dh}{dt}\right|_{t_s} \frac{a}{A} \quad (1)$$

where q is the specific discharge [L/t], $\left.\frac{dh}{dt}\right|_{t_s}$ is the change in head with respect to time evaluated at t_s (i.e., the time when the head inside the Shelby tube passes through the head value in the stream) [L/t], A is the cross-sectional area of the Shelby tube [L^2], and a is the cross-sectional area of the standpipe [L^2].

The specific discharge was calculated by evaluating the slope of the recovery line as the head in the Shelby tube passes through the head value of the stream multiplied by the ratio of the cross-sectional area of the Shelby tube to the standpipe. The ratio of the cross-sectional area of the Shelby tube to the amplifier standpipe (A/a) is also referred to as the amplification factor.

The equation for hydraulic conductivity is

$$K = \frac{\left.\frac{dh}{dt}\right|_{t=0} - \left.\frac{dh}{dt}\right|_{t_s}}{\frac{A(h_s - h_0)}{aL}} \quad (2)$$

where K is the hydraulic conductivity [L/t], $\left.\frac{dh}{dt}\right|_{t=0}$ is the change in head with respect to time at time = 0 (i.e., the start of the test) [L/t], h_s is the head in the stream [L], h_0 is the head inside the Shelby tube at time = 0 [L], and L is the length of sediment inside the Shelby tube [L].

The data needed to evaluate Equations 1 and 2 are head as a function of time inside the standpipe (H(t)) and the stream head outside the standpipe (H_S). These can be measured with a differential pressure transducer and a data logger. While it was not necessary to have a real-time readout of the differential pressure, the readout made it

possible to determine the time to completion of the test (i.e., when the head inside the pipe has crossed through head in the stream) and whether an amplifier was needed.

Measurement Method

The Shelby tube was vertically inserted into the stream bottom with the two holes perpendicular to the stream flow. The drilled holes should be just above the stream bottom and free from any obstruction. The differential pressure transducer was inserted in one of the holes and "leveled" (by propping the transducer or lightly removing sediment) to achieve a voltage readout close to zero. The transducer did not have to be perfectly zeroed. When open to the stream the total head difference between the tube interior and the stream was zero. Any offset in the measured pressure head was from the differential pressure transducer having its two ports at slightly different elevations. This value can be taken as zero, or the head in the stream (H_S), and used to determine the correct time to evaluate the slope of the recovery curve. After the transducer was "leveled" and with the tube open to the stream, the data logger should be activated. The data logger was allowed to record > 50 measurements of the stream pressure and an average value noted by the operator and later used to indicate when the test has completed. When the Shelby tube was closed off to the stream by installing a stopper in the remaining hole, the water inside the Shelby tube was perturbed (removal of water for a gaining reach and addition of water for a losing reach) and allowed to recover. The Shelby tube should remain undisturbed until the readout has gone past the stream pressure noted earlier by the operator. The differential pressure transducer had fine enough resolution to be altered by the presence of a nearby obstruction (e.g., the operator), and disturbance of stream flow

was minimized during the test. The pressure head in the stream was again measured by removing the stopper to document any change in stage or transducer movement during the test and to indicate the end of an individual test in the data logger file. The data logger is stopped at this point.

In the case of a slow recovery time, the process was expedited by use of an amplifier. It was important to remove the differential pressure transducer from the Shelby tube during the amplifier installation as it avoided overpressurizing the transducer. The PVC cone amplifier was used in conjunction with a shortened Shelby tube cut off 5 cm above the top of the perpendicular holes. A no-hub coupling was used to attach the amplifier or a section of Shelby tube for an unamplified test. The stream level should be well above the top of the shortened Shelby tube. After the amplifier was in place, the transducer could be installed, and the test could continue as outlined above. The use of a syringe attached to rigid tubing was shown to be useful for the removal/addition of water.

In the case of a very slow test in which the amplification factor was not sufficient to achieve a reasonable test period or the user wished to use the unamplified configuration in low discharge conditions, the measurement sequence was altered to expedite the test. The "step measurement method" involved measuring the recovery curve for shorter periods at various head levels. The goal of this method was to measure the sections of the recovery curve at various points such that the head differential was large between measured sections (reducing uncertainty in K measurement) while not waiting for a full recovery from the large disturbance. The test was similarly started by activating the data logger with the Shelby open to the stream to record stream head, inserting the plug and closing the Shelby, and perturbing the interior water level. After recording for a short

period (~1–2 minutes) a small amount of water would be added to (or removed from) the interior, changing the head level, and water level would be allowed to recover at the new level for a short period. In this way the user could measure many sections of the curve without waiting for a full recovery. The user then added/removed water to just below/above the stream head and allowed the water inside the Shelby to recover undisturbed through the stream head. Once the water level passed through the stream head the plug was removed, equilibrating the interior with the stream, and completing the test.

Discharge Analysis

The data logger records a time stamp and a voltage measurement, which was correlated to an elevation of water (pressure head). The elapsed time from the start of the test should be plotted against the pressure (Fig. 1.4).

From this plot, two subsets of the data needed to be parsed out. The first was the ambient stream level or zero line, which are the intervals at the start and end of the test when the Shelby tube was open to the stream. The second data subset was the section of the recovery curve that crossed over the zero line. The two subsets, zero line and recovery curve, were then plotted together. A regression analysis was performed on each data subset, with the zero line getting a linear treatment and the recovery curve getting a second-order polynomial regression (Fig. 1.5). The recovery curve is logarithmic but a second-order polynomial was a useful approximation for fitting a portion of the recovery. This does not affect the robustness of the test as it is the slope of the recovery curve as it passes through the stream level that was relevant. For a test that recovers quickly, it was

particularly prudent to use a limited portion of the recovery to fit the polynomial.

The specific discharge was calculated by evaluating the first derivative of the recovery polynomial at the time when the recovery curve crosses the zero line. Equating the two fit lines and solving for the variables using the quadratic equation calculated the exact intersection point.

Hydraulic Conductivity Analysis

The K of the sediment inside the Shelby tube was determined using Equation 2. The polynomial fit used to calculate discharge was used to evaluate the slope at time = t_s. The slope of the recovery at time = 0 could be determined from the same polynomial fit, or a secondary fit was used based on an alternate subset of the recovery curve. The time chosen for t_0 was arbitrary with the consideration that the solution was most numerically stable with a large change in head over the time period from t_0 to t_s. For a test with a slow recovery, the polynomial was fit over a large portion of the recovery curve and covered a large range of head values. For a test that recovered quickly, the polynomial was fit to a limited portion of the recovery. For very slow recovery, the step method was used and separate fits were calculated for the respective steps. The K of the sediment was determined by evaluating the slope of a portion of the curve with high head differential between the interior and stream ($t = 0$) and the slope of a portion of the curve that crossed the stream head ($t = t_s$).

Sampling Device

The Shelby tube can be configured as a self-purging groundwater sampling device (Fig. 1.6). With the Shelby tube installed in the stream bed at the desired depth, one of the drilled holes would be closed with a stopper and the remaining drilled hole would have a piece of tubing that connects the interior of the Shelby tube to the stream. The tubing would be oriented so that the end was just below the water level inside the Shelby tube and was tightly sealed in the drilled opening in the Shelby tube. The water level inside the Shelby tube will be equilibrated with the stream at this point. In a gaining location, the groundwater captured by the Shelby tube will displace the reservoir of free water inside the Shelby tube. With the outlet tube positioned near the top of the free water surface, the entire volume will be purged. The time needed to purge the system could be determined from the measured q. Depending on the depth of the stream, the available volume to sample from inside the Shelby tube could be multiple liters. The self-purging groundwater reservoir is also an ideal location to deploy diffusion type samplers [e.g., Gardner and Solomon, 2009].

Empirical Testing

University of Utah Seepage Drum

A seepage tank built at the University of Utah (UU) was used to test the performance of the Shelby tube using a 55-gallon drum and a peristaltic pump. The water was routed to the base of the drum by PVC pipe and well screen (Fig. 1.7) covered with 20-cm of washed stream pebbles. The stream pebbles were covered with water permeable cloth and course sand, the purpose of which was to keep sand out of the pore space of the

pebbles. Two separate configurations were tested, the first with 50-cm of coarse angular quartz sand and the second replacing 45-cm of the sand with fine glass beads. The 55-gallon drum was filled with water and allowed to sit overnight (prior to addition of the sediment) to degas the water and ensure that the sediments were fully saturated with no captured air. The peristaltic pump was attached to the top of the PVC pipe (Fig. 1.8) with the intake/return placed in the free standing water and was used to simulate a gaining or losing streambed. The Shelby tube was tested with upward and downward seepage in the course sand, but limited to upward seepage in the fine glass beads.

USGS Denver Federal Center

The Shelby tubes were tested in the Denver Federal Center (DFC) seepage tank as described by Rosenberry and Menheer [2006]. The Denver tank was filled with rounded medium quartz sand during Shelby tube testing of upward and downward seepage conditions.

Lab Results

The performance of the Shelby tube was evaluated by comparing known pumping rates and falling head permeability tests (following the procedure outlined in Genereux et al., 2008) to the q and K, respectively, calculated by the Shelby tube. Pumping rates were determined by bucket gauge and/or paddle wheel flow meter. Tables of complete results are presented in Appendix B.

Discharge Measurement Efficiency of Shelby Tube from University of Utah

For the angular coarse sand and pump q ranging from 0.6 to 50 m day^{-1}, the Shelby tube measurements averaged 3% more than the pumping rate, while for q ranging from -8 to -50 m day^{-1}, the Shelby tube measurements averaged 8% more than the pumping rate.

Three measurements were made with the Shelby tube at each pump rate. The Shelby measured q plotted against the pump rate, showed strong correlation and fell along the one-to-one line (R^2 = 0.998, m = 1.07, n = 38, where m = slope and n = sample number) (Fig. 1.9). For fine glass beads and q ranging from 0.4 to 1 m day^{-1}, the Shelby tube measurements averaged 10% more than the pumping rate. When the unamplified Shelby measured discharge was plotted against the pump rate the data were strongly correlated and fell along the one-to-one line (R^2 = 0.95, m = 0.96, n =10) (Fig. 1.10). Given the inherent variability of flow in the seepage drum, it was expected that the pumping rate would not exactly match the measured seepage rate.

Discharge Measurement Efficiency of Shelby Tube from USGS Denver Federal Center

For the unamplified Shelby tests conducted in round medium sand at the DFC with upward seepage rates from 0.2 to 0.6 m day^{-1}, the Shelby tube averaged 2% less discharge than the pumping rate. For downward seepage rates from -0.2 to -0.47 m day^{-1}, the Shelby tube averaged 23% more discharge than the pumping rate. The Shelby q plotted against the pump rate and showed strong correlation and fell along the one-to-one line (R^2 = 0.994, m = 1.05, n = 13) (Fig. 1.11). The larger size of the DFC seepage tank made it more susceptible to flow heterogeneity than the smaller UU seepage drum, as

shown in the increased variability of measurements in the DFC tank (Appendix B). It was suspected that these are real differences in seepage rates, as opposed to any effects of Shelby tube installation or measurement error. Similar to findings from the UU testing, the DFC Shelby tube results matched the pump rates better during upward seepage than downward.

Hydraulic Conductivity Measurements with Shelby Tube

The Shelby measured values of K for angular coarse sand and fine glass beads agreed well with falling-head permeameter measurements (Table 1.1). No falling-head permeameter test was conducted in the medium sand, but the Shelby measured K for the medium sand fell between the K of the coarse sand and fine glass beads, as would be expected. Both the UU and DFC results showed that the Shelby calculated K for upward seepage was less than the Shelby calculated K for downward seepage rates (Appendix B). Furthermore, the standard deviation of the repeated measurements of K during upward seepage was smaller than during downward seepage. It was unclear why the Shelby tube behaves differently during upward and downward seepage when measuring q and K.

Amplification Factor Calibration

Results from glass beads in the UU seepage drum for the observed amplification factor using the PVC cone amplifier are presented in Table 1.2. The apparent amplification factor was defined as the amplified Shelby q divided by the unamplified Shelby q. For specific discharge rates from 0.04 to 1 day^{-1}, the average apparent amplification factor for the PVC cone was 22.4. It is unclear why the apparent AF was

different from the physical AF and why the amplified tests would result in flow rates that are higher than expected. If head loss within the amplifier were suspected, it would be expected that the amplification factor would be smaller (e.g., amplified Shelby q would be reduced) at lower flow rates. The empirical data showed that the amplification factor increased as the flow rate decreased. Furthermore, a cursory analysis using empirical pipe flow equations showed that the expected head loss from constriction and friction was much smaller than the observed difference in flow. The issue of the fluctuating amplification factor was not immediately clear and warrants further investigation.

Field Testing

A field comparison of q and K measured by both Shelby tubes and a Darcian approach [Kennedy et al., 2007; Genereux et al., 2008] was conducted on West Bear Creek in North Carolina, USA. The sandy bottom stream in the Atlantic Coastal Plain has been extensively studied [Genereux et al., 2008; Kennedy et al., 2009a; Kennedy et al., 2009b; Kennedy et al., 2010]. Amplified and unamplified Shelby data, vertical hydraulic gradient, and falling head hydraulic conductivity measurements were collected at 24 sites along 8 transects. The Darcian discharge is the product of the vertical hydraulic gradient and the vertical K as determined by falling head permeability tests. Three transect measurements (right, center, and left) were made at locations chosen based on ease of piezometer penetration and water production. The Shelby tube was inserted toward the center of the stream from the piezometer location at the right and left positions and upstream of the piezometer at the center position. The falling head permeameter was located nearby the Shelby tube, but in undisturbed sediment (i.e., not the same location as

the Shelby). The comparative data for Shelby and Darcian approach presented here are for nearby locations, and it was not expected that the results agree for each location. Unamplified and amplified Shelby tests were completed with the modified Shelby tube and PVC cone amplifier, allowing the test to be completed in the same location and sediment. The physical amplification factor of 17.6 was used in the calculation of the amplified q and K. In addition to Equation 2 derived Shelby K values, the Shelby data were used to determine K using the falling-head equation [Hrovslev, 1951].

Comparison of Amplified to Unamplified Shelby Measurements

Shelby tube measurements of q and K were completed with the amplified and unamplified configuration at 17 of the 24 sites. The tests were conducted in the same sediment and location using the modified Shelby tube. Both amplified and unamplified tests were not completed at all the sites because some locations were not suitable for the unamplified test (low specific discharge). The mean q from the unamplified Shelby was 0.58 m day^{-1}, and for the amplified Shelby it was 0.43 m day^{-1}. The geometric mean K with outliers removed for the unamplified Shelby was 16.5 m day^{-1}, and for the amplified Shelby it was 12.6 m day^{-1}, which is relatively good agreement. Plots of amplified and unamplified Shelby q (Fig. 1.12) and K (Fig. 1.13) showed that the results roughly clustered around the one-to-one line. The outliers for the calculation of geometric mean K were visually selected from the amplified to unamplified plots. The outliers were chosen based on significant deviation from the overall trend (e.g., the two far right values in Fig. 1.13). The outliers were removed because lab results showed that amplified versus unamplified Shelby K were in good agreement, and the field results were subject to

additional measurement error, particularly the unamplified configuration in low discharge conditions. With regards to q, the majority of the data fell slightly below the one-to-one line suggesting that the unamplified Shelby tube was overestimating q rates with respect to Darcian method. Given the modest seepage rates (< 1 m day^{-1}) and relatively low K (< 40 m day^{-1}), the unamplified Shelby configuration was not ideal, and subsequent comparison of Shelby and Darcian methods made use of the amplified Shelby tube values. The discrepancy between the mean apparent field measured AF (13.4) and the physical AF (17.6) (Fig. 1.14) might be attributed to difficulties in data analysis of the unamplified Shelby tube at low q (< 0.5 m day^{-1}) and emphasizes the inability of the unamplified Shelby method to accurately resolve low q. The apparent field AF approached the physical AF, and the spread narrowed at higher specific discharge rates, suggesting that the apparent and physical AF were in good agreement at higher flows. The empirical results of the apparent AF as a function of q (Table 1.2) showed that the amplification factor increased as q decreased, which was opposite of the field results. It should be noted though that both field and lab data showed that the apparent and physical amplification factor converged as flow rate increased. For this reason, we suggest that the physical amplification factor be trusted and used for Shelby calculations. It was unclear why the amplification factor was variable at low flow rates, although the limited ability of the Shelby tube to resolve low flows may be a factor. Further research should be directed at resolving this issue.

Shelby Versus Darcian Method

The mean q as determined by Darcian approach was 0.54 m day^{-1} while the amplified and unamplified Shelby suggested 0.43 and 0.58 m day^{-1}, respectively. The Darcian q plotted against the amplified Shelby q showed moderate correlation and roughly clustered along the one-to-one line (Fig. 1.15). Complete results are presented in Appendix C. The geometric mean K with outliers removed as determined by the Darcian approach was 5.4 m day^{-1} while the amplified and unamplified Shelby suggested 12.6 and 16.5 m day^{-1}, respectively. The outliers were similarly visually selected and removed because of likely measurement error. Given the variation in measurement location and moderate heterogeneity of the stream bottom, the mean K results from the Darcian and Shelby approaches were in reasonable agreement. The Darcian K plotted against the amplified Shelby K showed moderate correlation and roughly clustered along the one-to-one line (Fig. 1.16).

Hvorslev K Analysis of Shelby Data

The Shelby derived data set for a given location was analyzed using the Hrovslev falling head equation in the work of Genereux et al. [2008] to check the robustness of Eq. 2 derived K of the sediments within the Shelby tube. The Hrovslev equation (commonly referred to as the falling-head equation) for the amplified tests was modified (following Hrovslev, 1951, Pg. 43, Case E) by multiplying the result by D^2/d^2 (where D is the Shelby tube diameter, and d is the amplifier standpipe diameter). Results for the Hrovslev derived Shelby K showed a geometric mean unamplified value of 13.9 m day^{-1} (compared to an Eq. 2 K of 18.4 m day^{-1}) and geometric mean amplified value of 7.9 m

day^{-1} (compared to an Eq. 2 K of 10.5 m day^{-1}). The Hrovslev amplified Shelby K plotted against the Hrovslev unamplified Shelby K (Fig. 1.17) clustered around the one-to-one line. Similarly, the Hrovslev and Eq. 2 derived Shelby K (both the unamplified (Fig. 1.18) and amplified tests (Fig. 1.19)) clustered around the one-to-one line, suggesting that the determination of K using Eq. 2 is consistent with the Hrovslev method.

Discussion

Lab results from the University of Utah and Denver Federal Center showed that the unamplified Shelby tube was reliably measuring upward specific discharge for flow rates ranging between 50–0.2 m day^{-1}. Lab results from the University of Utah showed that the unamplified and amplified Shelby tubes were reliably measuring K during upward seepage in various sediments (K = 15–200 m day^{-1}). Furthermore, field results from West Bear Creek show that the Shelby derived q and K compared well to a Darcian approach. Advantages of the Shelby tube method included ease of installation and measurement, reduced sediment and surface water disturbance, and increased direct specific discharge measurement quality (e.g., no correction factor). The reduced spatial coverage (as compared to traditional seepage meters) and thus the integration of heterogeneities can be compensated for by sampling density and design (i.e., sufficient number of sampling locations and high sampling density perpendicular to stream flow [Kennedy et al., 2008]). In addition, K was derived from the same data set used to determine q, thus reducing the time spent in the field and insuring that K and q are spatially correlated. The unamplified Shelby tube was less reliable in downward seepage conditions in the lab, with Shelby measured q up to 23% more than the seepage tank pumping rate. In addition, the Shelby

calculated K value during downward seepage was consistently higher and more variable than the Shelby K determined in the same sediment during upward seepage. The reason for the difference in measurement accuracy based on the direction of seepage was unclear.

Testing of the amplified Shelby tube produced some unexpected results. PVC cone amplifier testing in the lab and field showed that the apparent amplification factor (AF) did not always agree with the physical AF. The PVC cone had a physical AF of 17.6, while lab and field results suggested an AF of 22 and 13, respectively. Although the head loss due to constriction and friction as determined by empirical pipe flow equations was insignificant compared to measured flow, the apparent AF was more consistent and closer to the physical AF at higher specific discharge rates, suggesting that some head losses were occurring. The difference in apparent and physical AF was only recognizable at low flow rates suggesting that the head loss was small. The relatively small difference between the physical-, lab-, and field-derived AF might be attributed to difficulty in data analysis, particularly in low specific discharge conditions with the unamplified Shelby configuration.

Analysis of the Shelby data was difficult and nonunique if the recovery profile contains excess noise, there was a fast recovery with a small gradient or measuring very low flow rates. All of these issues stem from either poor approximation of the recovery curve with a second-order polynomial regression, inability to accurately determine the intersection of the recovery and zero line, or both. Given the constant fluctuation of the stream head in the field and the high sensitivity of the transducer, extra noise was an inherent issue. The analysis of the amplified tests was more straightforward as the rapid

recovery cancels out much of the stream noise. But this must be carefully weighed against the issues of the amplification factor variation. In the case of a fast recovery and small gradient (e.g., high K material with a low q) the Shelby method was not well suited to make specific discharge measurements. The slope of the recovery curve is rapidly changing, and the analysis became very sensitive to the evaluation time and regression fit. The Shelby method was also challenged in measuring very low flow rates (< 5 cm day^{-1}) regardless of the amplifier as the recovery can take a very long time and any noise along the recovery curve can confound the analysis. It is theoretically feasible to use a larger amplification factor (i.e., smaller diameter amplifier standpipe), although the smaller diameter tubing can significantly restrict flow. Although the Shelby tube was not well suited for use in low specific discharge and low gradient situations, seepage meter and Darcian methods are equally challenged in such conditions.

Conclusion

The thin-walled Shelby tube can be used to measure specific discharge (q) and hydraulic conductivity (K) in locations where the groundwater-surface water exchange is of interest. Both lab and field results show that the Shelby tube was reliably reproducing q and K as measured against established methods. The advantages of the Shelby tube are direct measurement of q, measurement of K from the same sediment, minimal disturbance to sediment and surface water flow, relatively fast and easy measurement compared to established methods, and greatly simplified equipment and fieldwork preparation. The Shelby tube could not accurately measure very low flows (< 5 cm day^{-1}) and the analysis can be nonunique in some extreme cases (e.g., high K with low q).

Additionally, the Shelby tube had greater variability when measuring q and K in downward seepage conditions, although there was not a theoretical basis that would explain this observation. The use of an amplifier with the Shelby tube reliably reproduced measured q and K while reducing the time to complete a measurement and the uncertainty associated with a given measurement. An amplifier can be easily constructed given a few considerations (such as secure attachment, consistent internal diameter, and appropriate amplification factor). Variation in the apparent amplification factor is, at this point, unexplained, although it seems reasonable that the physical amplification factor should be trusted and used in the Shelby calculations.

References

Cable, J. E., J. B. Martin, and J. Jaeger (2006), Exonerating Bernoulli? On evaluating the physical and biological processes affecting marine seepage meter measurements, *Limnol. Oceanogr.: Methods, 34,* 172–183.

Gardner, P., and D. K. Solomon (2009), An advanced diffusion sampler for the determination of dissolved gas concentrations, *Water Resour. Res.*, *45*, W06423, doi:10.1029/2008WR007399

Genereux, D. P., S. Leahy, H. Mitasova, C. D. Kennedy, and D. R. Corbett (2008), Spatial and temporal variability of streambed hydraulic conductivity in West Bear Creek, North Carolina, USA, *J. Hydro., 358*, 332–353, doi:10.1016/j.jhydrol.2008.06.017

Hvorslev, J. M. (1949), Subsurface exploration and sampling of soils for civil engineering purposes: Report of the research project, sponsored by the Engineering Foundation, the Graduate School of Engineering, Harvard University and the Waterways Experiment Station, Corps of Engineers, U.S. Army. American Society of Civil Engineers, Vicksburg, VA, http://hdl.handle.net/2027/mdp.39015068591497

Hvorslev, J. M. (1951), Time lag and soil permeability in ground-water observations, *Bull. No. 36*, 55 pp.,Waterways Experiment Station, Corps. Of Engineers, U. S. Army.

Kennedy, C. D., D. P. Genereux, D. R. Corbett, and H. Mitasova (2007), Design of a light-oil piezomanometer for measurement of hydraulic head differences and collection of groundwater samples, *Water Resour. Res.*, *43*, W09501, doi:10.1029/2007WR005904.

Kennedy, C. D., D. P. Genereux, H. Mitasova, D. R. Corbett, and S. Leahy (2008), Effect of sampling density and design on estimation of streambed attributes, *J. Hydro., 355*, 164–180.

Kennedy, C. D., D. P. Genereux, D. R. Corbett, and H. Mitasova (2009a), Relationships among groundwater age, denitrification, and the coupled groundwater and nitrogen fluxes through a streambed, *Water Resour. Res., 45*, W09402, doi:10.1029/2008WR007400.

Kennedy, C. D., D. P. Genereux, D. R. Corbett, and H. Mitasova (2009b), Spatial and temporal dynamics of coupled groundwater and nitrogen fluxes through a streambed in an agricultural watershed, *Water Resour. Res., 45*, W09401, doi:10.1029/2008WR007397.

Kennedy, C. D., L. C. Murdoch, D. P. Genereux, D. R. Corbett, K. Stone, P. Pham, and H. Mitasova (2010), Comparison of Darcian flux calculations and seepage meter measurements in a sandy streambed in North Carolina, United States, *Water Resour. Res., 46*, W09501, doi:10.1029/2009WR008342.

Landon, M. K., D. L. Rus, F. E. Harvey (2001), Comparison of instream methods for measuring hydraulic conductivity in sandy streambeds, *Ground Water, 39*, 870–885.
Libelo, E. L., and W. G. MacIntyre (1994), Effects of surface-water movement on seepage-meter measurements of flow through the sediment-water interface, *Appl. Hydrogeol. 2*, 49–54.

Murdoch, L. C., and S. E. Kelly (2003), Factors affecting the performance of conventional seepage meters, *Water Resour. Res., 39*, doi: 10.1029/2002WR001347.

Rosenberry, D. O., and Menheer, M. A., 2006, A system for calibrating seepage meters used to measure flow between ground water and surface water, *U.S. Geological Survey Scientific Investigations Report 2005-5053*, 21 pp., U. S. Geological Survey, Reston, VA.

Rosenberry, D. O., and J. W. LaBaugh (2008), Field techniques for estimating water fluxes between surface water and ground water, *U. S. Geological Survey Techniques and Methods 4–D2*, 128 pp., U. S. Geological Survey, Reston, VA.

Shinn, E. A., C. D. Reich, and T. D. Hickey, (2002). Seepage meters and Bernoulli's Revenge, *Estuaries, 25*, 126–132.

Todd, D. K. (1959), Ground water hydrology, *Qtr. J. Royal Meteor. Soc., 87,* 122–130

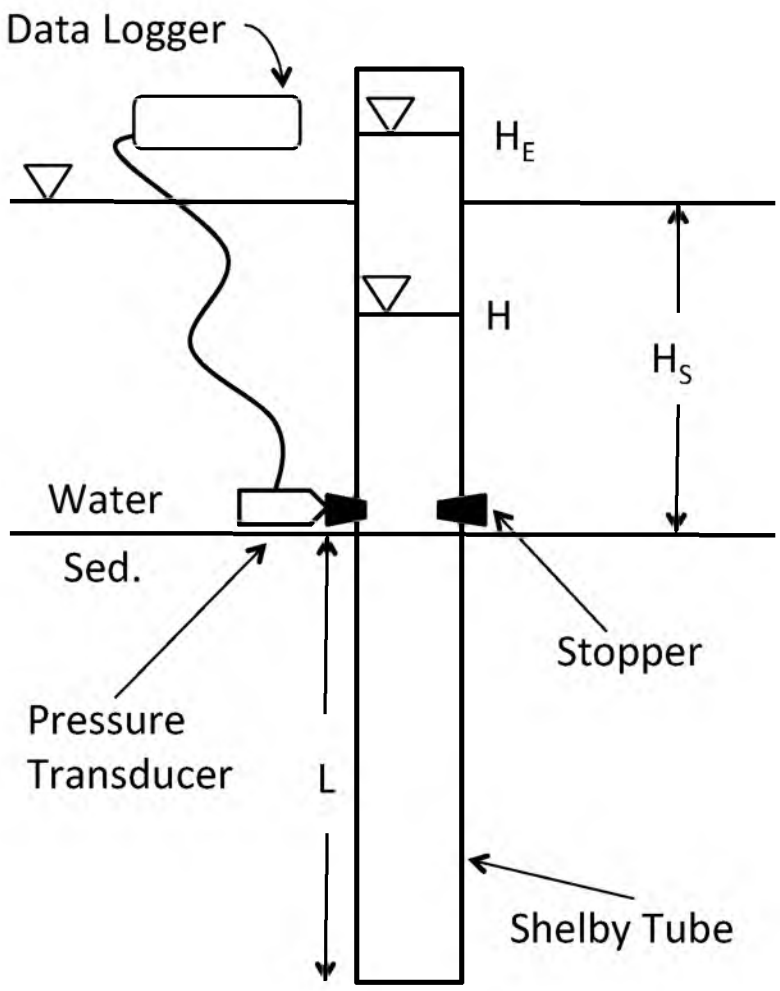

Figure 1.1. Diagram of Shelby tube seepage meter, differential pressure transducer, data logger, and rubber stoppers. L is the insertion depth, A is the cross-sectional area inside the tube, H_S is stream height, and for a gaining measurement, H is the time-varying water level inside the Shelby tube during the measurement, and H_E is the equilibrated head in the Shelby tube (equal to the head at the base Shelby tube).

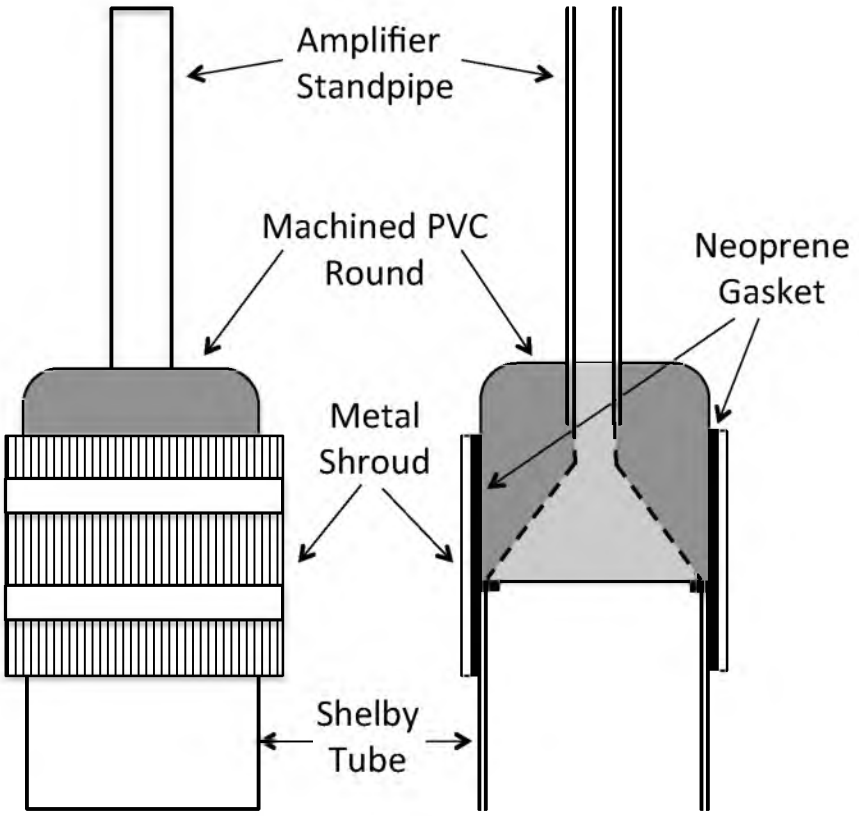

Figure 1.2. Diagram of amplifier attached to modified Shelby tube base in exterior side view and cut-away side view showing machined interior of PVC round, neoprene gasket and shroud of the coupling, and amplifier standpipe.

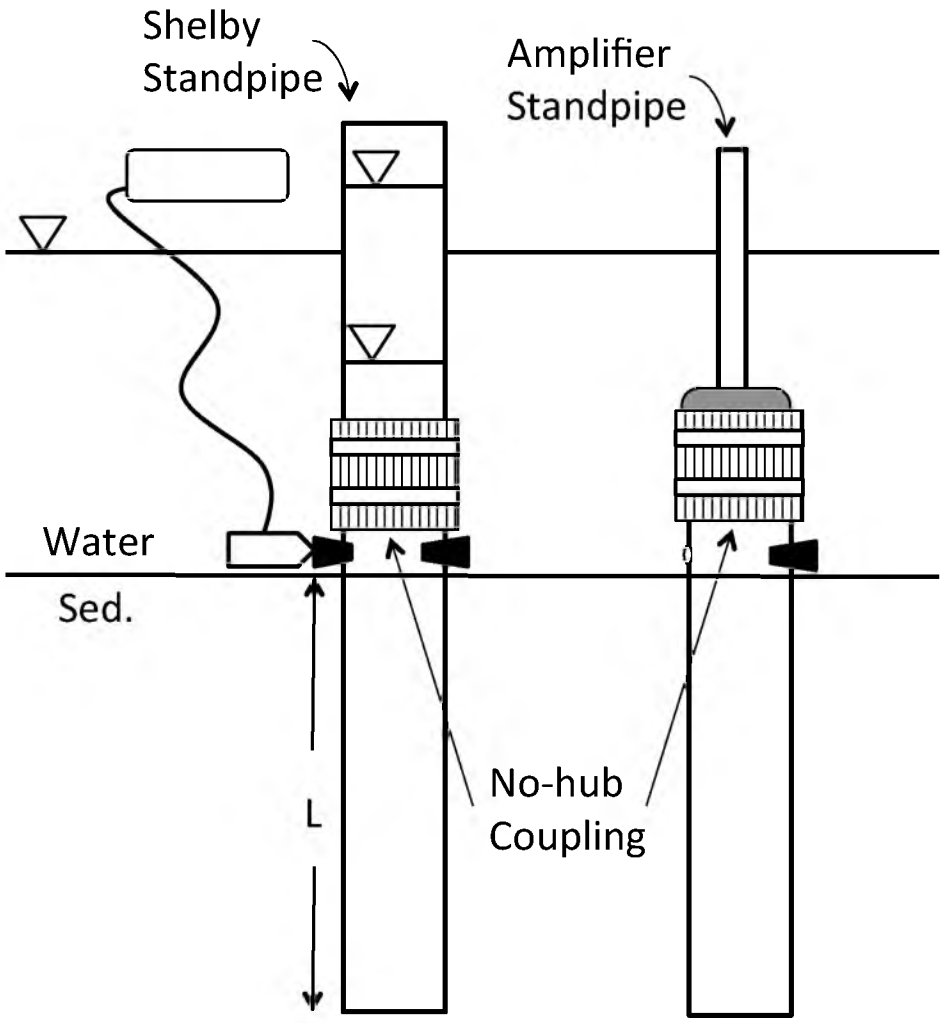

Figure 1.3. Diagram of modified unamplified Shelby tube with differential pressure transducer and data logger and amplified Shelby tube.

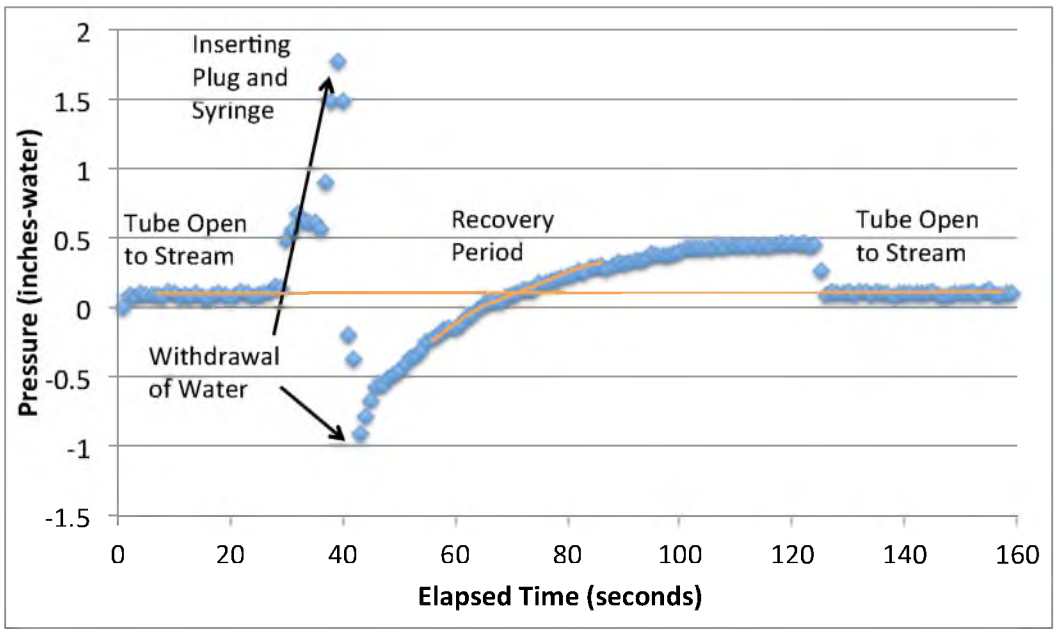

Figure 1.4. Pressure vs. time for a Shelby tube seepage meter test in a natural sandy streambed. Baseline transducer values were recorded during the two time periods when the Shelby tube was open to the stream. The orange lines indicate the baseline and recovery subsets in Figure 1.5.

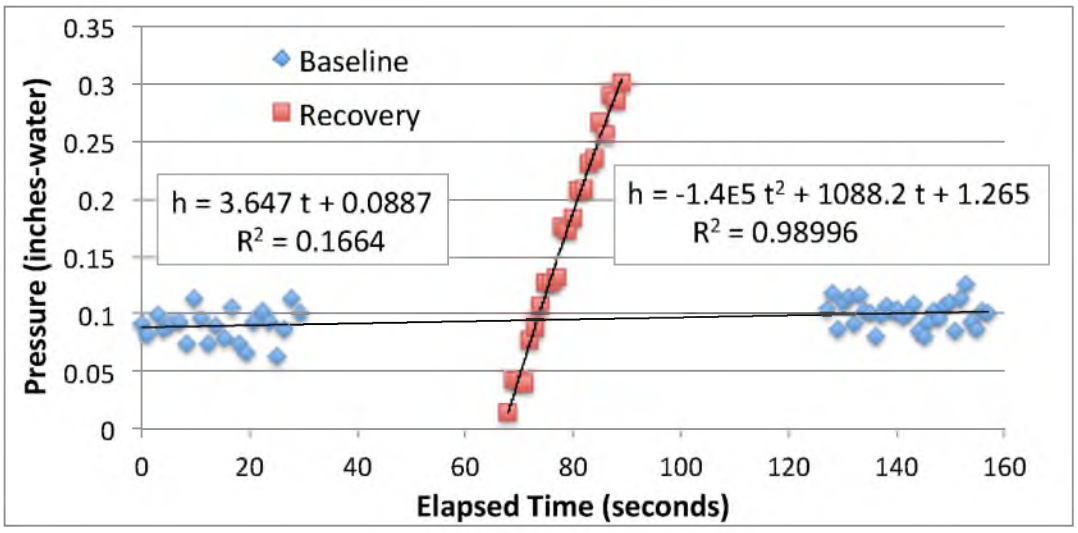

Figure 1.5. Pressure vs. time for the baseline transducer value and the recovery data from Figure 1.4 and the respective best-fit regressions.

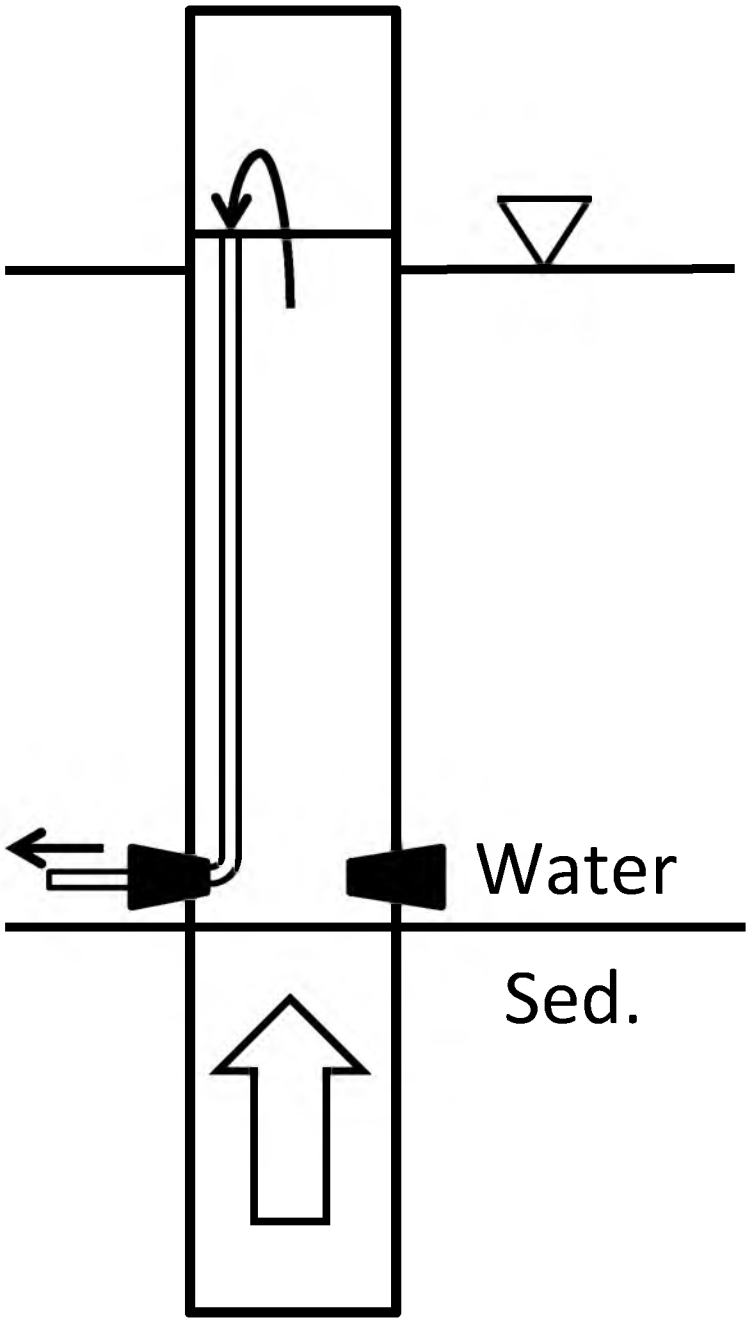

Figure 1.6. Diagram of Shelby tube configured as self-purging groundwater sampling device. The interior discharge tube is placed above stream level to ensure no streamwater is captured.

Figure 1.7. PVC pipe and well screen use to direct water to the base of a 55-gallon drum.

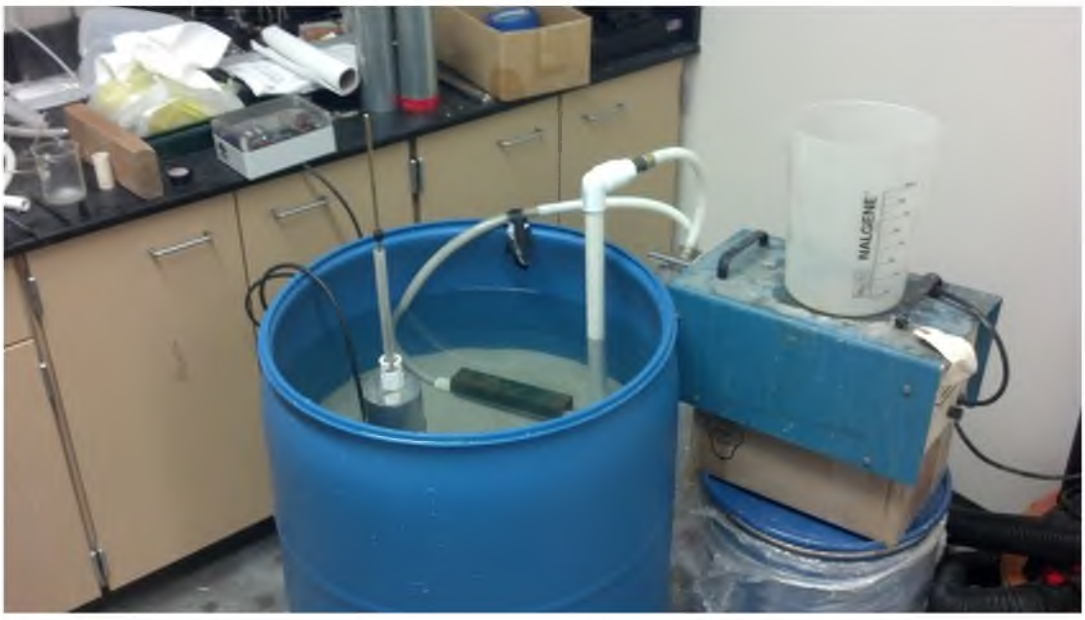

Figure 1.8. 55-gallon seepage drum showing peristaltic pump, well screen pump return, and installed Shelby tube with amplifier.

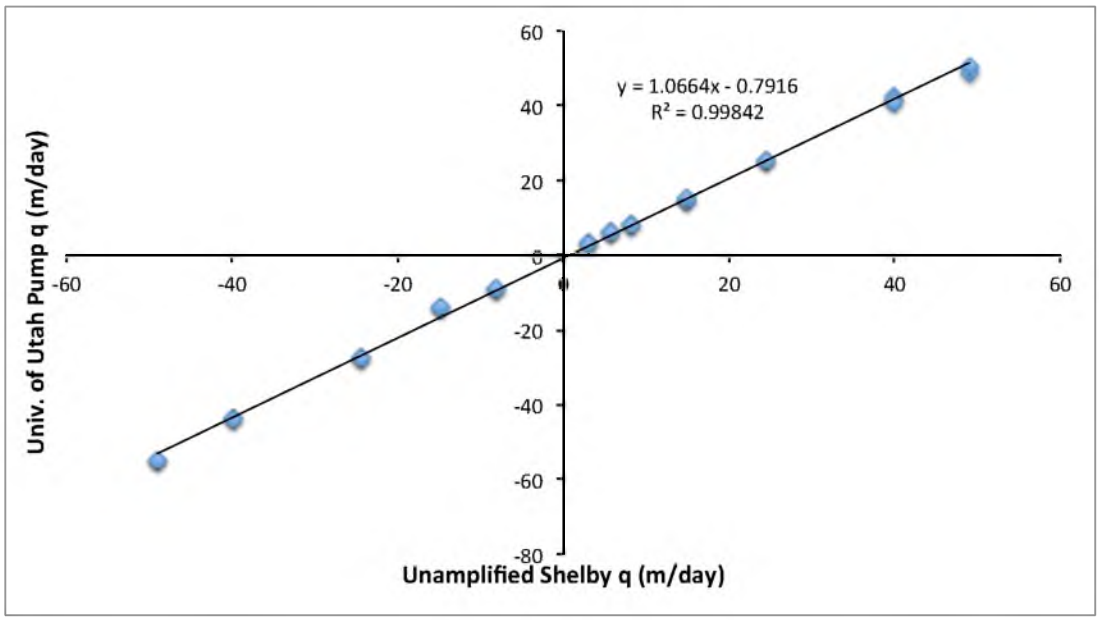

Figure 1.9. Plot of unamplified Shelby measured specific discharge (q) against the pump specific discharge for coarse sand in the University of Utah seepage drum. Negative values denote downward flow, while positives are upward flow.

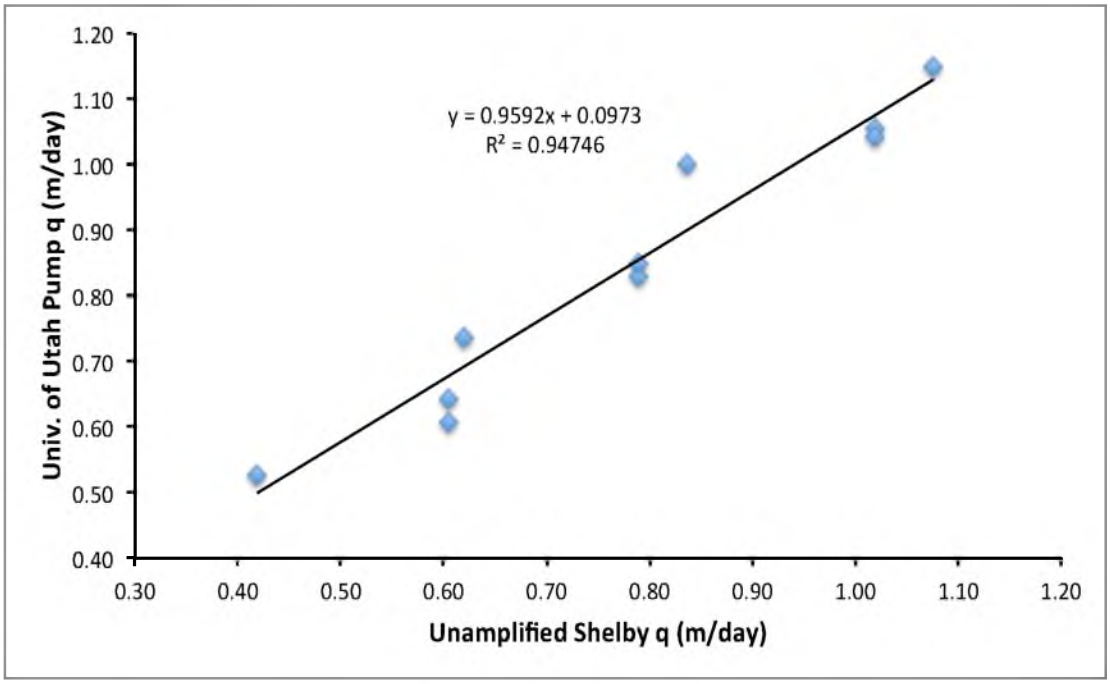

Figure 1.10. Plot of unamplified Shelby measured specific discharge (q) against the pump specific discharge for fine glass beads in the University of Utah seepage drum.

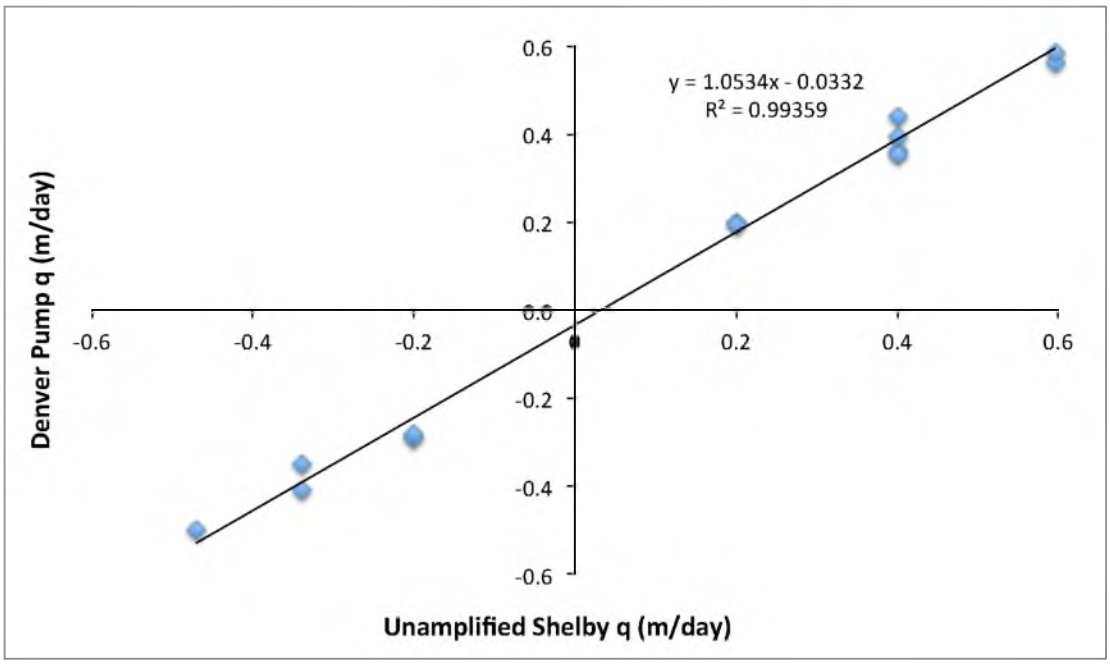

Figure 1.11. Plot of unamplified Shelby measured specific discharge (q) against the pump specific discharge for medium sand in the Denver Federal Center seepage tank. Negative values are for downward flow and positive values are for upward flow.

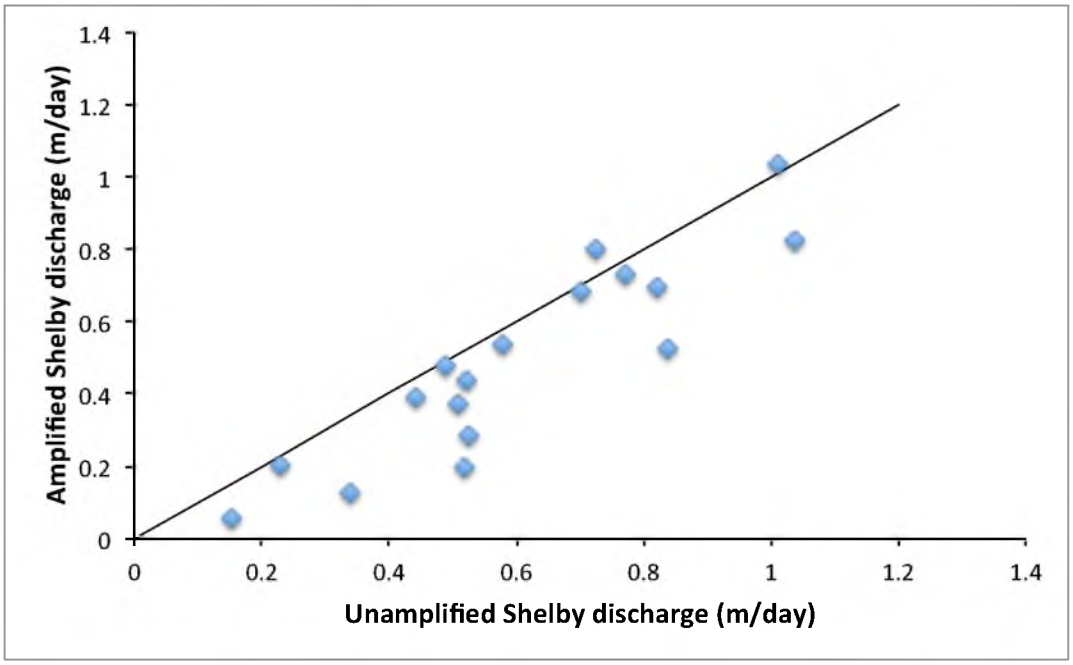

Figure 1.12. Plot of unamplified Shelby and amplified Shelby measured specific discharge (q) from West Bear Creek and one-to-one line.

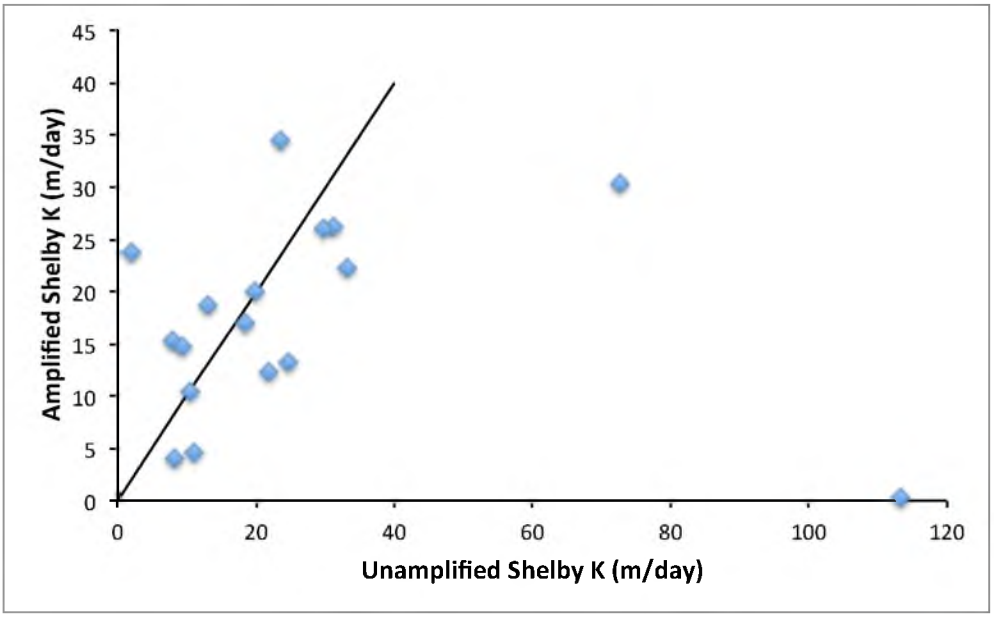

Figure 1.13. Plot of unamplified Shelby and amplified Shelby measured hydraulic conductivity (K) from West Bear Creek and one-to-one line.

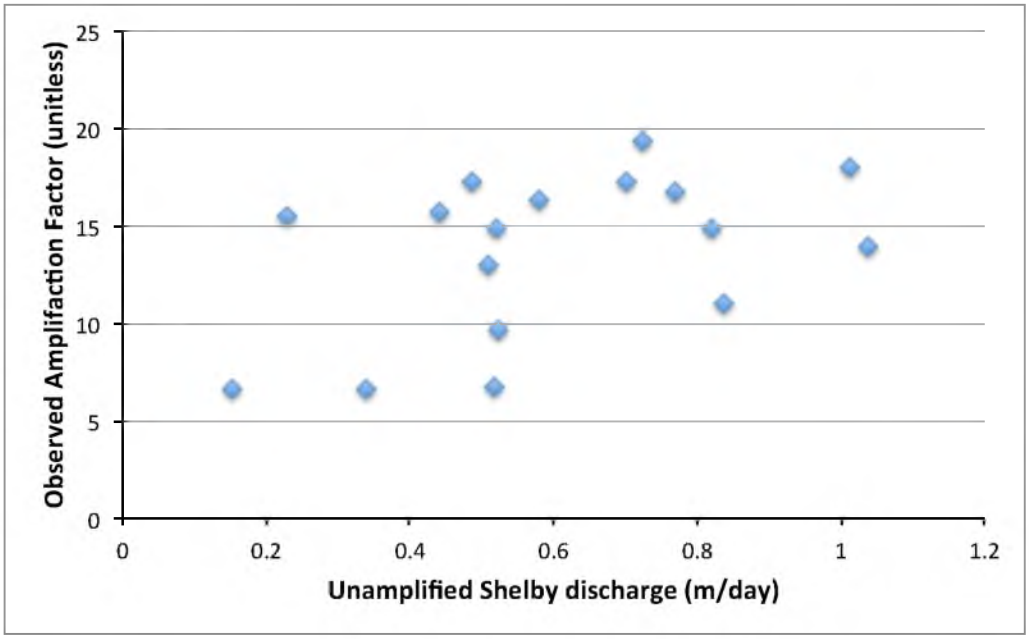

Figure 1.14. Plot of the unamplified Shelby specific discharge (q) against the apparent amplification factor (i.e., the ratio of amplified Shelby specific discharge to unamplified Shelby specific discharge) from West Bear Creek.

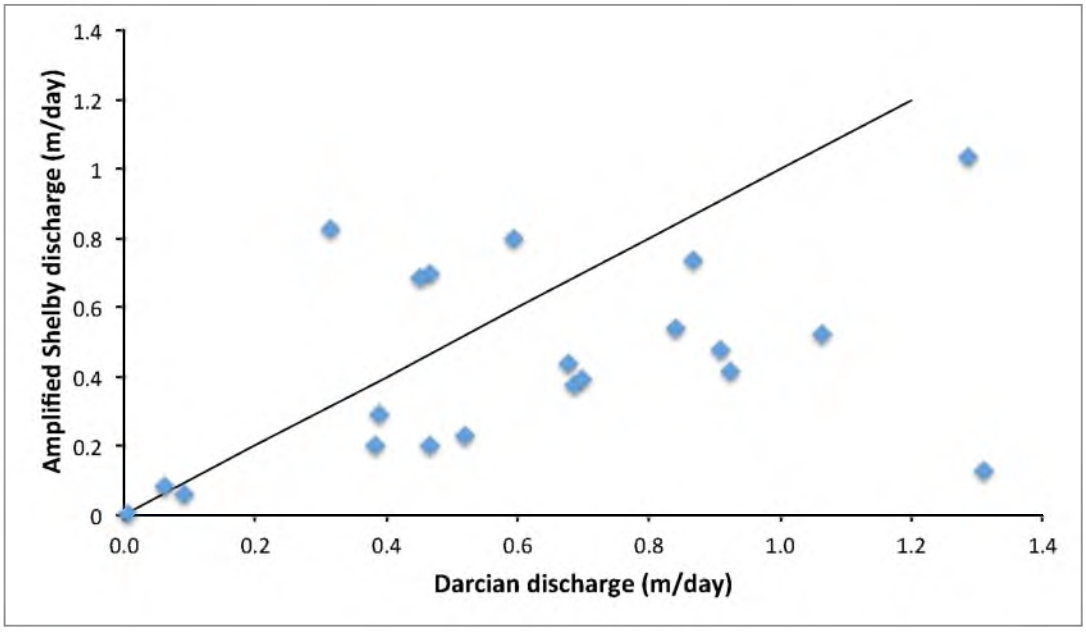

Figure 1.15. Plot of Darcian specific discharge (q) versus the amplified Shelby specific discharge from West Bear Creek and one-to-one line.

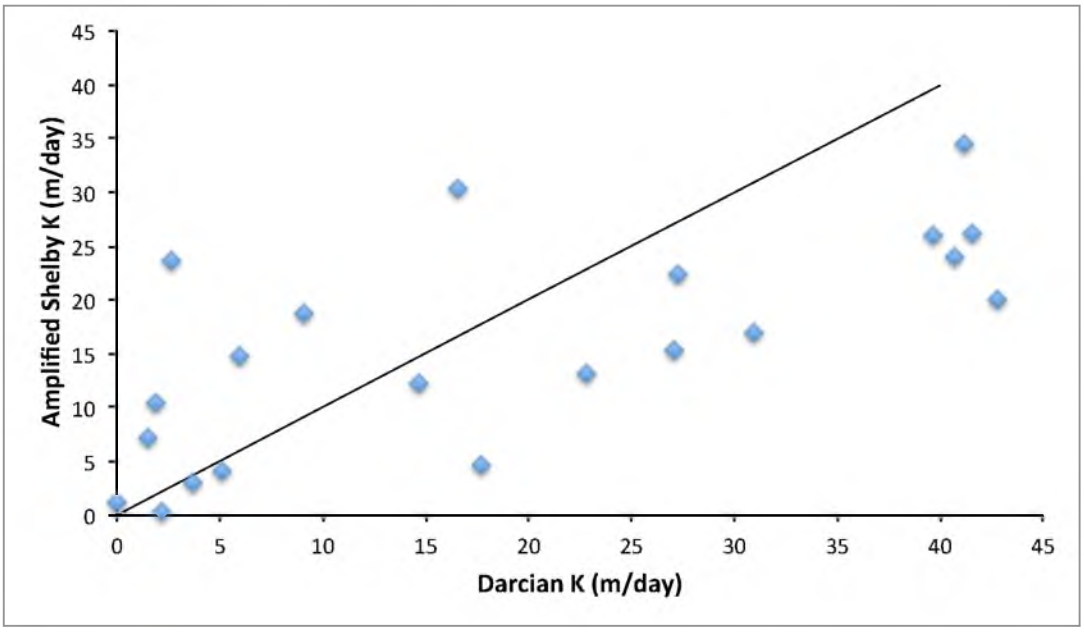

Figure 1.16. Plot of Darcian hydraulic conductivity (K) versus the amplified Shelby hydraulic conductivity from West Bear Creek and one-to-one line.

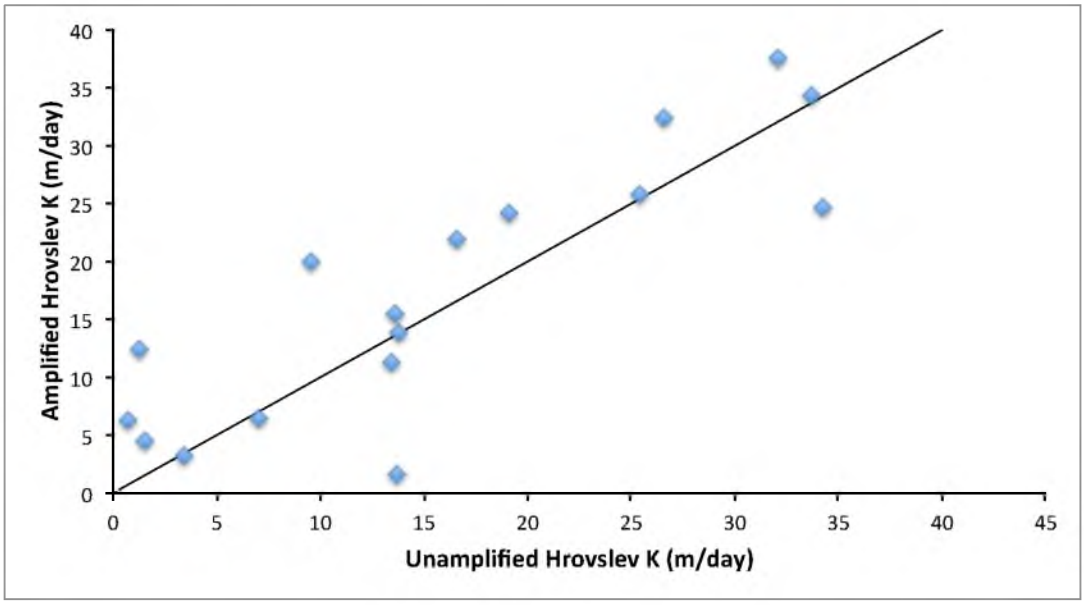

Figure 1.17. Plot of unamplified Shelby Hrovslev hydraulic conductivity (K) versus amplified Shelby Hrovslev hydraulic conductivity for Shelby tube data from the same location and sediment in West Bear Creek and one-to-one line.

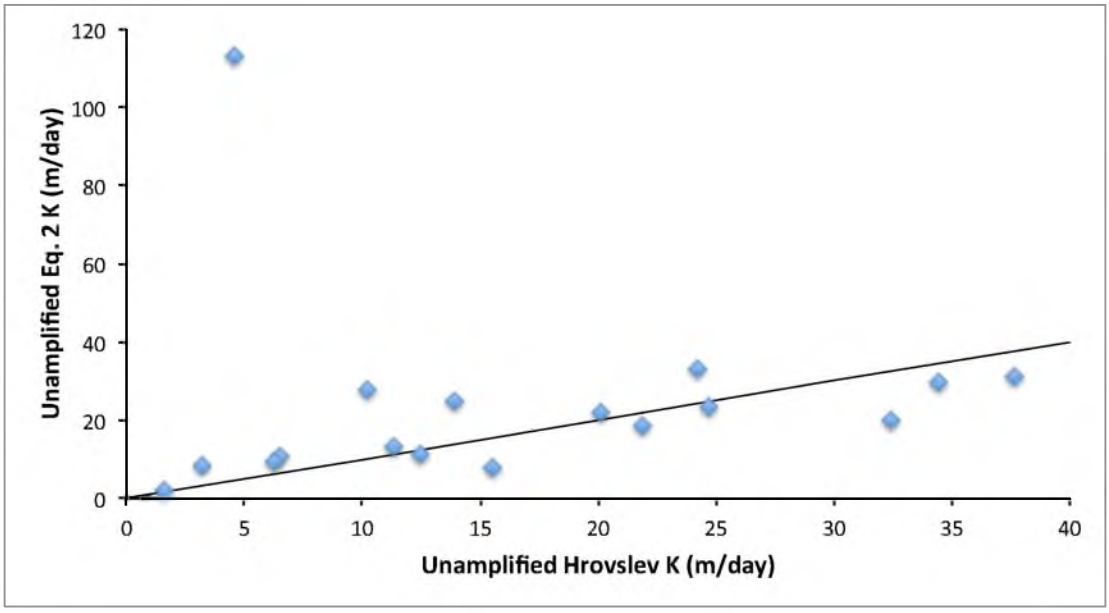

Figure 1.18. Unamplified Shelby Hrovslev hydraulic conductivity (K) versus unamplified Shelby Eq. 2 hydraulic conductivity for Shelby tube data from the same location and sediment in West Bear Creek and one-to-one line.

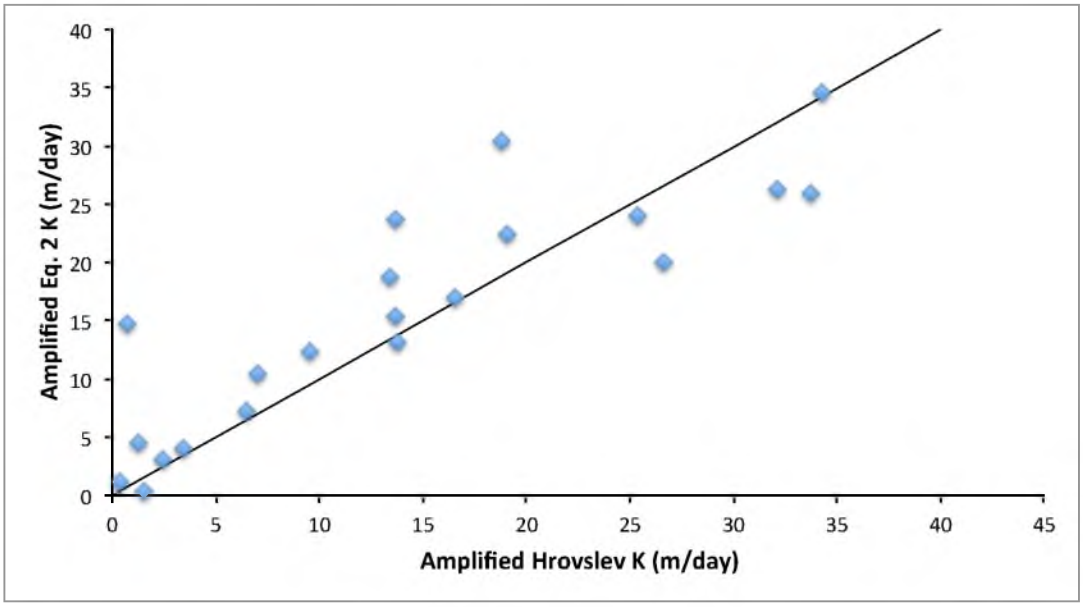

Figure 1.19. Amplified Shelby Hrovslev hydraulic conductivity (K) versus the amplified Shelby Eq. 2 hydraulic conductivity for Shelby tube data from the same location and sediment in West Bear Creek and one-to-one line.

Table 1.1. Mean hydraulic conductivity with 95% confidence intervals as measured by Shelby tube for coarse sand and fine glass beads from the University of Utah and medium sand from the Denver Federal Center. s.d. is standard deviation and n is number of measurements.

Material		Shelby			Falling Head		
	Flow Dir.	K (m day^{-1})	s.d.	n	K (m day^{-1})	s.d.	n
Coarse Sand	Up	212 ± 16	43	29	158 ± 13	10	5
	Down	249 ± 32	57	15			
Glass Beads	Up	16 ± 1.5	4.1	30	14 ± 0.2	0.2	5
Medium Sand	Up	102 ± 11	15	10	N/A		
	Down	152 ± 40	75	16			

Table 1.2. Specific discharge (q) as determined by pump rate, unamplified Shelby tube, amplified Shelby tube, and apparent amplification factor of PVC cone amplifier. Tests completed in glass beads at the University of Utah.

Pump q (m day^{-1})	Unamplified Shelby q (m day^{-1})	Amplified Shelby q (m day^{-1})	Apparent Amplification Factor
0.04	0.04	0.86	24.41
0.1	0.11	2.42	22.74
0.15	0.16	4.12	25.51
0.2	0.21	4.51	21.23
0.8	0.8	17.65	22.05
1.1	0.99	18.09	18.21
		Mean	22.36

CHAPTER II

SEEPAGE BLANKETS: A NOVEL STREAM-BOTTOM SEEPAGE COLLECTION DEVICE

Abstract

A flexible stream-bottom seepage collector (seepage blanket) has been designed and tested in both the laboratory and field. The goals of the blankets were to measure groundwater discharge and isolate streamwater from groundwater for sampling purposes. Attributes of the seepage blanket include a) automated flow meter, b) reduced perimeter to area ratio, c) metal edging inserted to cut-off shallow hyporheic flow, d) minimal profile and obstruction to flowing water, and e) a flexible medium across which pressure differences were minimized. A simple dilution flow meter for use with the seepage blanket was developed tested against bucket-gauged flows between 20 and 200 mL min^{-1}.

Lab testing of the seepage blankets was conducted in a seepage tank at the USGS Denver Federal Center, and field testing was conducted during two campaigns (July 2012 and March 2013) on West Bear Creek near Goldsboro, NC. Lab results showed that the seepage blanket dischargecwas on average 78% of the half-barrel meter discharge for flow rates between -50 and +60 cm day^{-1} in high-permeability sediments. Field results from July 2012 and March 2013 showed that mean specific discharge measured by the blankets was variable with respect to other methods. The ability of the blankets to isolate

groundwater was evaluated using field samples taken from blanket, stream, and 31-cm depth during July 2012 in West Bear Creek and analyzed for anions, CFC's, SF^6, dissolved gas, and Noble gas. Results showed that the blanket captured a mixture of groundwater and streamwater. The effect of the blankets on hyporheic flow was assessed during the March 2013 campaign, and results showed that the blankets can be used to manipulate hyporheic flow.

Introduction

Quantification of groundwater-surface water exchange has become increasingly important as the physical, chemical, and biological process understanding of the hyporheic zone has advanced, and there is increased recognition that groundwater and surface water are one resource. The most direct method to measure this water exchange, a seepage meter, was developed by Israelsen and Reeve [1944] and first used to measure groundwater inflow by Lee [1977]. These original seepage meters were a cut-off 55-gallon drum fitted with a port and flexible bag inserted into the sediment so that naturally discharging water is captured in the bag. The benefit of seepage meters, other than being the only direct discharge measurement device, is the spatial integration of discharge heterogeneity and the potential to collect flow-weighted spatially integrated samples from the devices. The basic design of the half-barrel seepage meter has been widely used to measure groundwater discharge in lakes and ponds [e.g., Lee, 1977; Shaw and Prepas, 1990b; Boyle, 1994; Rosenberry, 2000], streams and rivers [e.g., Libelo and MacIntyre, 1994; Landon et al., 2001; Rosenberry, 2008], and near-shore submarine settings [e.g., Cable et al., 1997; Burnett et al., 2001]. Decades of use and testing has revealed that

half-barrel seepage meters are subject to a number of potential errors [Murdoch and Kelly, 2003; Rosenberry and LaBaugh, 2008] although careful design, installation, measurement technique, and meter calibration [e.g., Rosenberry and Menheer, 2006] can provide reliable field results.

The seepage blankets presented here were designed for use in flowing water with the objective of advancing seepage meter design in this setting by minimizing potential sources of error. This was achieved by a) using an automated flow meter, b) reducing the perimeter to area ratio, c) minimizing the profile and obstruction to flowing water, d) using inserted metal edging to cut off shallow hyporheic flow, and e) providing a flexible medium across which pressure differences were minimized. The primary objective of the blankets was to isolate groundwater from streamwater, providing a representative sample of the exchange across the sediment-water interface and secondly to measure discharge.

Methods

Blanket Construction

A set of five low profile seepage blankets was installed across the width of a stream. The blankets were constructed from rubberized cloth (Hypalon©), providing a lightweight flexible device with a 71 x 107 cm footprint (0.76 m^2) and maximum height of 3.175-cm (1 ¼") (Fig. 2.1). The surface of the blanket coming into contact with the groundwater was covered in a stainless steel foil (Fig. 2.2) to limit contact of groundwater with noninert surfaces. The stainless steel foil was adhesive backed and trimmed to fit the contours of the blanket. A 1" PVC tee and flange was inserted into the top of the blanket to serve as a sampling and flow measurement port. Four-inch sections

of PVC ran along the ridgeline of the blanket providing structure to ensure that the blanket was not directly against the stream bottom, which might have inhibited water flow toward the outlet port. A gas release port (PVC plate and a rubber stopper) opposite the outlet port along the high point of the blanket allowed the operator to expel gases derived from the near stream sediment (exsolution or biogenic) from the blanket. Shallow hyporheic flow was blocked and the blanket was retained by 6" sections of stainless steel bar stock and 2" x 1" aluminum L. The stainless steel bar was drilled and countersunk and the aluminum L was tapped allowing the "edging" to attach to the blanket via machine screws. Holes punched in the rubber material allowed passage of the machine screw through the blanket, making a relatively plumb edge between rubber and metal edging. The five blankets were designed to be placed end to end and cover a 71-cm wide transect across the stream.

Dilution Flow Meters

Dilution flow meters (DFM) were designed and developed at the University of Utah for use with seepage blankets. The device was inspired by a similar technique used at Woods Hole Oceanographic Institute [Sholkovitz et al., 2003] based on the concept that the dilution of a tracer in a well-mixed fixed volume is directly proportional to the thru-flow (either inflow or outflow) in the given volume. Numerous adaptations of the seepage meter described in Sholkovitz et al. [2003] were made to reduce cost and improve reliability of measurements. Working in nonmarine systems was inherently easier and cheaper because salt can be used as a tracer, simplifying the detection system, and component corrosion was a minor issue. A polycarbonate box (Fig. 2.3a) was used as

both the mixing chamber and a framework to retain the other components. An electrical conductivity meter (Milwaukee MW301 Standard Portable Conductivity Meter) was the detection device and table salt was used as the tracer. The salt was injected into the chamber manually using a syringe, and a time series of EC measurements were made. The volume was mixed with a submersible inline centrifugal pump (Whale High Flow Inline 16 lpm 12 V d.c., prod # GP1692) that discharges through a perforated manifold within the mixing chamber. The purpose of a perforated manifold was primarily to limit the possible Bernoulli effects of the "jet" of water across the outlet from the mixing pump, resulting in "apparent flow" when the seepage meter was placed in a stagnant water body and also to aid in mixing and achieve more stable readings from the detection device. Two short sections of 1-inch PVC pipe on the inlet and outlet of the mixing chamber allowed attachment to the blanket and created a buffer volume inhibiting "back dilution" of streamwater into the chamber. The meters attached to the outlet port of the blankets (Fig 2.3b), measuring the water flux between the stream and the stream bottom covered by the blanket. Each blanket was outfitted with a complete dilution flow meter (Fig. 2.3c), and a long harness allowed discharge measurements to be made from the bank.

The concentration of a tracer (e.g., dyes, salts) in the mixing chamber follows an exponential dilution model [Sholkovtiz et al., 2003]. The data set needed to determine through-flow in the dilution flow meter was a time series of specific conductance of water inside the mixing chamber (C_t) and the background specific conductance of the groundwater (C_{int}). Following Sholkovtiz et al. [2003] the concentration of tracer in the mixing volume with respect to time (C_t) is described by the exponential dilution

equation:

$$C_t = C_{int}\, e^{-kt} \qquad (3)$$

where C_t is the specific conducatance in the mixing chamber at time t [μS cm^{-1}], C_{int} is the background specific conductance [μS cm^{-1}], k is the dilution rate constant [min^{-1}], and t is the elapsed time since injection of the tracer [min].

The dilution rate constant (k) is equal to the flow rate (Q, $mL\ min^{-1}$) divided by the internal volume (V, mL) of the mixing chamber (k = Q/V). The volume of the mixing chamber was not easily measured directly given the complex geometry of the mixing manifold, the specific conductance probe, and the circulation pump; thus the volumes of each of the five chambers were calibrated (Appendix D). In addition, the instantaneous flow rate (Q_{inst}, measured flow between any two specific conductance measurements) can be approximated with a first-order finite difference:

$$Q_{inst} = -V * \ln\left((C_t - C_{int})/(C_0 - C_{int})\right)/\Delta t \qquad (4)$$

where Q_{inst} is the instantaneous flow rate [mL min^{-1}], C_t is the specific conductance in the mixing chamber at a given time [μS cm^{-1}], C_0 is the starting specific conductance [μS cm^{-1}], and Δt is the elapsed time between measurements of C_0 and C_t [min].

The usefulness of calculating the flow (Q) by two methods (total dilution and finite steps) was that 1) the average of the instantaneous flows could be compared to the total dilution flow, 2) they can identify specific conductance measurements that were outliers, and 3) they provided contrasting measures of uncertainty associated with a given measurement. Appendix E displays example calculations and plots for measuring flow with the DFM. Comparison of DFM flow rates and bucket-gauged (graduated cylinder and stopwatch) pumping rates (Fig. 2.4) showed that the DFM was a robust measurement

device for flow rates between 20 mL min^{-1} and 200 mL min^{-1}, although it is expected that the dilution flow meter will function well at flows up to 500 mL min^{-1} as the mixing chamber was sufficiently large to handle higher flows.

Blanket Performance Evaluation

The performance of the seepage blanket was evaluated in a controlled laboratory environment (USGS Denver Federal Center) and in the field (West Bear Creek, North Carolina, USA). The performance was evaluated based on comparisons to discharge measurements and water samples collected from established methods, as detailed in the respective sections below.

Empirical Testing in USGS Seepage Tank

The seepage blankets were tested in a seepage tank at the U. S. Geological Survey Denver Federal Center, Lakewood, Colorado as detailed in Rosenberry and Menheer [2006]. The blanket discharge was compared to the controlled specific discharge in the tank and specific discharge measured by standard half-barrel seepage meters [Rosenberry, 2008]. The blanket discharge (i.e., the mean specific discharge captured by the blankets) was determined by dividing the DFM measured flow by the area of the blanket (0.76 m^2). Measurements with seepage blankets and standard half-barrel seepage meters were made with the seepage tank running over the full range of specific discharge rates achievable with the tank (-0.4 to 0.6 m day^{-1}). Complete results are presented in Appendix F. The measured specific discharge for the respective techniques is herein referred to as tank, blanket, or half-barrel discharge.

Blanket discharge was on average 39% of tank discharge for downward seepage and 40% of tank discharge for upward seepage (Table 2.1). The blanket discharge measurements were consistent for a given discharge rate with the mean coefficient of variation of 6.4% for all measurements, with a maximum of 14.4% for downward seepage at -0.47 m day^{-1} (n = 4), and 9.1% for upward seepage at 0.60 m day^{-1} (n = 5) (Appendix F). Standard half-barrel seepage meter measurements made across the same range of seepage rates show half-barrel discharge was 54% of tank discharge during downward seepage and 62% of tank discharge during upward seepage (Table 2.1). Similar to the blankets, the half-barrel discharge better matches the tank discharge during upward seepage. The average efficiency for the half-barrel seepage meters with 2 meters installed is 58%. Additional tests with 3 half-barrel meters were performed as detailed in Appendix F.

Blanket discharge was on average 92% of half-barrel discharge for downward seepage and 66% of half-barrel discharge for upward seepage (Table 2.1). The blanket discharge was on average 78% of the half-barrel discharge for flow rates between -0.4 and 0.6 m day^{-1}. The comparison of the blankets to the half barrel meters was a more valid means of measuring the efficiency of the blankets given the inefficiency of both seepage devices in the relatively high K (~100–150 m day^{-1}) sediments of the tank. The blankets were more efficient (measure closer to tank discharge) at lower flow rates, while the half-barrel meters are more efficient at higher flow rates. This suggested that the blankets were restricting higher flows (likely along the flow paths between the blanket and sediment and at the flow meter inlet/outlet) while the half-barrel meters had less resistance to flow. Additionally, the rectangular footprint of the blanket made

diversion of discharge flow paths and subsequent noncapture more likely than with the circular half-barrel. The blankets were designed to be deployed together across a transect, so flow path diversion was at a maximum with the single blanket installed alone. Given the size limitations of the seepage tank, we were unable to test more than one blanket along side each other, although we would expect the performance to be improved with additional blankets.

Field Implementation of Seepage Blankets at West Bear Creek, NC

The seepage blankets were deployed during two separate field campaigns, July 2012 and March 2013, on West Bear Creek near Goldsboro, NC. The blankets were installed adjacent to each other to form a transect across the width of the stream for a given location (Fig. 2.5). The sample naming convention followed the format WBC ###, with the three digit number indicating meters downstream from the tracer injection site. The injection site was located 1 km upstream of the North Beston Road bridge (35°21'31.01" N, 77°50'46.54" W, WGS84). The location along the transect was indicated by the relative position of the blankets when facing downstream (e.g., right bank, right, center, left, and left bank). In July 2012 the blankets were installed at three different transects (WBC 478,513, 521) providing groundwater discharge rates at all three and the full sample suite (as detailed in the Sample Suite section) at two of the transects (WBC 478, 513). For the March 2013 campaign the blankets were installed at a single transect (WBC 715) and five groundwater discharge measurements were made over a period of 3 days, and a single sample suite was collected. A transect of five Darcian method discharge measurements and samples (detailed below) were completed at the above transects with

the seepage blanket removed. In July 2012 Darcian measurements were made at a total of 39 locations along 8 transects clustered over a ~60 meter reach of stream (WBC 479 to 537). Additional locations (30 total along 6 transects) during the March 2013 campaign were spaced over the 2.7 km study reach. Standard diffusion samplers [Gardner and Solomon, 2009] and USGS minipoint samplers [Duff et al., 1998] were deployed along vertical transects with the blankets installed during March 2013 to determine the extent of hyporheic flow. Further detail is outlined in the respective sections below. The measured discharge from the blankets was evaluted by comparing results to the Darcian method (points), reach mass balance (RMB), and Flowtracker™ (velocity area method) measurements. Groundwater isolation was evaulated by comparing blanket samples to piezometer samples screened from 31–36 cm depth.

Darcian Measurement Method

North Carolina State University (NCSU) completed measurements of vertical hydraulic gradient (J [L L^{-1}]) and vertical hydraulic conductivity (K [L t^{-1}]) with the product equal to the specific discharge for a given point location. The Darcian method is also referred to as points in the following discussion. The vertical hydraulic gradient was measured by light-oil piezomanometer [Kennedy et al., 2007] and vertical hydraulic conductivity by falling-head permeability tests as described in Genereux et al. [2008]. The piezomanometer was screened from 31 to 36 cm depth and also used to collect groundwater samples. A full sample suite (as detailed in Sample Suite section) was collected from each point location.

Reach Mass Balance

A reach mass balance (RMB) was performed along the study reach using a conservative tracer (NaBr) to determine the groundwater inflow. The design of the injection, sample collection, and analysis followed the procedure of Kimball et al. [2004]. Details of the July 2012 reach mass balance are presented in Appendix G, while the March 2013 reach mass balance was analyzed by NCSU. Stream samples from both campaigns were analyzed at the U. S. Geological Survey Utah Water Science Center with ion chromatography. For the July 2012 campaign, two separate synoptic samples were collected along the reach. Given an average stream width of 7 meters and no observed surface water inflows, the interpreted groundwater discharge per 100 m section of reach based on bromide dilution is presented in Fig. 2.6. A mass balance was performed on bromide for the July 2012 campaign to determine the extent of hyporheic flow and bank storage. The mass balance analysis indicated that 81.4 +/- 1.9 kg of Br was injected into the stream and 75.1 +/- 10.4 kg was captured at 2700 meters downstream. The relatively larger uncertainty associated with the bromide mass at WBC 2700 was attributed to the change in stream stage over the duration of the test, and the difficulties of estimating the stream flow (see Appendix G for details). Given that there was not a statistically significant loss of bromide mass between the injection site and WBC 2700 in July 2012, we concluded that hyporheic and bank storage flow paths were completed (e.g., flow paths were short compared to test duration and bromide was returned back to the stream) and there were no unmeasured losses of streamwater along the reach.

Field Sample Suite Collected from Blankets and Points

A variety of samples were collected from the blankets with the goals of a) evaluate the "seal" of the blanket and efficacy of this device in isolating groundwater and streamwater, b) provide a basis for comparing the blanket sample collection method to an established stream bottom groundwater sampling method (e.g., points), and c) provide spatially- integrated flow-weighted samples for an ongoing study exploring spatial integration of groundwater transit times. The sample suite was collected from the blankets using a peristaltic pump (or otherwise noted) pumping at a rate less than the dilution flow meter measured discharge from a given blanket. The tubing for the peristaltic pump was fashioned from 1/8-inch copper tubing and a ~15-cm section of Viton rubber tubing for the pump head to operate on. The tee port on the blanket was fitted with a ~40-cm piece of 1-inch PVC tubing into which the pumping tubing was inserted. The sample suite was collected from the points by North Carolina State with a similarly configured peristaltic pump. Blanket pumping rates were kept at 80% of measured discharge from the blankets to limit streamwater being pulled into the blanket artificially. Table 2.2 outlines the sample, collection method, container, and analysis location for the blankets. The bromide sample would indicate the presence of surface water as the injected tracer was the only source of significant bromide in the system. Noble gases, which along with tritium provide the basis of $^{3}H/^{3}He$ dating, should be different in groundwater than surface water because of ^{3}He exchange with the atmosphere that occurs in streams. Similarly, CFC's and SF_6 that are used for groundwater dating readily exchange with the atmosphere in streams and thus should be different in groundwater than surface water. Dissolved gas (CO_2, N_2, O_2, CH_4), NO_3, and cation

samples inform the physical, chemical, and biological processes in the subsurface between 31-cm (piezometer depth) and the sediment-water interface. During the March 2013 campaign a time series of bromide samples were collected from the stream and blankets during the first arrival of bromide stream tracer. The goal of the bromide arrival time series was to discern the lag time of bromide arrival in the stream versus the blankets. USGS minipoint [Duff et al., 1998] vertical profile samples were collected prior to blanket installation, and upstream/downstream of blankets after installation, to determine the extent of natural hyporheic flow and the effect of the blanket on that flow. Lastly, a vertical transect of standard diffusion samplers for noble gases [Gardner and Solomon, 2009] were deployed beneath the blankets that would indicate the existence of hyporheic flow paths in the center of the blankets.

Results

July 2012

A summary for the July 2012 campaign is presented below with full details in Appendix H. Groundwater discharge was measured along three transects (WBC 478, 513, and 521) with the blankets. The specific discharge measurements from the three methods showed that the points agree reasonably well with the RMB, and the blankets were the outlier (Table 2.3). It should be noted that blankets results were not corrected with an efficiency factor, as is common with seepage meter discharge measurements, from the USGS Denver Federal Center because the sediments in the testing tank were not matched to field conditions.

Dissolved gas results showed a lower dissolved gas concentration for the more reactive gases in the samples collected by the blankets than the points (Table 2.4 and Fig.

2.7). The mean concentration of argon between blanket (0.51 mg L^{-1}) and point (0.56 mg L^{-1}) samples suggested that the discrepancy was not a blanket degasing sampling artifact, but rather natural processes between 31-cm depth and the sediment-water interface.

Noble gas results showed that the blankets were collecting representative samples (when compared to the points) for the conservative gases at a given transect (Table 2.5 and Fig. 2.7). Given the extended period of storage in the copper tube, the N_2 results should be interpreted cautiously as there was likely biological activity in the sample prior to analysis.

Results from bromide samples collected from the blankets showed that the blankets were capturing some streamwater. It is clear that the presence of bromide in the blankets at WBC 478 and WBC 513 was not solely a result of pumping as there was a strong bromide signal in the blankets prior to extended pumping. At WBC 478, the bromide samples were the first sample collected from the blanket, and no time series was collected. At WBC 513, the bromide samples were collected as the first, intermediate, and last sample from the blanket (except for an intermediate sample from the left position). Whether the presence of bromide indicated a leak, in which the seal was insufficient to exclude streamwater or capture of hyporheic flow, could not be evaluated with July 2012 data. However, the results from the March test discussed below suggested that the presence of bromide resulted from shallow hyporheic flow.

The CFC and SF_6 results have been corrected for the presence of streamwater in the blankets to determine the concentration of CFC and SF_6 in groundwater. This correction was done by mass balance of bromide and CFC/ SF_6. Since the bromide concentration in groundwater was below the analytical detection limit (0.01 mg L^{-1}), one can solve for the

amount of streamwater collected by a given blanket using the known concentration of bromide in the stream for a given transect and the flow rate from the blanket. With a measured stream concentration of CFC and SF_6 at each transect, the blanket sample CFC and SF_6 was corrected for presence of streamwater. A large measured variation in CFC concentration between the stream samples collected above and below the blanket transects creates some uncertainty in the blanket CFC correction. To capture the magnitude of the uncertainty, three separate corrected blanket CFC concentrations were determined. The best estimate made use of a linear regression between the two measured stream CFC concentrations to estimate the stream CFC at a given transect. The maximum and minimum blanket CFC concentrations indicated the upper and lower bounds of the corrected blanket CFC concentrations. Details of the correction calculations are in Appendix H.

The CFC and SF_6 comparison between blankets and points was done on a flow-weighted basis. For the blankets, the measured concentration was multiplied by the weighted flow (groundwater discharge for a given blanket divided by the total groundwater discharge across the transect) to arrive at the mass flow of CFC and SF_6 for a given blanket. The transect flow-weighted value was the sum of the mass flows from each blanket (Tables 2.6 and 2.7). Similarly, the points CFC and SF_6 were flow-weighted by assigning a representative area (10-cm^2) to the measured specific discharge, calculating the mass flow for each point, and taking the sum across the transect. The piston-flow recharge year associated with a given flow-weighted SF_6 concentration represents the year in which the water parcel was isolated (i.e., transported below the water table) in the recharge area, assuming the parcel was not mixed with other

groundwater along the flow path. This value is derived following the USGS SF_6 laboratory calculations [Busenberg and Plummer, 2010].

The flow-weighted uncorrected (for additions of streamwater) blanket CFC concentrations matched the flow-weighted point CFC concentrations reasonably well. Flow-weighted bromide corrected blanket CFC concentrations did not match the points, and further the bromide correction adjusted the blanket CFC concentration in the opposite direction. A likely cause was difficulties in measuring and subsequent estimations of stream CFC concentration. It is worth noting that CFC-12 results were not reported here due to indication of modest gas stripping, which also likely affected the CFC-11 and CFC-113 results. The CFC results, for this reason, were more problematic for dating of the water sample when taken alone. All samples from points and blankets showed stripping of CFC-12, suggesting that gas stripping took place prior to sampling by the blankets and points, and the results inform the groundwater sample isolation of the blankets.

The flow-weighted bromide corrected blanket SF_6 concentrations matched the flow-weighted point measurements reasonably well and yielded apparent recharge year ranging from 1986.5 to 1988.5 compared to 1981.5 to1985.5 for samples collected from points.

March 2013

A summary for the March 2013 campaign is presented below with full details in Appendix I. While the full sample suite was again collected in March 2013, the samples are pending analysis and results will not be presented here. Discharge results, bromide

arrival time series samples, USGS Minipoint samples, and standard diffusion sampler vertical profiles are presented here.

Comparison of blanket, point, and RMB-measured specific discharge is presented in Table 2.8, with the mean blanket specific discharge being the average value of five measurements made over 3 days. In contrast to the July 2012 discharge results, the blankets were measuring more discharge than the points. In addition, on March 11, 2013, Sontec Flowtracker™ stream discharge measurements were made at the injection site (i.e., WBC 0) and WBC 800, with the difference between the two measurements taken as gain from groundwater (no observed surface inflows). The Flowtracker™ measurements indicated a gain of 1.2 cubic feet per second over the 800 m reach, or 4.25E-05 $m^3 s^{-1}$ of inflow per meter of reach. The measured mean volumetric discharge from the blankets on March 11 at WBC 715 was 1497 mL min^{-1} and given the 71-cm width of the blanket parallel to stream flow, the blankets measured 3.51E-05 $m^3 s^{-1}$ of groundwater inflow per meter of reach. Taking the average stream width from the injection site to WBC 800 to be the width covered by the blankets (5.334 m), the mean specific discharge as measured by the Flowtracker™ and the blankets at WBC 715 was 0.69 and 0.57 m day^{-1}, respectively.

A time series of bromide samples were taken from the stream and the right and center blankets during the first arrival of injected bromide at WBC 715. Samples were collected every 20 minutes as a stream grab sample and withdrawn from blankets with a 60 mL syringe and extension tubing, from 16:30 to 18:30 on March 13, 2013 (Fig. 2.8). Over the 2-hour period, the stream bromide concentration was steady at 0.74 mg L^{-1} (s.d. = 0.035, n = 6), while samples in the blankets show a distinct transition from background bromide concentrations to mixed water with some component of streamwater (Fig. 2.8). During

sampling the relative consistency in bromide suggested that the pumping from the blanket did not alter the flow field or pull in additional streamwater through a leak (Table 2.9). In fact the bromide concentration decreased across the sampling period at each of the blankets. Also, the plateau bromide concentration in the center blanket during arrival (0.2 mg L^{-1}) was significantly lower than the initial bromide concentration during sampling (0.62 mg L^{-1}).

USGS Minipoint piezometers [Duff et al., 1998] were used to collect samples from a vertical profile in the sediment at 3-, 7-, 10-, 15-, 20-, and 25-cm depth below the sediment-water interface. A USGS minipoint profile was collected prior to tracer injection and blanket installation at WBC 715 in the center, left, and right locations (Fig. 2.9). The goal of the preblanket/tracer (PBT) profiles was to determine the extent of hyporheic flow prior to installation of the blankets with the idea that at least some of the dissolved ion concentrations would be different in groundwater than streamwater. After installation of the blankets and an extended equilibration period (>48 hours) USGS minipoint profiles were collected upstream and downstream of the right and center blankets (Fig. 2.10). With injected bromide in the stream, the extent and effect of blanket installation on hyporheic flow could be determined. An additional single minipoint piezometer was used to collect samples from beneath the right and center blankets at 10- and 20-cm depth (Table 2.10). A single minipoint was used for all samples collected and was installed at an angle from the downstream edge of the blanket.

USGS minipoint vertical profiles of pretracer, natural dissolved ion concentrations suggested minimal hyporheic flow (~5-cm) or no hyporheic flow prior to blanket installation. The presence of injected bromide stream tracer in the subsurface indicated

that the blankets induce hyporheic flow (at one location) to at least 10-cm depth; however, there is evidence that beneath the center of the blanket, no hyporheic flow was induced. This suggested that the blankets can be used to manipulate hyporheic flow and potentially be used to the investigators advantage depending on specific research objectives (such as collection of a spatially-integrated flow-weighted groundwater samples).

The preblanket/tracer profile (Fig. 2.9) from the center location showed changes in the fluoride and nitrate concentrations suggesting hyporheic flow paths less than 5-cm deep, although using nitrate as a hyporheic tracer can be problematic given nitrate transformations in the subsurface. The bromide, chloride, and sulfate did not show the same trend with groundwater concentrations being closer to streamwater concentrations, and any mixing of the two end members in the shallow sediment was undecipherable. The preblanket/tracer profile (Fig. 2.9) from the right and left locations did not show a clear trend in ion concentrations with respect to depth. The profile from the left and right location showed clearly different end member waters (except for bromide and chloride at the left and bromide, fluoride, and sulfate at the right), but there were no intermediary waters, which was interpreted as indicating no hyporheic flow for those locations. The shallow natural hyporheic flow in the center of the stream channel was likely associated with the increase in mean sediment grain size toward the center.

The upstream and downstream minipoint profile (Fig. 2.10) from the right location showed changes in ion concentrations consistent with induced hyporheic flow. It is interesting to note that the groundwater end member concentration of sulfate was nearly doubled from the preblanket/tracer (PBT) results. The upstream minipoint profile (Fig.

2.10) from the center location shows a similar trend to the PBT profile, suggesting no change to the system with the addition of a blanket. The fluoride, nitrate, and bromide concentrations suggested a hyporheic flow path up to 10-cm deep. Note that the stream concentration of bromide was significantly higher due to the tracer injection. The downstream minipoint profile showed groundwater analyte concentrations not trending toward the streamwater concentrations at shallower depths, suggesting no mixing and/or hyporheic flow. We reasoned that the blanket blocking streamwater from flowing into the sediment caused this. Samples collected by the single minipoint under the right and center blanket at 10- and 20-cm depth (Table 2.10) showed consistent concentrations of the ions between the two depths, and had background bromide concentrations. This suggested that the blankets were not driving deeper hyporheic flow paths.

Groundwater has a different helium isotope ratio than streamwater due to ingrowth of ^{3}He in groundwater from tritium (^{3}H) decay and exchange of ^{3}He with the atmosphere in streamwater. Samples for ^{3}He and other noble gases were collected by standard diffusion sampler [Gardner and Solomon, 2009] beneath the center of the blankets to examine the extent of surface water penetration and mixing with subsurface fluids (i.e., hyporheic flow). Results from standard diffusion samplers installed at 0-, 5-, 10-, 20-, and 30-cm depth below the center of the blankets showed no significant variation in the helium isotope ratio (R/R_a) (Fig. 2.11). The results from the diffusion samplers further confirmed the lack of deep hyporheic flow paths beneath the blankets. These samples were not datable given the lack of collected tritium, but the three transect profiles showed clear differences between the streamwater and all depths in the subsurface (Table 2.11).

Discussion

Lab and field results showed that absolute discharge measurements made with a seepage blanket were variable with respect to other methods (i.e., Darcian (points), reach mass balance, velocity-area (Flowtracker™)). Although it is a common method to use an efficiency correction factor in traditional seepage meter measurements [D. Rosenberry, personal communication, 2013], a correction factor was not used in the data presented here.

In the Denver federal Center seepage tank the blankets measured ~40% of the total flow thorough the sediment and measured ~78% of the flow measured by the half-barrel seepage meters. The testing completed at the Denver Federal Center was an extreme case because half-barrel meters have been previously shown to be up to 90% efficient in the same tank with different sediments (D. Rosenberry, personal communication, 2013), while during this test they were only capturing ~55% of the tank discharge. Furthermore, a single blanket was tested in the Denver seepage tank by itself, as opposed to a set of five designed to be used in the field. The increase in perimeter to area ratio of one blanket (0.046) from five blankets (0.031) could explain some of the blanket inefficiency. Additionally, we reasoned that the rectangular blanket footprint provides limited resistance to diversion of flow paths around the blanket (particularly around the corners of the blanket), as opposed to the circular half-barrel footprint. It should be noted that for both the blanket and half-barrel meter the efficiency compared to tank discharge was greatly improved at lower seepage rates. This suggested that in highly permeable sediments, even at low seepage rates (~10 cm day^{-1}), the restriction in flow caused by the device can significantly alter the measured seepage rate, as noted in previous research

[Rosenberry, 2008].

For the field component, the July 2012 campaign showed that the blankets were on average measuring less specific discharge (0.12 m day^{-1}) than the points (0.43 m day^{-1}) and the reach mass balance (0.38 m day^{-1}). In contrast, during the March 2013 campaign the blankets measured an average specific discharge of 0.5 m day^{-1}, which was similar to velocity-area measurements made along the same reach, while the points and reach mass balance measured significantly less specific discharge (0.31 and 0.33 m day^{-1}, respectively). It is unclear why the blankets measured more specific discharge than indicated by the points and reach mass balance during the March 2013 campaign, but spatial and temporal variations in discharge were likely to be factors.

Results from previous comparisons of specific discharge between Darcian and seepage meter methods [e.g., Kennedy et al., 2010] have shown that the absolute specific discharge measurements are not expected to agree. Measurements made by the dilution flow meter and subsequent blanket specific discharge had an approximate uncertainty of ± 20% (Appendix J), which was in line with the accuracy of other specific discharge measurement methods. It should be noted that accuracy of specific discharge measurements were improved (< ±7 % of expected) for dilution flow meter calculated flow rates above 100 mL min^{-1}. The accuracy might be further improved for the lower range of flow rates if a smaller mixing volume was used. All this suggests that the blankets as a groundwater discharge measurement device should be used with care and might provide reasonable results given calibration and testing of the blankets similar to procedures used for the half-barrel meter [e.g., Rosenberry and Menheer, 2006].

The presence of injected bromide in samples collected from the blankets suggests

that, even in low gradient streams such as West Bear Creek, there was some hyporheic flow. USGS minipoint profiles collected prior to blanket installation showed some natural hyporheic flow occurring in the center of the stream. The blankets are effectively capturing this hyporheic flow and furthermore might be used to manipulate the hyporheic flow. Thus, based on field data, seepage blankets showed promise as a sediment-water interface sampling device.

The July 2012 campaign showed a moderate amount of bromide in the blankets, although it is unclear whether this was a leak (direct connection of blanket interior to surface water) or hyporheic flow path capture. For the March 2013 campaign, bromide arrival time series samples showed a steady concentration in the stream of 0.74 mg L^{-1}, while samples from the blankets showed a clear transition from background bromide to mixed groundwater and streamwater with a bromide concentration of ~0.2 mg L^{-1}. This suggested that the blankets are not leaking, as there was some lag between bromide arrival in the stream and the blankets. The relatively short lag time (~40 min) to reach plateau in the blankets suggested that the hyporheic flow paths being captured by the blankets in West Bear Creek were short. Additionally, at the center location during March 2013, it was unclear why the first sample collected has a much higher bromide concentration (0.62 mg L^{-1}) than the plateau bromide concentration during arrival (~0.2 mg L^{-1}). While the July 2012 campaign sampling might have pulled some streamwater into the blanket during pumping, results from the March 2013 campaign sampling showed this is clearly not the case, as the bromide concentration from all the blankets decreased somewhat over the course of sampling in March 2013. Overall, the experiment shows that careful sampling of the blankets can provide representative samples of the

sediment-water interface flux.

The July 2012 points and blankets noble gases comparison showed that the blankets were capturing the same groundwater as points without degassing the sample. Using the blanket as a flow-weighted spatially integrated medium scale-sampling device for dating of water was possible, but it was less practical given the need for a conservative stream tracer and subsequent corrections. The blankets should be viewed as a separate type of sampling device from more traditional groundwater sampling. The July 2012 results for reactive gases and dissolved ions showed that the blankets can effectively capture the sediment-water interface fluxes, and furthermore the samples can be used to document transformations of the reactive species in the near surface sediment. Sampling both "deep" groundwater with piezometers and the sediment-water interface flux with blankets could be very informative in regards to hyporheic processes.

Stream bottom vertical profiles suggested that the seepage blankets have a significant effect on hyporheic flow. March 2013 results from USGS minipoint profiles collected prior to blanket installation showed some natural hyporheic flow occurring in the center of the stream, while the left and right locations showed no hyporheic flow. Given the presence of finer grain sediments along the banks of the stream, that transition to medium grain sands toward the center, the spatial variance in hyporheic flow was likely controlled by the hydraulic conductivity of the stream bottom. Installation of the seepage blanket induced ~10-cm deep hyporheic flow at the right location (both upstream and downstream), while the center blanket hyporheic flow was unaltered at the upstream location and completely cutoff at the downstream location. Given the lack of variation at the upstream center blanket location, we suggest that streambed disturbance rather than

alteration of stream flow induced hyporheic flow at the right location. During installation of the blankets along the edges of the stream, pushing the blankets down through thick layers (5–10 cm) of loosely consolidated fine grain sediments was unavoidable. Much of the sediment around the blanket was transported away, reducing the depth of fine grain sediments around the edges of the blankets and thus altering vertical hydraulic conductivity. Turbid water from the interior of the blanket was observed to be flushing out of the port for 15–20 minutes after installation, suggesting the depth of interior fine grain sediments was reduced as well. Furthermore, single minipoint samples and standard diffusion samplers from beneath the center of the blankets showed little to no variation with depth, indicating that the blankets cut off hyporheic flow over the footprint of the blankets. From the results regarding depth of induced hyporheic flow, it is prudent to have continuous edging if the goal is to exclude induced hyporheic flow from the blanket sample. Additionally, for a low gradient sandy bottom shallow stream, the edging should be inserted > 10-cm depth.

The vertical profile results from March 2013 suggested that the blankets can be used to manipulate hyporheic flow. The blankets could be used to induce shallow hyporheic flow, capture the natural flow paths for quantification of the sediment-water interface flux, or cut off naturally occurring hyporheic flow. We posit that a narrow (along the length of the stream) seepage collection device would have minimal effect on hyporheic flow, while a wide device sealed against the streambed would be effective in cutting off most, if not all, hyporheic flow. The narrow blanket configuration would be a good option for investigation of shallow sediment processes and nutrient fluxes, while a wide blanket would provide an ideal location for deployment of diffusion samplers for

collection of dissolved gases. Alternatively, the use of a wide blanket (that cuts off streamwater penetration) over the top of a narrow blanket (that captures groundwater inflows) would be a useful configuration for collecting spatially integrated flow-weighted groundwater samples for dating and determination of mean transit times.

Conclusion

Seepage blankets can be used to quantify groundwater discharge and were an effective sample collection device, capturing the water-sediment interface exchange. The use of a dilution flow meter allowed semi-automated discharge measurements from the blankets that were relatively precise, repeatable, and have reasonable levels of uncertainty. Raw groundwater specific discharge results from the blankets did not match Darcian and reach mass balance derived specific discharge, which is in agreement with previous studies comparing Darcian methods to uncalibrated seepage meters [e.g., Kennedy et al., 2010]. The blanket discharge result from this study could be improved with calibration and use of a correction factor, as is common practice for seepage meter measurements [Rosenberry and Menheer, 2006]. Lab results show the low-profile flexible design of the blankets did not show significant improvement over traditional seepage meters for groundwater discharge quantification in standing water. A comparison between seepage blankets and meters in flowing water was not conducted in this study, but field results (ion concentration vertical profiles) suggest that the blankets limit the disturbance to the stream flow field.

The seepage blanket has displayed utility as a sediment-water interface sampling device. Samples collected from blankets and piezometer gave relatively similar results for

the nonreactive analytes, suggesting the blankets captured the same groundwater sampled at 31-cm depth. Comparison of reactive species results between blanket and piezometer samples showed that shallow subsurface processes (physical, chemical, and biological) might be reasonably quantified with the blankets. Samples collected from the blankets are clearly a mixture of streamwater and groundwater, as would be expected in a stream with hyporheic exchange, and can be used to quantify sediment-water interface fluxes. Results from vertical profiles in the stream bottom show that the blanket might be used to manipulate hyporheic flow. Streamwater penetration into sediments can be amplified or cutoff depending on the specific goals of the study. Further, we suggest that the blanket can be designed to minimize alteration of the natural system, potentially allowing quantification of unmanipulated groundwater-surface water exchanges.

References

Boyle, D. R. (1994), Design and seepage meter for measuring groundwater fluxes in the nonlittoral zones of lakes—Evaluation in a boreal forest lake, *Limnol. Oceanogr., 39*, 670–681.

Burnett, W. C., M. Taniguchi, and J. Oberdorfer (2001). Measurement and significance of the direct discharge of groundwater into the coastal zone, *J. Sea Res.*, *46*, 109–116.

Busenberg E., and L. N. Plummer (2010), SF6 results sheet and piston flow recharge year, U. S. Geological Survey, Reston VA.

Cable, J. E., W. C. Burnett, J. P. Chanton, D. R. Corbett, and P. H. Cable (1997), Field evaluation of seepage meters in the coastal marine environment, *Est., Coastl. Shelf Sci., 45*, 367–375.

Duff, J. H., F. Murphy, C. C. Fuller, F. J. Triska, J. W. Harvey, and A. P. Jackman (1998), A mini drivepoint sampler for measuring pore water solute concentrations in the hyporheic zone of sand-bottom streams, *Limnol. Oceanogr., 43*, 1378–1383.

Gardner, P., and D. K. Solomon (2009), An advanced diffusion sampler for the determination of dissolved gas concentrations, *Water Resour. Res., 45*, W06423,

doi:10.1029/2008WR007399

Genereux, D. P., S. Leahy, H. Mitasova, C. D. Kennedy, and D. R. Corbett (2008), Spatial and temporal variability of streambed hydraulic conductivity in West Bear Creek, North Carolina, USA, *J. Hydro., 358*, 332–353, doi:10.1016/j.jhydrol.2008.06.017

Israelsen, O. W., and R. C. Reeve (1944), Canal lining experiments in the delta area, Utah, *Utah Agricultural Experiment Station Technical Bulletin 313*, Utah State Agricultural College, Logan, UT.

Kennedy, C. D., D. P. Genereux, D. R. Corbett, and H. Mitasova (2007), Design of a light-oil piezomanometer for measurement of hydraulic head differences and collection of groundwater samples, *Water Resour. Res., 43*, W09501, doi:10.1029/2007WR005904.

Kennedy, C. D., L. C. Murdoch, D. P. Genereux, D. R. Corbett, K. Stone, P. Pham, and H. Mitasova (2010), Comparison of Darcian flux calculations and seepage meter measurements in a sandy streambed in North Carolina, United States, *Water Resour. Res., 46*, W09501, doi:10.1029/2009WR008342.

Kimball, B. A., R. L. Runkel, T. E. Cleasby, and D. A. Nimick (2004), Quantification of metal loading by tracer injection and synoptic sampling, 1997–98, *U.S. Geological Survey Professional paper 1652-D6*, In *Integrated Investigations of Environmental Effects of Historical Mining in the Basin and Boulder Mining Districts, Boulder River Watershed, Jefferson County, Montana*, edited by D. A. Nimick, S. E. Church, and S. E. Finger, U. S. Geological Survey, Reston, VA.

Landon, M. K., D. L. Rus, and F. E. Harvey (2001), Comparison of instream methods for measuring hydraulic conductivity in sandy streambeds, *Ground Water, 39*, 870–885.

Lee, D. R. (1977), A device for measuring seepage flux in lakes and estuaries, *Limnol. Oceanogr.*, *22*.

Libelo, E. L., and W. G. MacIntyre (1994), Effects of surface- water movement on seepage-meter measurements of flow through the sediment-water interface, *App. Hydrogeo., 2*, 49–54.

Murdoch, L. C., and S. E. Kelly (2003), Factors affecting the performance of conventional seepage meters, *Water Resour. Res., 39*, 1163–1180.

Rosenberry, D. O. (2000), Unsaturated-zone wedge beneath a large, natural lake, *Water Resour. Res., 36*, 3401–3409.

Rosenberry, D. O. (2008), A seepage meter designed for use in flowing water, *J. Hydro.*, 359, 118–130.

Rosenberry, D. O., and J. W. LaBaugh (2008), Field techniques for estimating water

fluxes between surface water and ground water, *Techniques and Methods 4–D2*, 128 pp., U.S. Geological Survey, Reston, VA.

Rosenberry, D. O. and M. A. Menheer (2006), A system for calibrating seepage meters used to measure flow between ground water and surface water, *Scientific Investigations Report 2006-5053*, 21pp., U.S. Geological Survey, Reston, VA.

Shaw, R. D., and E. E. Prepas (1990). Groundwater-lake interactions: II. Nearshore seepage patterns and the contribution of ground water to lakes in central Alberta. *J. Hydro.*, *119*, 121–136.

Sholkovitz, E., C. Herbold, and M. Charette (2003), An automated dye-dilution based seepage meter for the time-series measurement of submarine groundwater discharge, *Limnol. Oceanogr.: Methods,1*, 16–28.

Figure 2.1. Seepage blanket showing rubber material construction, outlet port, and metal edging.

Figure 2.2. Photo displaying stainless steel foil bottom of the seepage blanket. Author for scale.

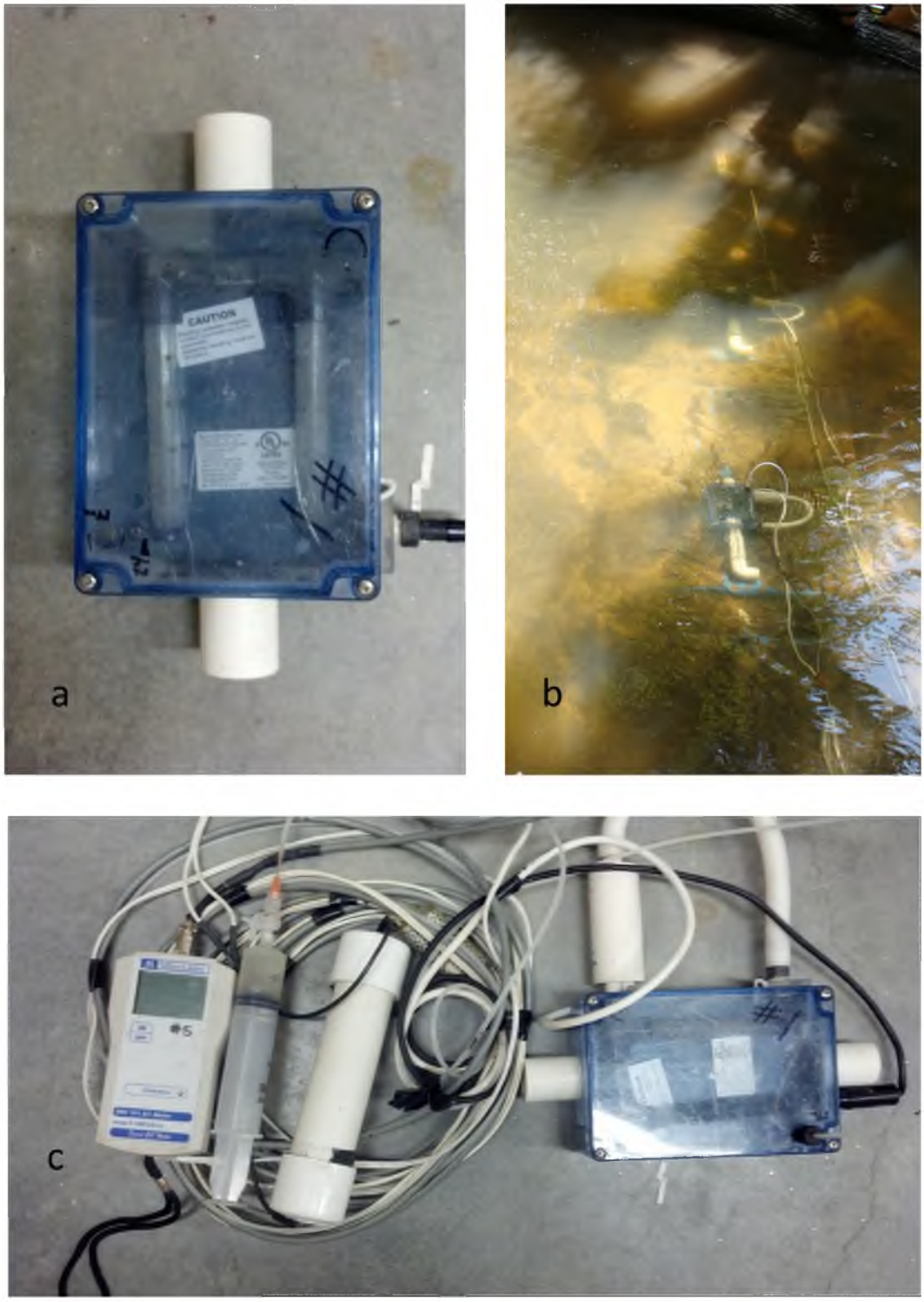

Figure 2.3. Dilution flow meter. a) close-up of mixing chamber and manifold, b) deployed with blanket in the field, c) the complete flow meter with EC probe and readout, syringe, battery pack, circulation pump, and mixing chamber.

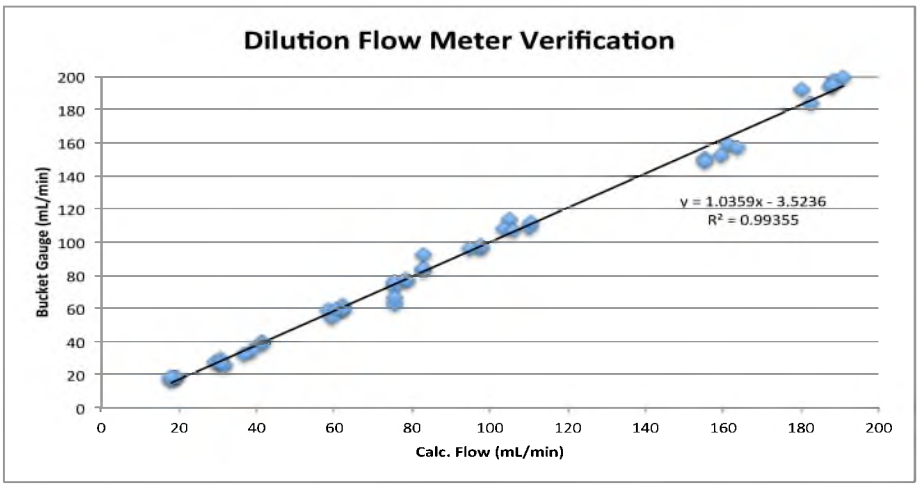

Figure 2.4. Plot of bucket gauge flow rates against dilution flow meter calculated flow rates.

Figure 2.5. Photo of blankets installed lengthwise along a transect at West Bear Creek. Note the near complete coverage of the stream bottom across the transect by the blankets.

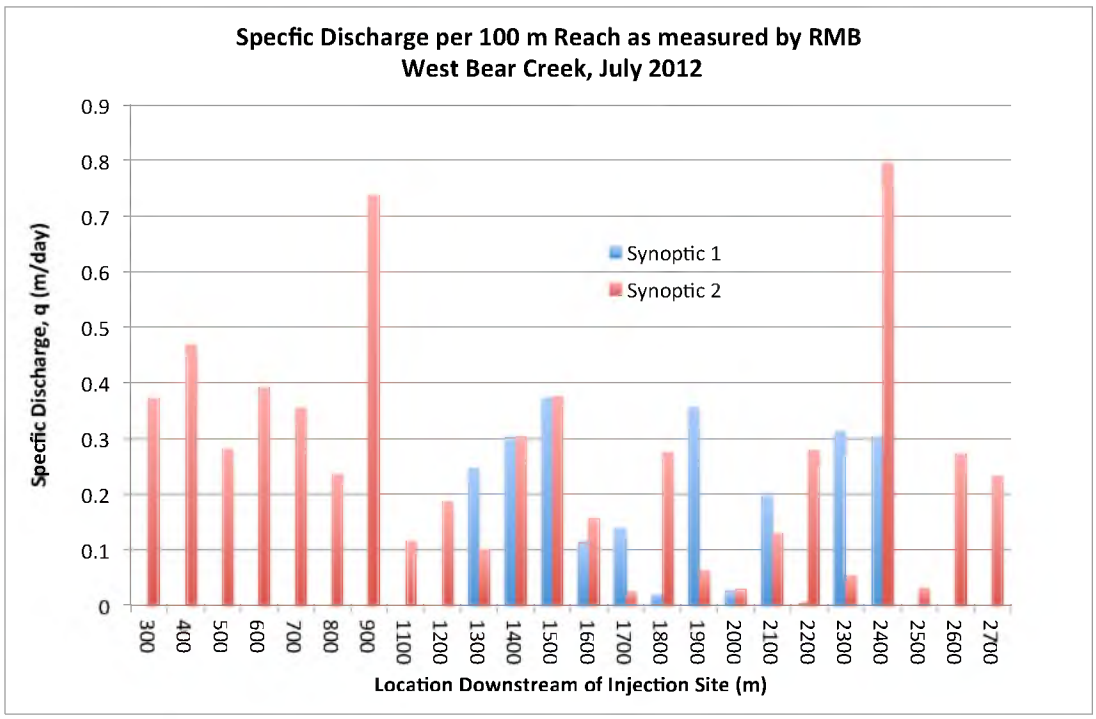

Figure 2.6. Interpreted specific discharge for 100-meter sections of stream as determined by reach mass balance from July 2012, West Bear Creek. An average stream width of 7 meters was used in the calculation.

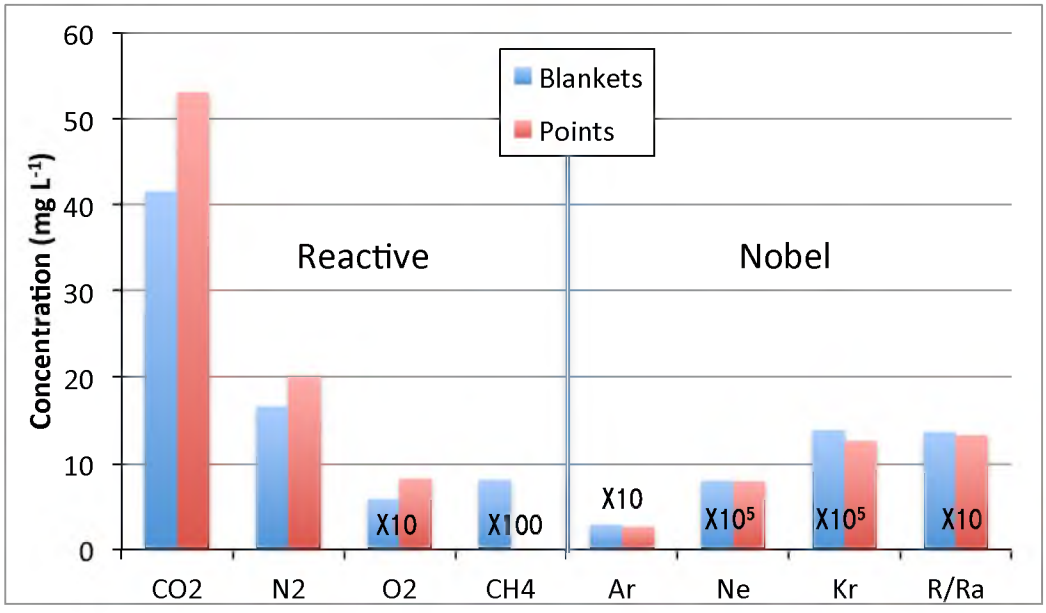

Figure 2.7. Dissolved gas concentrations from blankets and points for a representative sample from West Bear Creek.

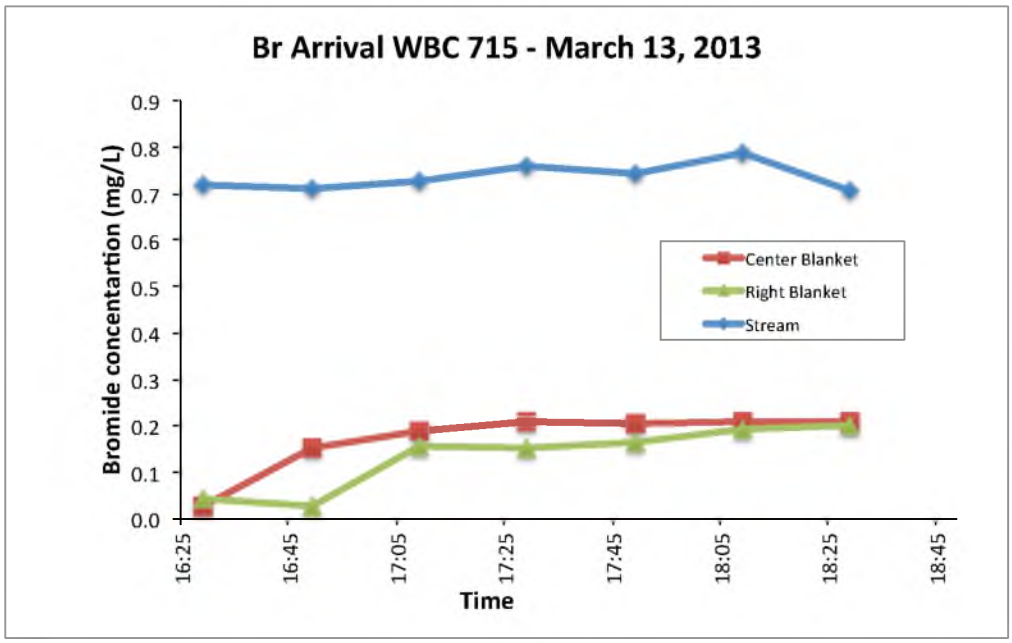

Figure 2.8. Injected bromide arrival at WBC 715 for the right blanket, center blanket, and stream in West Bear Creek on March 13, 2013.

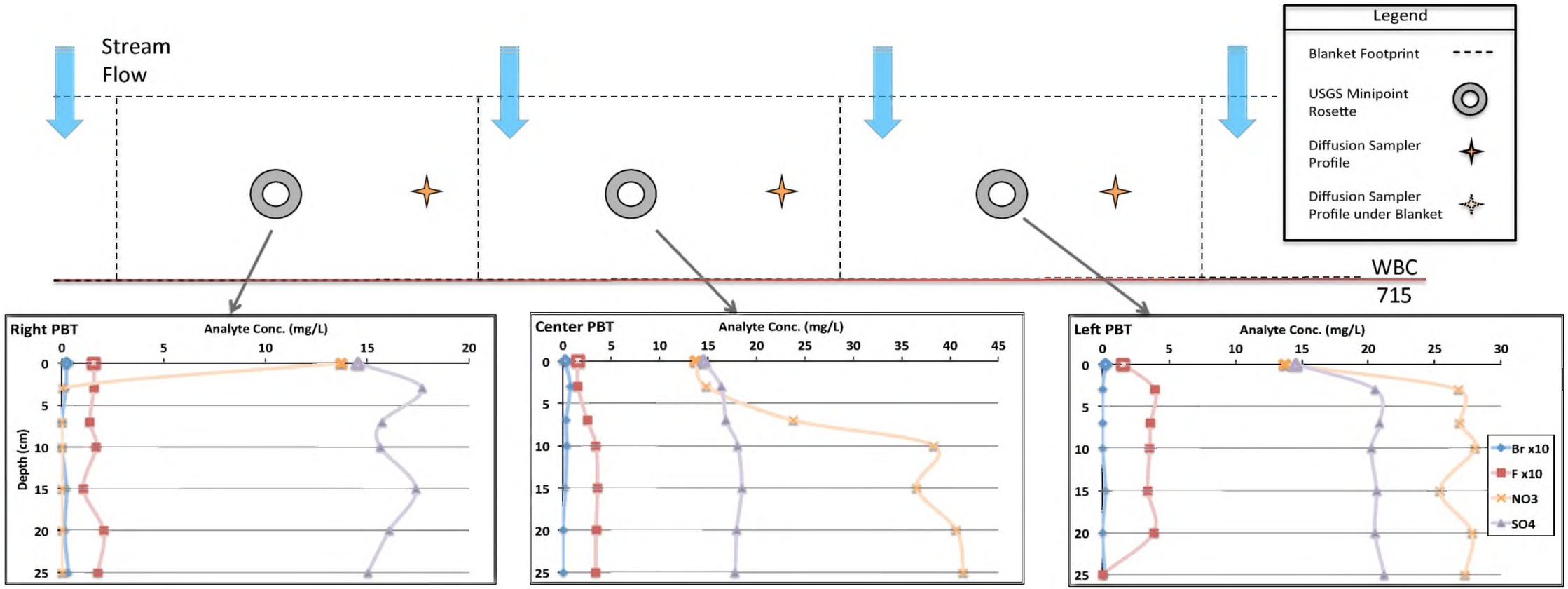

Figure 2.9. Pre-Blanket/Tracer USGS minipoint vertical profiles from the left, right, and center locations at WBC 715 on West Bear Creek, NC in March 2013. Open symbol (0 cm) indicates surface water sample.

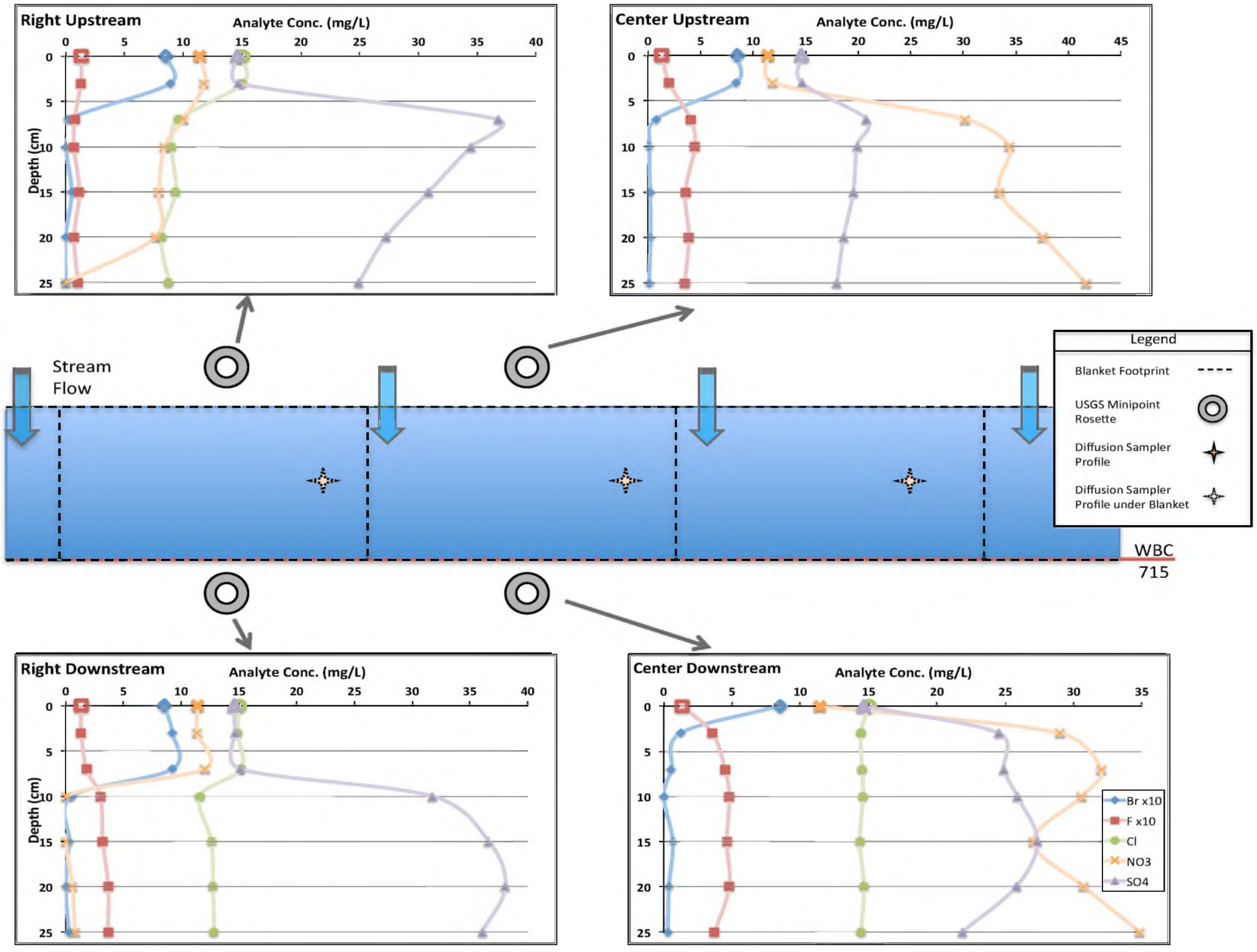

Figure 2.10. USGS minipoint vertical profiles from upstream and downstream of the right and left blankets at WBC 715 on West Bear Creek, NC in March 2013. Open symbol (0 cm) indicates surface water sample. The bromide tracer in the stream penetrated to less than 10 cm suggesting the existence of only shallow hyporheic flow paths.

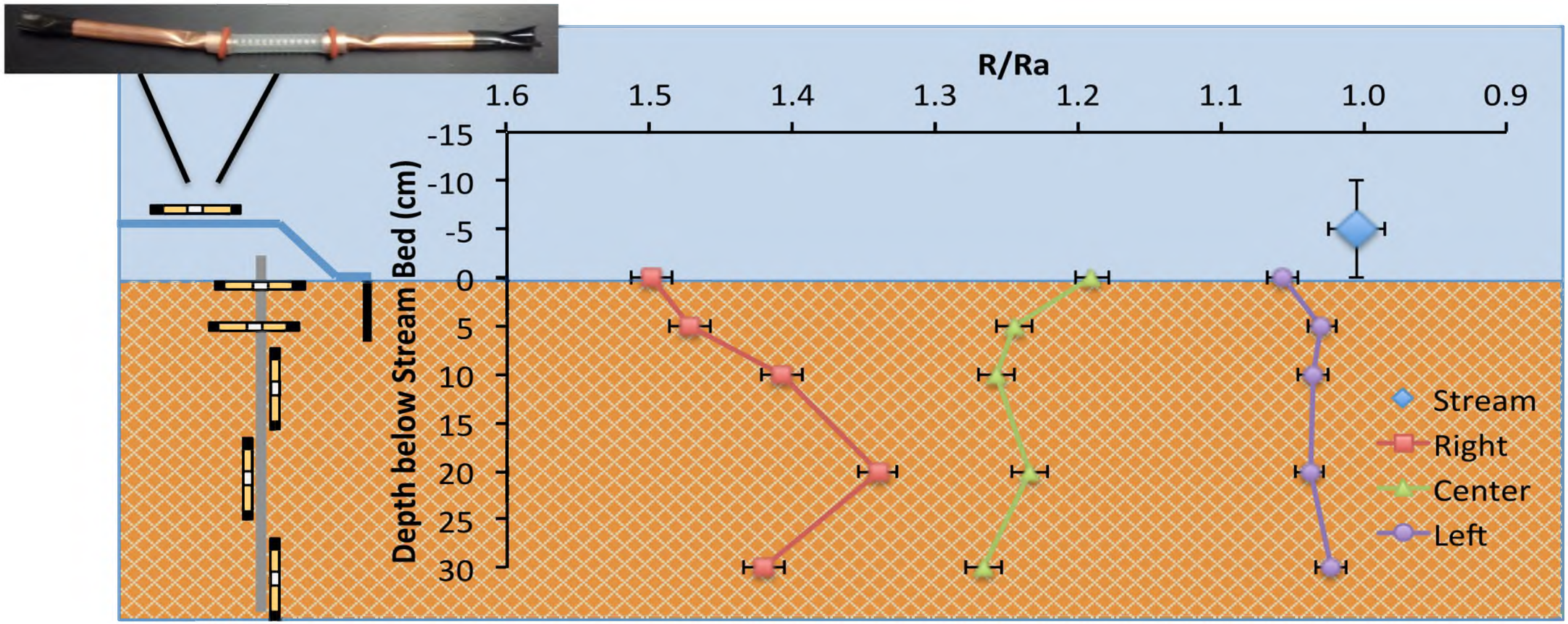

Figure 2.11. Schematic of standard diffusion samplers deployed beneath the center of the blankets for the respective locations at WBC 715, West Bear Creek, NC in March 2013. The helium isotope ratio (R/R_a) is plotted for the respective transect locations and shows clear difference from the stream value. Error bars show 2% uncertainty, which is a maximum value for the analysis.

Table 2.1. Tank, blanket, and half-barrel specific discharge from Denver Federal Center seepage tank. Tank/Blanket is the ratio of tank discharge to the blankets, Tank/Half-barrel is the ratio of tank discharge to half-barrel seepage meters, and Blanket/Half-barrel is the ratio of blanket discharge to half-barrel seepage meters.

Tank Discharge (m day^{-1})	Blanket Discharge (m day^{-1})	Half-barrel Discharge (m day^{-1})	Tank/ Blanket	Tank/ Half-barrel	Blanket/ Half-barrel
-0.1	-0.05	-0.03	0.5	0.31	1.62
-0.2	-0.08	-0.11	0.4	0.55	0.73
-0.34		-0.21		0.62	
-0.47	-0.13	-0.31	0.28	0.67	0.42
		Mean	0.39	0.54	0.92
0.1	0.05	0.06	0.5	0.59	0.86
0.2	0.09	0.11	0.43	0.57	0.76
0.4	0.14	0.24	0.35	0.62	0.59
0.6	0.19	0.41	0.32	0.72	0.45
		Mean	0.4	0.62	0.66

Table 2.2. Water samples, collection method, vessel, and analysis location for field blanket and point samples from West Bear Creek.

Sample	Collection Method	Vessel	Analysis Location
Bromide	Peristaltic Pump	20 mL Scintillation Vile	U of U[1], USGS UTWSC[2]
Noble Gases	Check Valve/ Syringe Manifold	Cu Tube	U of U Noble Gas Lab[1]
Tritium	Peristaltic Pump	0.5 L HDPE Bottle	U of U Noble Gas Lab[1]
SF^6	Peristaltic Pump	2 L Brown Glass	USGS SF6 Lab[3]
CFC	Peristaltic Pump	100 ml glass bottle	USGS CFC Lab[3]
Dissolved Gas	Peristaltic Pump	250 mL glass bottle w/ stopper	USGS Dissolved Gas Lab[3]
NO3	Peristaltic Pump	20 mL Scintillation Vile	NCSU[4]
Cations	Peristaltic Pump	20 mL Scintillation Vile	NCSU[4]
Silica	Peristaltic Pump	20 mL Scintillation Vile	NCSU[4]

[1] University of Utah, Salt Lake City, UT; [2] U.S. Geological Survey, Utah Water Science Center, West Valley City, UT; [3] U.S. Geological Survey, Reston, VA; [4] North Carolina State University, Raleigh, NC.

Table 2.3. Mean specific discharges for blankets, points, and reach mass balance (RMB) for West Bear Creek in July 2012. Units are m day^{-1}.

Location	Blankets (n = 5)	Points (n = 5)	RMB*
521	0.04	0.05	N.A.
513	0.11	0.45	N.A.
478	0.22	0.79	N.A.
Mean	0.12	0.43	0.38

* The mean RMB discharge is calculated by dividing the average gain (m^3 day^{-1}) from WBC 400 to WBC 600 by the average stream width (7 m) and the distance between measurement points (200 m).

Table 2.4. Dissolved gas results from USGS Dissolved Gas Lab for blanket and point samples from West Bear Creek in July 2012.

Transect	Method	Mean Concentration (mg L^{-1})				
		CO_2	N_2	O_2	Ar	CH_4
478	Blankets	41.53	16.57	0.58	0.51	0.08
	Points	53.02	20.01	0.82	0.56	0.001
513	Blankets	45.67	16.27	0.41	0.51	0.03
	Points	64.05	19.10	1.01	0.57	0.01

Table 2.5. Noble gas results from the University of Utah Dissolved Noble Gas Lab for blanket (Blkt) and point (Pt) samples from West Bear Creek in July 2012.

Transect	Method	Mean Concentration (mg L^{-1})						R/Ra	Tritium (TU)
		N_2	Ar	Ne	Kr	Xe	^4He		
478	Blkt	7.96	0.28	7.96E-05	1.38E-04	3.05E-05	3.19E-05	1.36	2.12
	Pt	7.03	0.26	7.85E-05	1.26E-04	1.20E-05	3.08E-05	1.32	2.96
513	Blkt	7.45	0.29	7.86E-05	1.54E-04	1.12E-05	3.60E-05	1.26	3.05
	Pt	8.26	0.29	8.55E-05	1.42E-04	3.02E-05	3.47E-05	1.1	3.44

Table 2.6. Transect flow-weighted CFC concentrations of blankets, bromide corrected blankets, and points from West Bear Creek in July 2012. Units are pmol kg^{-1}.

Transect	Uncorrected Blankets		Corrected Blankets						Points	
			Best Est.	Max	Min	Best Est.	Max	Min		
	CFC-11	CFC-113	CFC-11			CFC-113			CFC-11	CFC-113
513	1.618	0.117	1.360	1.368	1.344	0.073	0.075	0.068	1.542	0.151
478	1.463	0.086	1.516	1.534	1.516	0.066	0.70	0.066	1.038	0.117

Table 2.7. Transect flow-weighted SF_6 concentrations and piston-flow mean apparent recharge year from blankets, bromide corrected blankets, and points from West Bear Creek in July 2012. SF_6 concentrations are in units of pptv and have been corrected for excess air.

Transect	Uncorrected Blankets		Corrected Blankets		Points	
	SF_6	Recharge Year	SF_6	Recharge Year	SF_6	Recharge Year
513	2.97	1992.5	1.76	1986.5	1.55	1985.5
478	2.95	1992.5	2.05	1988.5	1.04	1981.5

Table 2.8. Mean specific discharge as measured by points, uncorrected blankets, and reach mass balance (RMB) from West Bear Creek in March 2013.

Transect	Location	Uncorrected Blankets n = 5	Points n = 1	RMB
715	RB	0.61	0.13	N.A.
	R	0.65	0.14	N.A.
	C	0.64	0.74	N.A.
	L	0.59	0.14	N.A.
	LB	0.01	0.38	N.A.
Mean		0.5	0.31	0.33

Table 2.9. Bromide concentration from blanket samples at WBC 715 on West Bear Creek in March 2013.

Location	Time	Bromide (mg L^{-1})
LU	13:34	0.4851
	15:10	0.3631
CU	11:20	0.6232
	13:15	0.4575
RU	11:00	0.2599
	13:16	0.2197
RBU	13:40	0.7762
	14:09	0.6726

Table 2.10. Dissolved ion concentrations from single minipoint samples beneath the right and center blankets at WBC 715, West Bear Creek in March 2013.

Location	Depth	Concentration in mg L^{-1}				
		F	CL	Br	NO_3	SO_4
R	10	0.35	14.07	0.033	28.33	20.59
	20	0.35	14.43	0.030	29.15	20.58
C	10	0.09	5.85	0.023	0	17.52
	20	0.07	7.93	0.032	0	21.71

Table 2.11. Noble gas concentrations from standard diffusion sampler vertical profiles beneath center of blanket at the respective locations at WBC 715, West Bear Creek in March 2013.

Location	Depth (cm)	Concentrations in ccSTP cc^{-1}					
		^{3}He	^{4}He	Ne	Ar	Kr	Xe
Stream		7.45E-12	5.31E-06	1.70E-05	9.69E-03	1.74E-06	6.39E-07
Right	0	1.13E-11	5.39E-06	1.44E-05	8.78E-03	1.05E-06	8.23E-08
	5	1.11E-11	5.41E-06	1.56E-05	8.62E-03	1.05E-06	4.47E-08
	10	1.08E-11	5.49E-06	1.49E-05	9.17E-03	1.14E-06	4.13E-08
	20	1.09E-11	5.81E-06	1.54E-05	9.78E-03	1.17E-06	6.27E-08
	30	1.11E-11	5.62E-06	1.44E-05	9.19E-03	1.18E-06	7.52E-08
Center	0	9.35E-12	5.63E-06	1.86E-05	9.40E-03	1.12E-06	7.95E-08
	5	9.60E-12	5.53E-06	1.85E-05	9.45E-03	1.08E-06	7.86E-08
	10	9.72E-12	5.54E-06	1.85E-05	9.30E-03	1.12E-06	7.99E-08
	20	9.47E-12	5.51E-06	1.82E-05	9.46E-03	1.13E-06	8.00E-08
	30	9.61E-12	5.45E-06	1.83E-05	9.60E-03	1.18E-06	8.23E-08
Left	0	9.16E-12	6.23E-06	2.07E-05	1.01E-02	1.20E-06	8.44E-08
	5	8.79E-12	6.13E-06	1.91E-05	1.00E-02	1.04E-06	8.19E-08
	10	8.83E-12	6.13E-06	2.16E-05	9.88E-03	1.24E-06	8.30E-08
	20	9.16E-12	6.34E-06	2.07E-05	1.02E-02	1.12E-06	8.42E-08
	30	9.08E-12	6.39E-06	2.11E-05	9.78E-03	1.21E-06	8.21E-08

THESIS CONCLUSION

The thin-walled Shelby tube can be used to measure specific discharge (q) and hydraulic conductivity (K) in locations where the groundwater-surface water exchange is of interest. Both lab and field results show that the Shelby tube reliably reproduced q and K as measured by established methods. The advantages of the Shelby tube are the direct measurement of q, the measurement of K is conducted in the same sediment as the q measurement, there is minimal disturbance to the system (e.g., sediment and surfacewater flow), the measurement is a relatively fast and easy compared to established methods, and the equipment and preparation needed for fieldwork are greatly simplified. The Shelby tube could not accurately measure very low flows (< 5 cm day^{-1}), and the analysis could be nonunique in some extreme cases (e.g., high K with low q). Additionally, the Shelby tube had greater variability when measuring q and K in downward seepage conditions, although there is not a theoretical basis that would explain this observation. The use of a simple amplifier with the Shelby tube reliably reproduced measured q and K while reducing the time to complete a measurement and the uncertainty associated with a given measurement. Although some variations between calibrated and physically measured amplification factors were observed, the physical amplification factor (i.e., ratio of areas) is recommended.

Seepage blankets can be used to quantify groundwater discharge and were an effective sample collection device, capturing the water-sediment interface exchange. This

study indicated that the blankets had the potential to be an accurate and reliable groundwater discharge measurement device but require calibration and use of a correction factor. The use of a dilution flow meter allowed semi-automated discharge measurements that are relatively precise, repeatable, and have reasonable levels of uncertainty. The practice of seepage meter calibration (such as performed in Rosenberry and Menheer, 2006) was not conducted in this study; thus no correction factor was applied to the blanket specific discharge results. Raw groundwater specific discharge results from the blankets did not match Darcian and reach mass balance derived specific discharge, which was in agreement with previous studies comparing Darcian methods to seepage meters (e.g., Kennedy et al., 2010). The low-profile flexible design of the blankets did not show significant improvement over traditional seepage meters in regards to groundwater discharge quantification. On the other hand, the seepage blanket had significant potential utility as a sediment-water interface sampling device. Samples collected from blankets and piezometer (31-cm depth) gave relatively similar results for the nonreactive analytes, suggesting the blankets were capturing the same groundwater as being sampled at depth. Comparison of reactive species results between blanket and piezometer samples showed that shallow subsurface processes (physical, chemical, and biological) might be reasonably quantified with the blankets. Samples collected from the blankets were clearly a mixture of streamwater and groundwater, as would be expected in a stream with hyporheic exchange, and can be used to quantify sediment-water interface fluxes. Results from vertical profiles in the stream bottom showed that the blanket might be used to manipulate hyporheic flow. Streamwater penetration into sediments can be amplified or cut off depending on the specific goals of the study. Further, we suggest that

the blanket can be designed to minimize alteration of the natural system, potentially allowing quantification of minimally or unmanipulated groundwater-surface water exchanges.

APPENDIX A

DERIVATION OF DISCHARGE AND HYDRAULIC CONDUCTIVITY EQUATIONS

Consider a gaining stream reach with a Shelby tube installed to a depth of L below the stream bottom. A riser pipe is installed with a cross-sectional area of a, while the Shelby tube has a cross-sectional area of A. The head at the bottom of the Shelby tube is h0, which is also the head inside the Shelby tube when it is allowed to reach equilibrium. The head in the stream (above the stream bottom) is hs.

To start the test, the water level inside the riser pipe is lowered (using a syringe) such that the head is h1 and corresponds to time = 0. The water level (h(t)) then rises as a function of time. The h(t) will pass through hs and asymptotically approach h0.

Discharge

The following derivation starts with the basic falling head equation [Todd, 1959].

The flow of water (Q) inside the tube is given by Darcy's Law as

$$Q = -\frac{KA(h - h_0)}{L}$$

where K is hydraulic conductivity [L/t], A is the cross sectional area of the tube [L^2], h_0

is the total head in the standpipe [L], h is the total head at the bottom of the Shelby tube [L], L is the height of sediment inside the Shelby tube [L] (from stream bed to the base of tube is ideal conditions), and Q is the flow inside the tube [L^3/t].

Within the standpipe, the flow is given by

$$Q = a\,\frac{\partial h}{\partial t}$$

Equating these we have

$$a\,\frac{\partial h}{\partial t} = -\frac{KA(h - h_0)}{L}$$

$$\frac{\partial h}{h - h_0} = -\frac{KA\partial t}{aL} \qquad (5)$$

Darcy's Law also gives groundwater flow within the streambed:

$$q = -\frac{K(h_s - h_0)}{L}$$

$$h_s - h_0 = -\frac{Kq}{L}$$

$$h_0 = -\frac{Kq}{L} + h_s \quad (6)$$

Now let $H = h - h_0$, then $\frac{\partial H}{\partial h} = 1$, so $\partial H = \partial h$. Also, at $t = 0, H_0 = h_1 - h_0$.

So,

$$\int_{H_0}^{H} \frac{\partial H}{H} = \int_{0}^{t} \frac{-KA\partial t}{aL}$$

and letting

$$\lambda = -\frac{KA}{aL}$$

and solving, we have

$$lnH - lnH_0 = \lambda t = ln\frac{H}{H_0}$$

so

$$\frac{H}{H_0} = e^{\lambda t}$$

Thus,

$$\frac{h - h_0}{h_1 - h_0} = e^{\lambda t}$$

OR

$$h = h_1 e^{\lambda t} - h_0\left(e^{\lambda t} - 1\right) \quad (7)$$

Now we substitute Eq. (6) into Eq. (7) to obtain

$$h = h_1 e^{\lambda t} - (\frac{qL}{K} + h_s)\left(e^{\lambda t} - 1\right)$$

expanding and re-organizing

$$h = (h_1 - \frac{qL}{K} - h_s)e^{\lambda t} + \frac{qL}{K} + h_s \quad (8)$$

when $h - h_s = 0$, the head in the Shelby tube is equal to the head in the stream. We will call this time t_s

$$0 = (h_1 - \frac{qL}{K} - h_s)e^{\lambda t_s} + \frac{qL}{K}$$

and solving for t_s

$$\frac{-qL}{K\left(h_1 - \left(\frac{qL}{K}\right) - h_s\right)} = e^{\lambda t_s}$$

$$\frac{\ln\left(\frac{-qL}{K\left(h_1 - \left(\frac{qL}{K}\right) - h_s\right)}\right)}{\lambda} = t_s \quad (9)$$

We now compute $\frac{dh}{dt}$ from Eq. (9) when $t = t_s$ (i.e. when $h = h_s$)

$$\left.\frac{dh}{dt}\right|_{t_s} = \lambda(h_1 - \frac{qL}{K} - h_s)e^{\lambda t_s}$$

substituting the definition of t_s from Eq. (9) we have

$$\left.\frac{dh}{dt}\right|_{t_s} = \lambda(h_1 - \frac{qL}{K} - h_s)\, e^{\left(\frac{\ln\left(\frac{-qL}{K\left(h_1 - \left(\frac{qL}{K}\right) - h_s\right)}\right)}{\lambda}\right)}$$

$$= \lambda(h_1 - \frac{qL}{K} - h_s)(\frac{-qL}{(Kh_1 - qL - Kh_s)})$$

Substituting the definition of λ and expanding

$$\left.\frac{dh}{dt}\right|_{t_s} = -\frac{KA}{aL}(h_1 - \frac{qL}{K} - h_s)(\frac{-qL}{(Kh_1 - qL - Kh_s)})$$

$$= -\frac{KA}{aL}(h_1 - \frac{qL}{K} - h_s)(\frac{-qL}{(Kh_1 - qL - Kh_s)})$$

$$= (-\frac{KA}{aL}h_1 + \frac{KA}{aL}\frac{qL}{K} + \frac{KA}{aL}h_s)(\frac{-qL}{(Kh_1 - qL - Kh_s)})$$

$$= (-\frac{KA}{aL}h_1 + \frac{Aq}{a} + \frac{KA}{aL}h_s)(\frac{-qL}{(Kh_1 - qL - Kh_s)})$$

$$= (\frac{qLKA\,h_1}{aL(Kh_1 - qL - Kh_s)} - \frac{Aq^2L}{a(Kh_1 - qL - Kh_s)} - \frac{h_sKAqL}{aL(Kh_1 - qL - Kh_s)})$$

$$= \left(\frac{qKA\,h_1}{a(Kh_1 - qL - Kh_s)} - \frac{Aq^2L}{a(Kh_1 - qL - Kh_s)} - \frac{h_sKAq}{a(Kh_1 - qL - Kh_s)}\right)$$

$$= \frac{qKA\,h_1 - Aq^2L - h_sKAq}{a(Kh_1 - qL - Kh_s)}$$

$$= \frac{qA(K\,h_1 - qL - h_sK)}{a(Kh_1 - qL - Kh_s)}$$

$$= q\frac{A}{a}$$

So when $h = h_s$,

$$\left.\frac{dh}{dt}\right|_{t_s \to h = h_s} = q\,A/a$$

OR

$$q = \left.\frac{dh}{dt}\right|_{t_s} \frac{a}{A} \qquad (10)$$

thus, the slope of the h versus t curve, when evaluated at h = hs, is independent of K and L, and the natural specific discharge (q) is given by this slope times the ratio of the standpipe area to the Shelby tube area.

Hydraulic Conductivity

From the same data set (dH/dt), the hydraulic conductivity can be determined as follows from Eq. (9).

At t = 0,

$$\left.\frac{dh}{dt}\right|_{t=0} = -\frac{KA}{aL}\left(h_1 - \frac{qL}{K} - h_s\right) = \frac{KA}{aL}h_1 + \frac{KA}{aL}\frac{qL}{K} + \frac{KA}{aL}h_s$$

$$= \frac{KA}{aL}(h_s - h_1) + q\frac{A}{a}$$

So

$$\frac{\left.\frac{dh}{dt}\right|_{t=0} - q\frac{A}{a}}{\frac{A(h_s - h_1)}{aL}} = K$$

And substituting Eq. (10) into the above we have

$$\frac{\left.\frac{dh}{dt}\right|_{t=0} - \left.\frac{dh}{dt}\right|_{t_s}}{\frac{A(h_s - h_1)}{aL}} = K \qquad (11)$$

So K is determined by measuring the slope of the head versus time curve at time = 0 (start of test) and at time = ts, which is when h = hs as the recovery curve passes through the stream pressure value, and the total water level displacement (hs − h1).

References

Todd, D. K. (1959), *Groundwater hydrology*, Wiley and Sons, New York.

APPENDIX B

RESULTS FROM LAB TESTING OF THE SHELBY TUBE

Table B.1. Discharge results from unamplified Shelby tube testing at the University of Utah in coarse sand under gaining conditions.

Pump Flow (m d^{-1})	Meas. Flow (m d^{-1})	% Eff
49.01	48.48	0.99
49.01	50.01	1.02
49.01	50.39	1.03
39.92	42.67	1.07
39.92	41.85	1.05
39.92	41.57	1.04
39.92	40.84	1.02
24.51	25.48	1.04
24.51	25.50	1.04
24.51	25.56	1.04
14.82	14.94	1.01
14.82	14.29	0.96
14.82	14.81	1.00
14.82	15.46	1.04
8.17	7.91	0.97
8.17	8.40	1.03
8.17	7.87	0.96
5.73	6.05	1.06
5.73	6.34	1.11
5.73	5.86	1.02
3.00	3.34	1.11
3.00	3.27	1.09
3.00	3.20	1.07
Mean	1.03	

Table B.2. Discharge results from unamplified Shelby tube testing at the University of Utah in coarse sand under losing conditions.

Pump Flow ($m\ d^{-1}$)	Meas. Flow ($m\ d^{-1}$)	% Eff
-8.17	-9.15	1.12
-8.17	-9.02	1.10
-8.17	-9.08	1.11
-14.82	-13.64	0.92
-14.82	-14.32	0.97
-14.82	-13.69	0.92
-24.51	-27.26	1.11
-24.51	-27.70	1.13
-24.51	-27.77	1.13
-39.92	-43.51	1.09
-39.92	-43.61	1.09
-39.92	-44.01	1.10
-49.01	-55.09	1.12
-49.01	-55.03	1.12
-49.01	-54.99	1.12
Mean		1.08

Table B.3. Discharge results from unamplified Shelby tube testing at the University of Utah in fine glass beads under gaining conditions.

Pump Flow ($m\ d^{-1}$)	Meas. Flow ($m\ d^{-1}$)	% Eff
1.02	1.05	1.03
1.02	1.04	1.02
0.79	0.83	1.05
0.79	0.85	1.08
0.60	0.61	1.00
0.60	0.64	1.06
1.08	1.15	1.07
0.84	1.00	1.20
0.62	0.73	1.18
0.42	0.53	1.26
Mean		1.10

Table B.4. Discharge results from unamplified Shelby tube testing at the USGS Denver Federal Center in medium sand under gaining conditions.

Pump Flow ($m\ d^{-1}$)	Meas. Flow ($m\ d^{-1}$)	% Eff
0.4	0.36	0.91
	0.36	0.89
	0.44	1.10
	0.39	0.98
0.596	0.63	1.06
	0.56	0.94
	0.59	0.98
0.2	0.20	0.99
	0.19	0.97
Mean		0.98

Table B.5. Hydraulic conductivity (K) results from Shelby tube testing at the University of Utah in coarse sand for gaining conditions.

Pump Flow ($m\ d^{-1}$)	K ($m\ d^{-1}$)
50	210.65
	231.02
	283.69
40	217.62
	227.12
	228.69
	310.79
25	221.15
	234.77
15	193.21
	148.88
	159.99
	176.93
8	162.58
	202.88
	150.5
6	189.82
	231.13
	163.2
3	222.22
	214.15
	280.92
1	132.45
	198.38
0.7	246.14
	173.89
0.5	243.55
	243.74
Mean	212.46
s.d.	43.36

Table B.6. Discharge results from unamplified Shelby tube testing at the USGS Denver Federal Center in medium sand under losing conditions.

Pump Flow ($m\ d^{-1}$)	Meas. Flow ($m\ d^{-1}$)	% Eff
-0.47	-0.5	1.06
-0.34	-0.41	1.21
	-0.35	1.03
-0.2	-0.29	1.45
	-0.28	1.40
Mean		1.23

Table B.7. Hydraulic conductivity results from Shelby tube testing at the University of Utah in coarse sand for losing conditions.

Pump Flow ($m\ d^{-1}$)	K ($m\ d^{-1}$)
-8	246.2
	237.94
	139.9
-15	152.26
	325.21
	179.56
-25	220.19
	309.2
	251.12
-40	269.56
	263.57
	311.52
-50	261.65
	317.16
	258.76
Mean	249.57
s.d.	57.27

Table B.8. Hydraulic conductivity results from Shelby tube testing at the University of Utah in fine glass beads.

Pump Flow ($m\ d^{-1}$)	K ($m\ d^{-1}$)
1.02	19.4
	15.13
	13.58
	12.78
	16.22
1	10.8
0.8	22.5
0.79	21.06
	18.88
	13.8
	14.9
	15.28
0.6	15.35
	18.79
	10.78
	17.67
	15.3
0.2	19.66
	9.51
	12.41
0.15	18.75
	18.01
	14.53
	16.73
	20.74
	6.57
	22.43
	11.84
0.1	13.4
	22.89
Mean	15.99
s.d.	4.09

Table B.9. Hydraulic conductivity results from Shelby tube testing at the USGS Denver Federal Center in medium sand under losing conditions.

Pump Flow ($m\ d^{-1}$)	K ($m\ d^{-1}$)
-0.2	132.72
	54.48
	60.81
	301.42
-0.34	171.85
	210.76
	100.92
	223.01
	81.25
	183.06
-0.47	263.96
	77.58
	233.16
	111.02
	128.06
	119.36
Mean	152.78
s.d.	75.27

Table B.10. Hydraulic conductivity results from Shelby tube testing at the USGS Denver Federal Center in medium sand under gaining conditions.

Pump Flow ($m\ d^{-1}$)	K ($m\ d^{-1}$)
0.596	104.36
	116.04
0.4	99.07
	100.13
	77.32
0.2	84
	128.15
	100.43
	91
	115.79
Mean	101.63
s.d.	15.43

APPENDIX C

FIELD RESULTS FOR SHELBY TUBE COMPARISON

TO DARCIAN METHOD

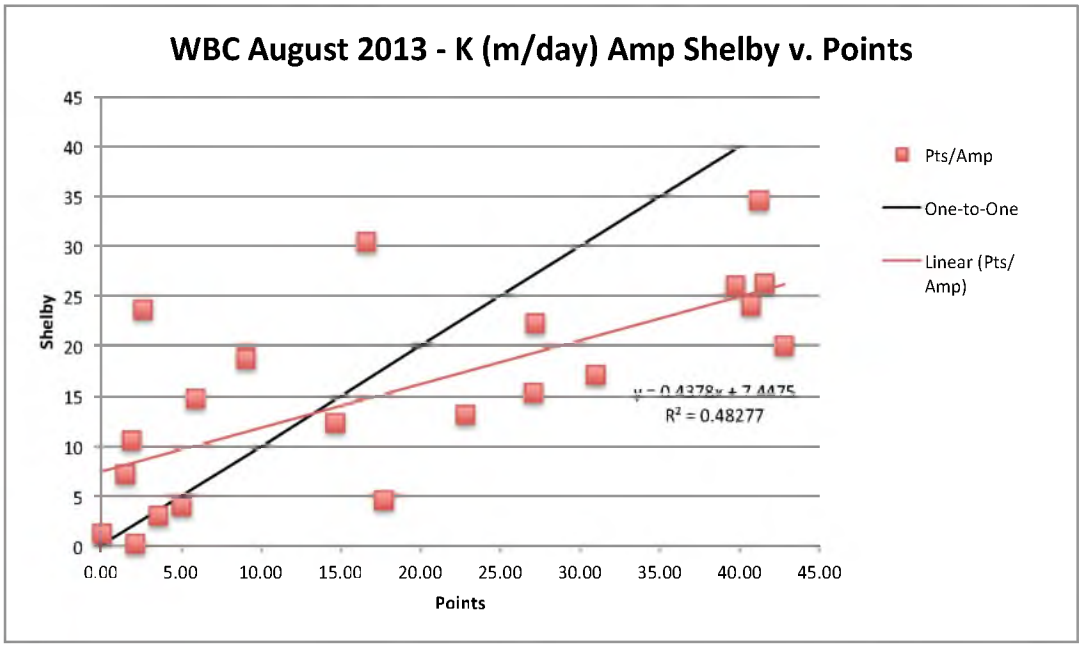

Figure C.1. Hydraulic conductivity (K) results for the amplified Shelby tube and Darcian (points) methods from West Bear Creek. Linear regression is with outliers removed.

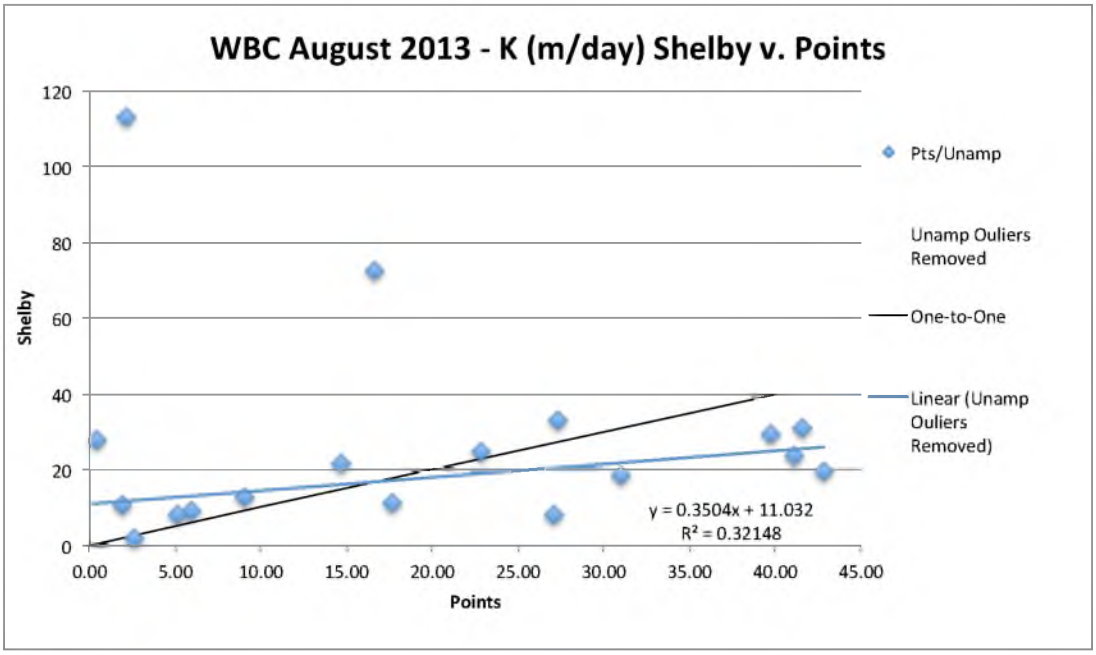

Figure C.2. Hydraulic conductivity (K) results for the unamplified Shelby tube and Darcian (points) methods from West Bear Creek. Linear regression is with outliers removed.

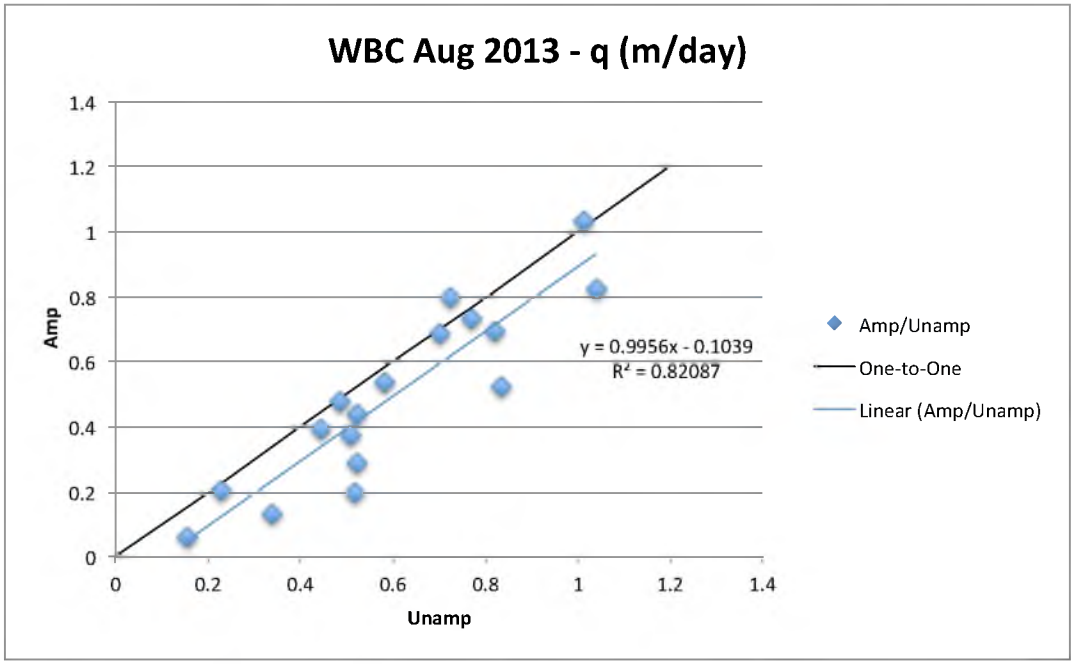

Figure C.3. Specific discharge (q) results for the amplified and unamplified Shelby tube method from West Bear Creek.

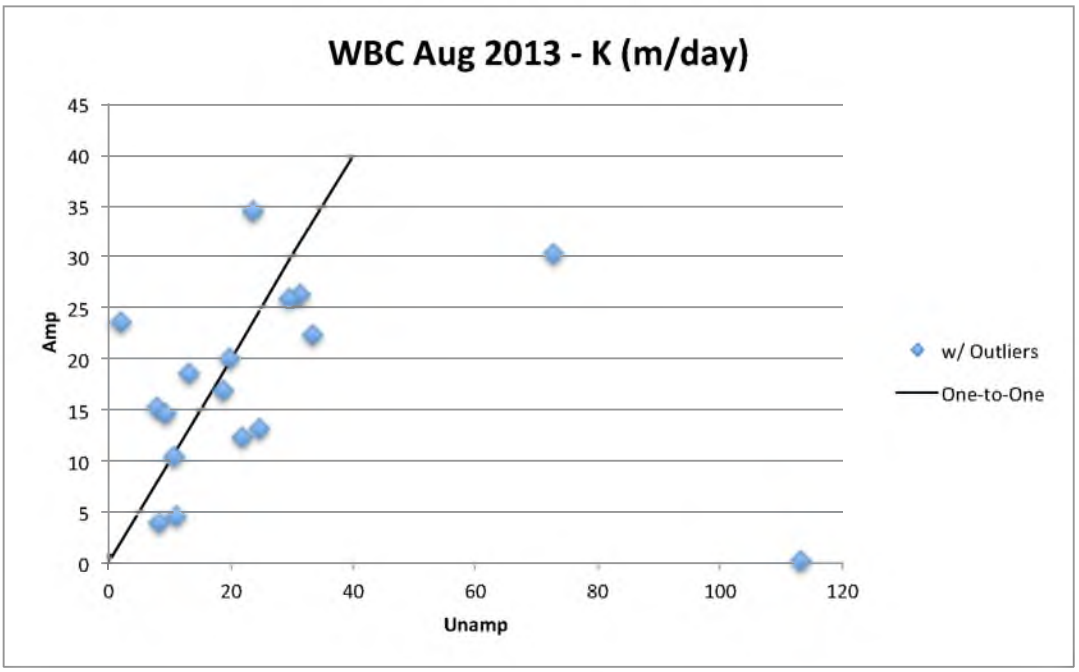

Figure C.4. Hydraulic conductivity (K) results for the amplified and unamplified Shelby tube method from West Bear Creek.

Table C.1. Specific discharge (q) and hydraulic conductivity (K) results for the amplified and unamplified Shelby tube and Darcian (points) methods from West Bear Creek in August 2013.

Location	q (m day^{-1})			K (m day^{-1})		
	Point	Shelby		Point	Shelby	
		Amplified	Unamplified		Amplified	Unamplified
479 R	0.01		0.15	0.45		27.78
479 C	0.09	0.06	0.15	2.16	0.27	113.25
479 L	0.01			0.02		
487 R	0.32	0.82	1.04	1.92	10.49	10.62
487 C	1.31	0.13	0.34	17.69	4.58	11.10
487 L	0.47	0.70	0.82	9.07	18.68	13.06
495 R	1.06	0.52	0.84	27.25	22.36	33.28
495 C	0.91	0.48	0.49	27.05	15.34	7.94
495 L	0.01			0.11		
504 R	0.47	0.20	0.52	14.66	12.33	21.78
504 C	0.69	0.37	0.51	30.99	17.02	18.57
504 L	0.84	0.54	0.58	42.80	20.01	19.82
512 R	0.70	0.39	0.44	22.82	13.22	24.68
512 C	0.93	0.41		40.70	23.97	
512 L	0.39	0.29	0.52	41.15	34.56	23.50
522 R	0.60	0.80	0.72	16.57	30.35	72.68
522 C	1.29	1.03	1.01	41.53	26.25	31.10
522 L	0.52	0.23		3.66	3.00	
529 R	0.45	0.69	0.70	5.92	14.74	9.42
529 C	0.87	0.73	0.77	39.71	25.97	29.67
529 L	0.68	0.44	0.52	5.09	4.07	8.11
537 R	0.01	0.00		0.03	1.13	
537 C	0.06	0.08		1.51	7.24	
537 L	0.38	0.20	0.23	2.64	23.69	1.94
Mean	0.54	0.43	0.58	16.48	15.68	26.57
Geomean				5.21	10.51	18.42
s.d.	0.40	0.28	0.26	16.01	9.95	26.71

Table C.2. Specific discharge (q), hydraulic conductivity (K), and the observed amplification factor (AF) results for the amplified and unamplified Shelby tube method from West Bear Creek in August 2013.

Location	q ($m\ day^{-1}$)	q amp ($m\ day^{-1}$)	AF	K ($m\ day^{-1}$)	K amp ($m\ day^{-1}$)
479 R	0.15			27.78	
479 C	0.15	0.06	6.64	113.25	0.27
479 L					
487 R	1.04	0.82	13.96	10.62	10.49
487 C	0.34	0.13	6.65	11.10	4.58
487 L	0.82	0.70	14.92	13.06	18.68
495 R	0.84	0.52	11.02	33.28	22.36
495 C	0.49	0.48	17.25	7.94	15.34
495 L					
504 R	0.52	0.20	6.78	21.78	12.33
504 C	0.51	0.37	12.95	18.57	17.02
504 L	0.58	0.54	16.30	19.82	20.01
512 R	0.44	0.39	15.68	24.68	13.22
512 C		0.41			23.97
512 L	0.52	0.29	9.69	23.50	34.56
522 R	0.72	0.80	19.42	72.68	30.35
522 C	1.01	1.03	17.98	31.10	26.25
522 L		0.23			3.00
529 R	0.70	0.69	17.24	9.42	14.74
529 C	0.77	0.73	16.77	29.67	25.97
529 L	0.52	0.44	14.83	8.11	4.07
537 R		0.00			1.13
537 C		0.08			7.24
537 L	0.23	0.20	15.51	1.94	23.69
Mean	0.58	0.43	13.74	26.57	15.68
Geomean				18.42	10.51
s.d.	0.26	0.28	4.14	26.71	9.95
Outliers Removed					
Mean				18.27	15.72
Geomean				15.09	12.04
s.d.				9.54	9.03

Table C.3. Hydraulic conductivity as determined by Eq. 2 (K) and Hvorslev (K Hvor) results for the unamplified Shelby tube method from West Bear Creek. Hvor 2 refers to analysis completed on a separate section of the recovery curve as obtained by the step method.

		Unamplified	
Location	K ($m\ day^{-1}$)	K Hvor ($m\ day^{-1}$)	K Hvor 2 ($m\ day^{-1}$)
479 R	27.78	10.21	20.97
479 C	113.25	4.56	0.31
479 L			
487 R	10.62	6.48	
487 C	11.10	12.43	6.41
487 L	13.06	11.35	11.35
495 R	33.28	24.24	97.03
495 C	7.94	15.51	79.26
495 L			
504 R	21.78	20.08	17.99
504 C	18.57	21.89	21.89
504 L	19.82	32.44	
512 R	24.68	13.93	16.17
512 C		25.80	97.46
512 L	23.50	24.73	28.96
522 R	72.68	64.12	64.12
522 C	31.10	37.66	36.11
522 L			
529 R	9.42	6.27	
529 C	29.67	34.40	42.23
529 L	8.11	3.19	4.83
537 R			
537 C			
537 L	1.94	1.61	1.36
Mean	26.57	19.52	34.15
Geomean	18.42	13.93	16.85
s.d.	26.71	15.29	32.93

Table C.4. Hydraulic conductivity as determined by Eq. 2 (K) and Hvorslev (K Hvor) results for the amplified Shelby tube method from West Bear Creek. Hvor 2 refers to analysis completed on a separate section of the recovery curve as obtained by the step method.

Location	K (m day^{-1})	Amplified K Hvor (m day^{-1})	K Hvor 2 (m day^{-1})
479 R			
479 C	0.27	1.52	1.58
479 L			
487 R	10.49	7.02	6.14
487 C	4.58	1.28	1.69
487 L	18.68	13.38	
495 R	22.36	19.09	19.09
495 C	15.34	13.62	
495 L			
504 R	12.33	9.55	9.55
504 C	17.02	16.58	17.76
504 L	20.01	26.59	
512 R	13.22	13.77	13.77
512 C	23.97	25.38	25.38
512 L	34.56	34.22	34.22
522 R	30.35	18.82	
522 C	26.25	32.11	
522 L	3.00	2.38	2.38
529 R	14.74	0.72	
529 C	25.97	33.73	29.34
529 L	4.07	3.44	
537 R	1.13	0.31	
537 C	7.24	6.47	6.47
537 L	23.69	13.67	13.67
Mean			
Geomean	15.68	13.98	13.93
s.d.	10.51	7.94	9.30

Table C.5. Hydraulic conductivity as determined by the Darcian method and the Hvorslev analysis of amplified and unamplified Shelby tube results (Hvorslev K) from West Bear Creek.

Location	Darcian K (m day^{-1})	Unamplified Hvor K (m day^{-1})	Amplified Hvor K (m day^{-1})
479 R	0.45	10.21	
479 C	2.16	4.56	1.52
479 L	0.02		
487 R	1.92	6.48	7.02
487 C	17.69	12.43	1.28
487 L	9.07	11.35	13.38
495 R	27.25	24.24	19.09
495 C	27.05	15.51	13.62
495 L	0.11		
504 R	14.66	20.08	9.55
504 C	30.99	21.89	16.58
504 L	42.80	32.44	26.59
512 R	22.82	13.93	13.77
512 C	40.70	25.80	25.38
512 L	41.15	24.73	34.22
522 R	16.57	64.12	18.82
522 C	41.53	37.66	32.11
522 L	3.66		2.38
529 R	5.92	6.27	0.72
529 C	39.71	34.40	33.73
529 L	5.09	3.19	3.44
537 R	0.03		0.31
537 C	1.51		6.47
537 L	2.64	1.61	13.67
Mean	16.48	19.52	13.98
Geomean	5.21	13.93	7.94
s.d.	16.01	15.29	11.23

APPENDIX D

MIXING CHAMBER VOLUME CALIBRATION AND TESTING FOR DILUTION FLOW METERS

The robustness of the dilution flow meter (DFM) as a discharge measurement device is dependent on accurate measurement of the mixing chamber volume. The validity of the calculated discharge was determined by comparing results to bucket gauged discharge. The volume of the mixing chamber was not easily directly measured given the complex geometry of the mixing manifold, specific conductance probe, and circulation pump. Thus, the volume of each individual mixing chamber was determined by using Equations 1 and 2 from the main text and solving for the volume (V) for a given flow rate (Q). This was done iteratively by varying the volume of a given mixing chamber to minimize the sum of Chi-Squared of the instantaneous flow and the slope-calculated flow for a range (~20–200 mL min^{-1}) of pump flow rates. A steady pump flow rate was maintained by peristaltic pump and measured by graduated cylinder, and the background specific conductance was held constant by discharging tracer-laden water from the pump to the sink and periodically refilling the container in which the dilution flow meter was submerged (Fig. D.1). The plot of bucket gauge measured flow against dilution flow meter measured flow for the calibration fell along a straight line ($R^2 = 0.9935$) and near the 1:1 line (m = 1.036) (Fig. D.2), and individual results of the mixing chamber

calibration are presented in Table D.1. The calibrated volumes for the five individual boxes are presented below in Table D.2. The volumes of the boxes differed slightly due to inconsistencies in the manufacturing of the boxes.

The calibration of the mixing chamber volume was tested by comparing the calculated flow rates to measured pumping rates (~30, ~160 mL min^{-1}) as presented in Table D.3 and D.4. The slope-calculated flow rate and the average instantaneous flow rate when plotted against the bucket gauged flow rate fell along a straight line (R^2 = 0.9993, 0.9986) and near the 1:1 line (m =1.014, 1.011) (Fig. D.3). The dilution flow meters are a proven robust measure of flow for rates between 20 mL min^{-1} and 200 mL min^{-1}, although we expect the dilution flow meters to function well at flows up to 500 mL min^{-1}. It should be noted that the meter is theoretically valid for much larger or smaller flows depending on the volume of the mixing chamber.

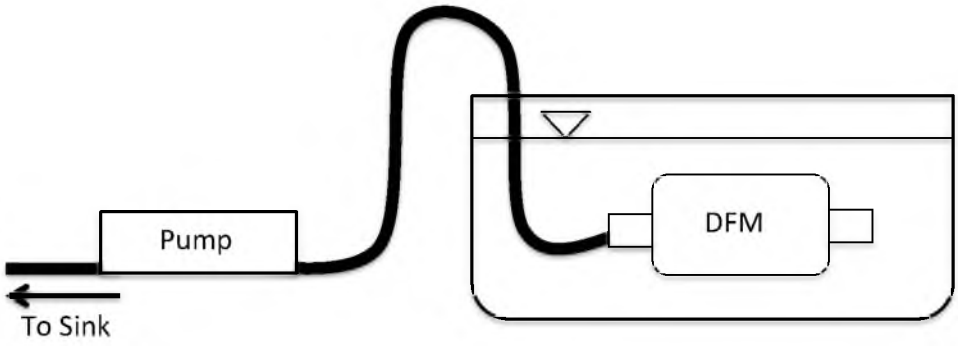

Figure D.1. Diagram of dilution flow meter calibration configuration with filled tank, dilution flow meter, and peristaltic pump.

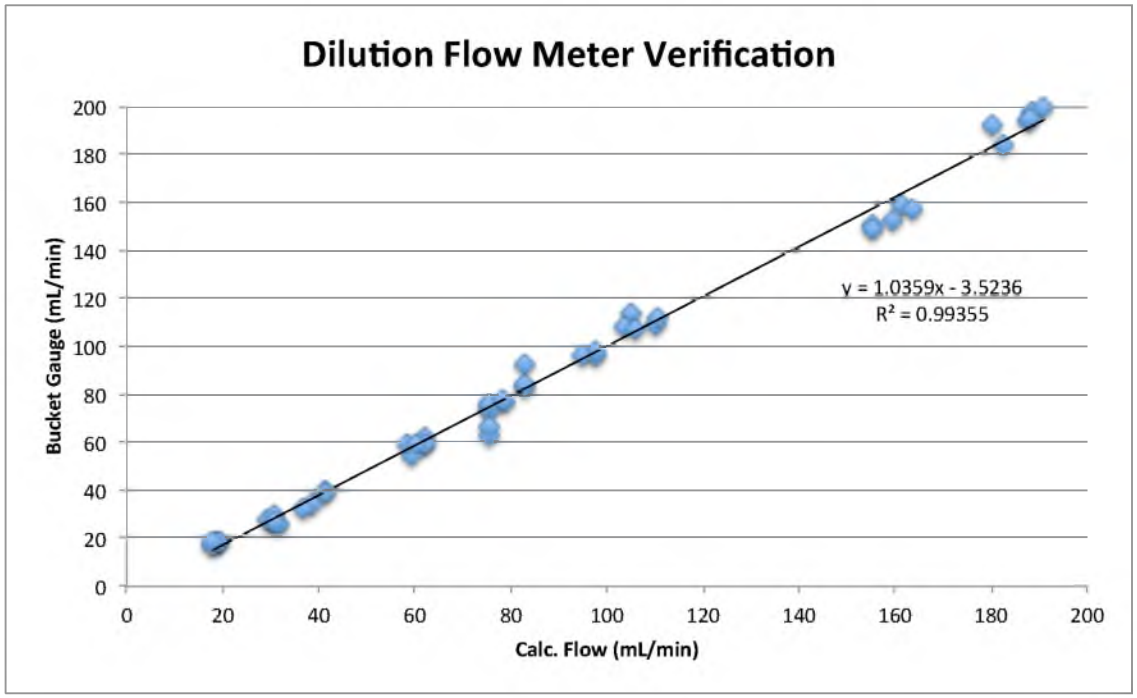

Figure D.2. Plot of bucket gauged flow against the linear regression calculated flow during the calibration of the dilution flow meter mixing chamber.

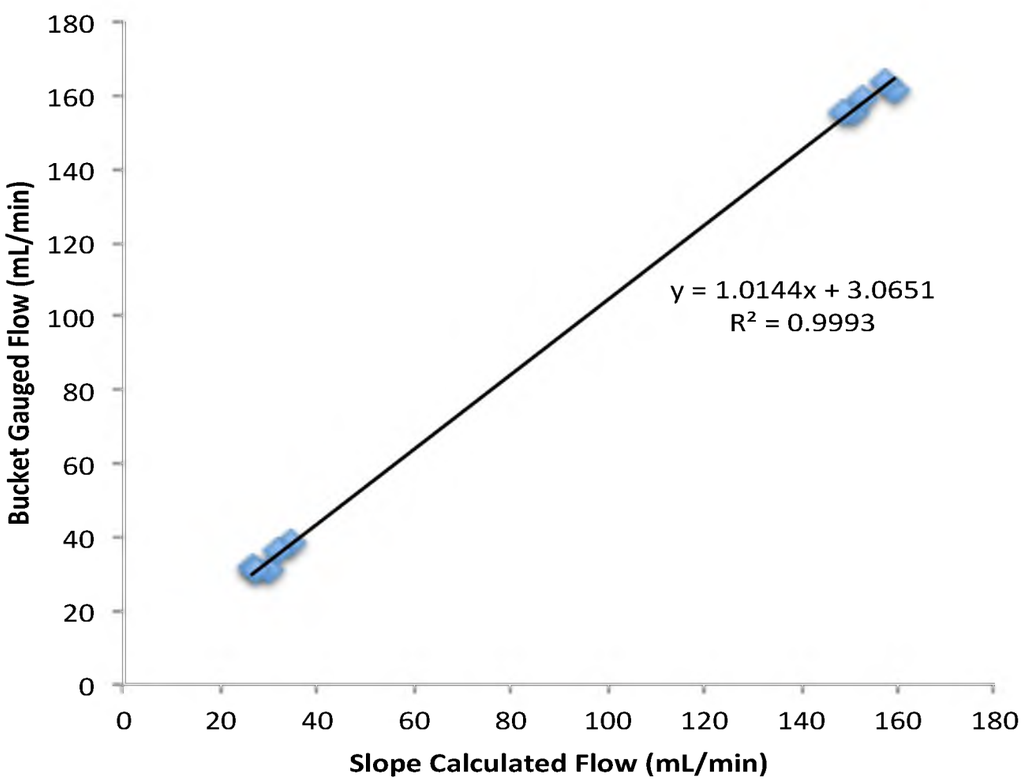

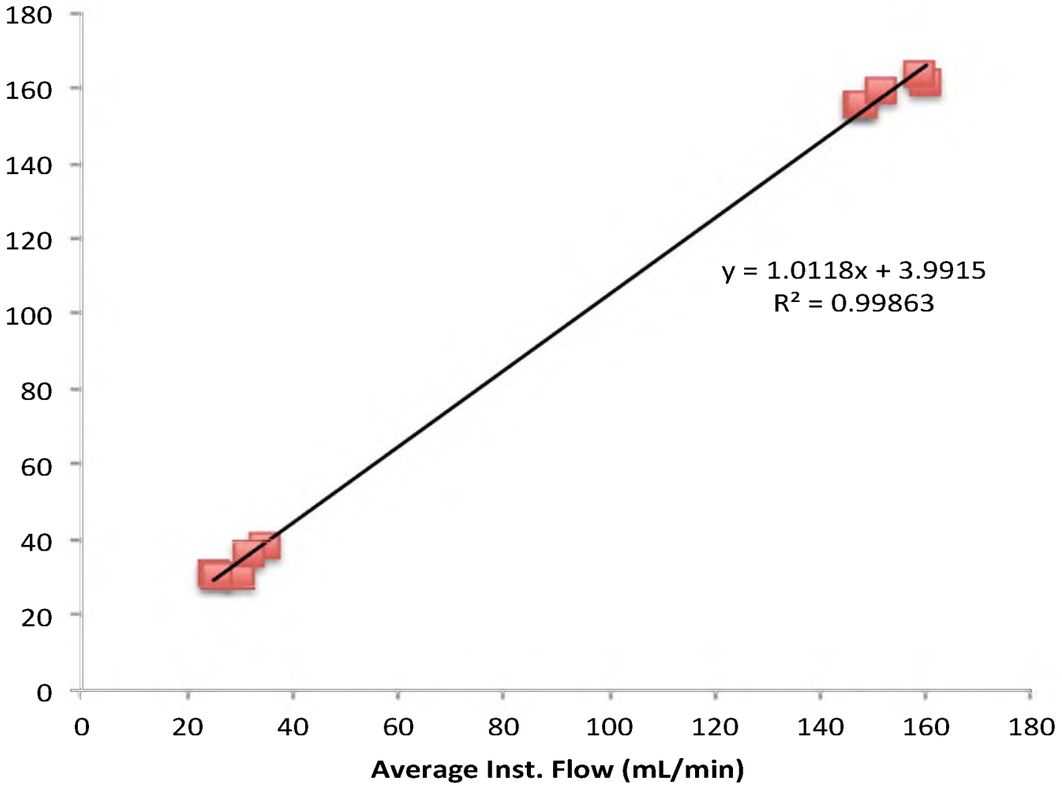

Figure D.3. Plots of bucket gauge flow rate against dilution flow meter linear regression and mean instantaneous flow.

Table D.1. Results from calibration of dilution flow meter mixing chamber volume by minimizing Chi-Squared.

Chamber	Bucket Gauge Q (mL min^{-1})	Mean Instant Q (mL min^{-1})	Linear Regress Q (mL min^{-1})
1	75.5	66.75	67.00
	41.25	39.84	39.51
	41.25	38.59	38.80
	95	92.00	96.07
	83	88.99	92.85
	188	188.42	194.82
2	75.5	73.95	75.54
	29.5	26.62	27.48
	60.25	57.93	58.95
	78.5	77.66	77.15
	78.25	75.64	77.83
	110.5	112.24	112.06
	187.75	190.54	194.43
3	75.5	64.04	62.72
	105	110.06	114.15
	110	101.25	109.42
	103.5	104.72	108.30
	106	105.22	107.54
	62	60.20	60.04
	61.5	59.30	60.17
	62	61.92	62.36
	62.25	60.44	59.55
	180	184.89	192.38
	182.5	184.63	183.83
	18.75	18.22	18.88
	19.25	18.54	18.31
	19.3	17.79	18.44
	18	17.85	18.36
4	75.5	73.28	73.49
	31.25	25.75	26.05
	97.6	95.68	96.36
	97.6	96.82	98.19
	58.33	59.33	59.57
	191	195.85	199.62

Table D.1. Continued

5	75.5	74.41	76.00
	18	15.40	16.65
	59.5	48.72	54.91
	83	82.51	82.93
	83	83.84	83.89
	188.5	194.19	198.05

Table D.2. Calibrated volumes for each of the DFM mixing chambers.

Chamber	Volume (mL)
1	911.7
2	902.5
3	902.4
4	933.35
5	908.6

Table D.3. Dilution flow meter check: Bucket gauge measured flow and DFM measured flow with statistics.

Chamber	Bucket Gauge			Dilution Flow Meter Calculated				
	Measure Q (mL min^{-1})		Mean Q (mL min^{-1})	Linear Regress Q (mL min^{-1})	R^2 of Linear Fit	Mean Instant Q (mL min^{-1})	s.d. Inst. Q	COV
1	31	32	31.5	26.42	0.98860	25.00	2.01	0.080
	154	157	155.5	150.94	0.99983	147.42	4.97	0.034
2	154	157	155.5	148.84	0.99984	147.69	5.82	0.039
	31	30.5	30.75	30.12	0.99999	29.96	0.26	0.009
3	31	30.5	30.75	27.38	0.99605	25.57	3.76	0.147
	160	163	161.5	159.29	0.99994	160.13	4.76	0.030
4	163	164	163.5	157.23	0.99985	158.81	8.66	0.055
	38.5	38.5	38.5	34.66	0.99870	34.64	3.12	0.090
5	36.5	36.5	36.5	32.12	0.99815	31.81	2.28	0.072
	162	157	159.5	152.58	0.99623	151.76	22.44	0.148

Table D.4. Statistics of dilution flow meter check.

Relative Flow	Statistic	Bucket Gauge	Dilution Flow Meter Calculated				
		Mean Q (mL min^{-1})	Linear Regress Q (mL min^{-1})	R^2 of Linear Fit	Mean Instant Q (mL min^{-1})	s.d. Inst. Q	COV
High	Avg.	33.60	30.14	0.996	29.39	2.286	0.080
	s.d.	3.64	3.38		4.11		
	COV	0.11	0.11		0.14		
Low	Avg.	159.10	153.78	0.999	153.16	9.331	0.061
	s.d.	3.58	4.36		6.03		
	COV	0.02	0.03		0.04		

APPENDIX E

EXAMPLE DILUTION FLOW METER

CALCULATION AND PLOTS

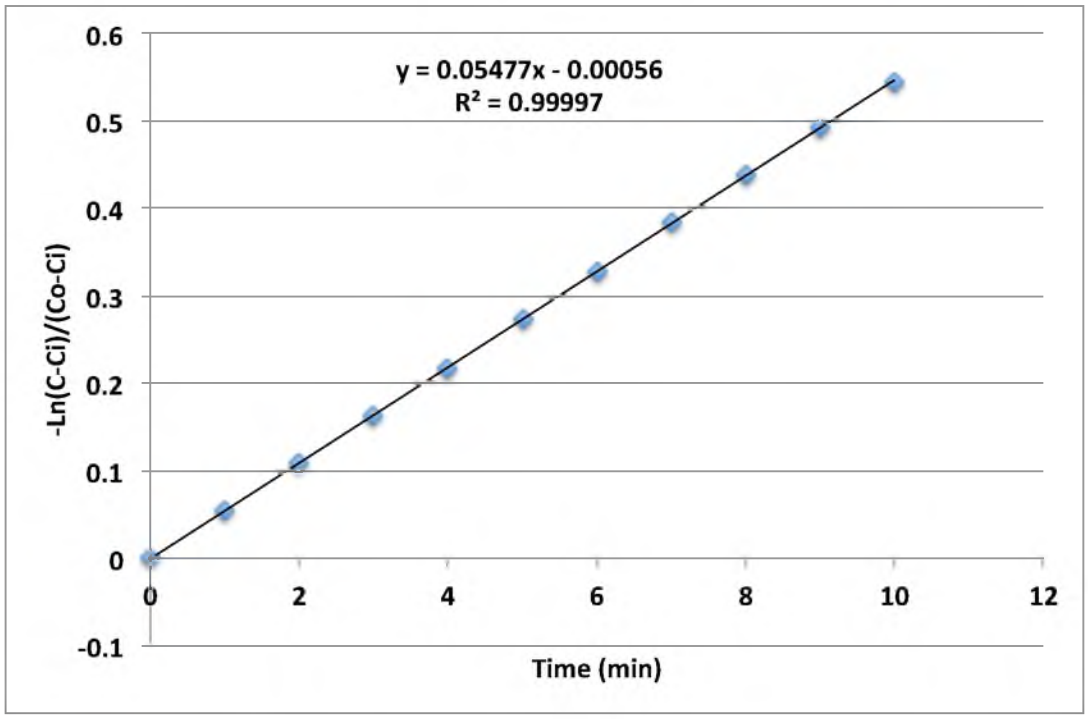

Figure E.1. Plot of the natural log transformed dilution curve with respect to time and linear regression.

Table E.1. Example calculations of blanket discharge (Q, mL min^{-1}) measured by dilution flow meter. EC is electrical conductivity, C is the electrical conductivity in the mixing chamber at a given time, Co is the electrical conductivity at the previous time, and Cint is the initial/background conductivity.

Chamber Vol. (ml)	Initial EC (uS cm^{-1})				
911.7	263				
Time (min)	EC (uS cm^{-1})	Delta Time	Ln{(C-Cinit) /(Co-Cinit)}	Instant Q (ml min^{-1})	-Ln{(C-Cinit) /(Co-Cinit)}
0	1524				0
1	1457	1	-0.0546	49.8	0.0546
2	1394	1	-0.0542	49.4	0.1088
3	1335	1	-0.0536	48.8	0.1624
4	1277	1	-0.0556	50.7	0.2180
5	1223	1	-0.0547	49.9	0.2727
6	1171	1	-0.0557	50.8	0.3284
7	1122	1	-0.0555	50.6	0.3839
8	1076	1	-0.0550	50.2	0.4389
9	1033	1	-0.0543	49.5	0.4933
10	994	1	-0.0520	47.4	0.5452
				Mean Inst. Q (mL min^{-1})	Linear Regress Q (mL min^{-1})
				49.71	49.97
				s.d.	Slope
				1.02	-0.0548
				Variance	
				1.04	
				COV	
				0.02	

APPENDIX F

USGS DENVER FEDERAL CENTER

SEEPAGE BLANKET TESTING

The tank discharge was measured by in-line paddle wheel flow meters and verified with a floating pan and bucket gauge measurement. Fig. F.1 shows the paddle wheel discharge plotted against bucket gauge discharge. Given the strong correlation between paddle wheel and bucket gauge discharge ($R^2 = 0.9992$, m = 0.987), all the subsequent analysis (and main text) that refers to "tank discharge" indicates the paddle wheel flow measurements. The seepage blanket measured discharge as compared to the tank discharge is presented in Table F.1 and Fig. F.2 and F.3.

The efficiency of the blanket was strongly influenced by the discharge rate of the tank, as shown in Fig. F.3. As the tank discharge increased, the efficiency of the blankets decreased. This suggested that, for high permeability sediments, the flow restriction caused by blanket capture during higher seepage rates had significant effect on the performance of the blankets.

Standard half-barrel seepage meter measurements made across the same range of seepage rates are presented in Table F.2 and Fig. F.4 and F.5. Separate tests and discharge measurements were completed with 2 and 3 half-barrel meters installed to determine the effects of areal coverage on seepage meter performance. The average half-

barrel discharges presented are typically based on three measurements from each seepage meter that is installed. Thus, for 2-meter measurements n = 6, and for 3-meter measurements n = 9.

Similar to the blankets, the half-barrel was more efficient during upward seepage (61.9%) than during downward seepage (53.8%). The average efficiency for the half-barrel seepage meters with 2 meters installed was 58.3%, and for 3 meters installed it was 74.7%. We suspected that the increased efficiency during tests with three meters was caused by the decreased area of the nonmetered tank and thus increased resistance to flow bypass.

Interestingly, the half-barrel meter efficiency increased as the tank discharge increased, the opposite of the trend for the blankets. The half-barrel meters show increased efficiency at increased flow rates, for both the 2 and 3 half-barrel meter configurations.

The efficiency of the blankets as compared to the half-barrel meters is presented below in Table F.3 and Fig. F.6 and F.7. The comparison of the blankets to the half barrel meters was a more valid means of measuring the efficiency of the blankets given the inefficiency of both seepage devices in the high K sediments of the tank.

The mean efficiency of the blankets as compared to the half-barrel was 77.5% for the 2-meter configuration and 52.5% for the 3-meter configuration. The efficiency for a given configuration increased at lower flow rates (Fig. F.7), which was a result of the observed negative correlation between blanket/tank efficiency and half-barrel/tank efficiency as the seepage rate was altered.

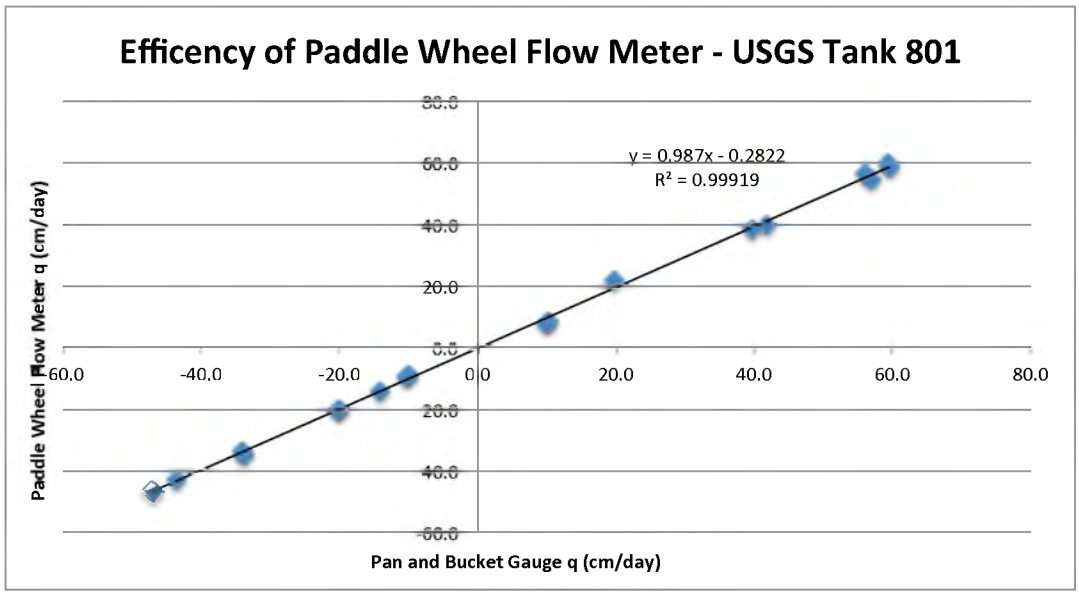

Figure F.1. Comparison of USGS Tank 801 flow measurements made with the paddle wheel flow meter and a pan and bucket gauge.

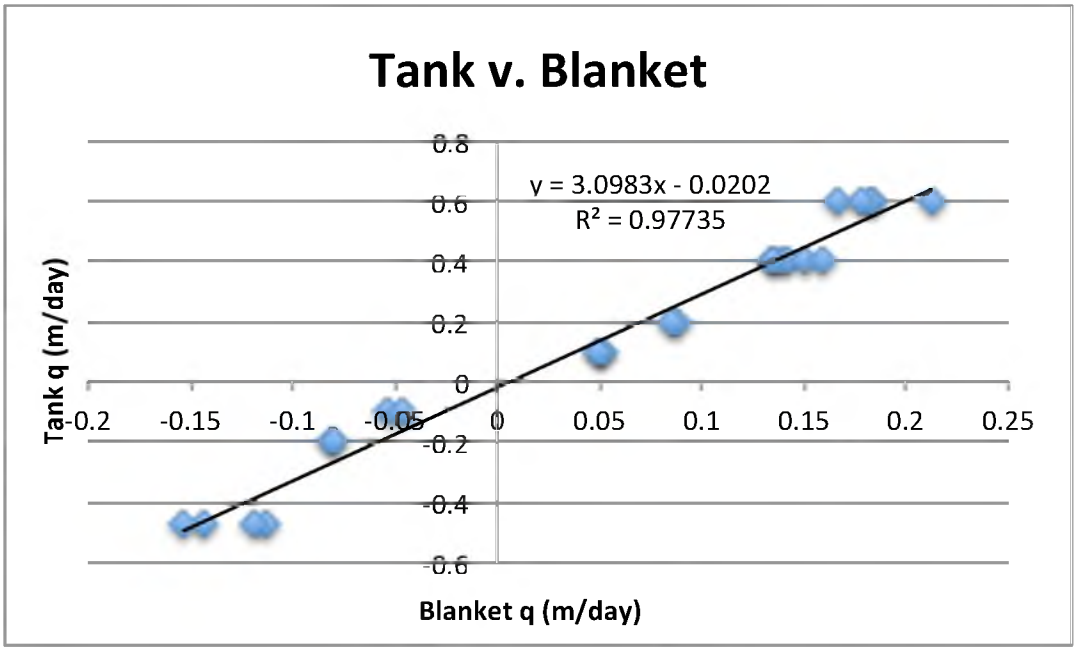

Figure F.2. Plot of tank discharge against blanket discharge.

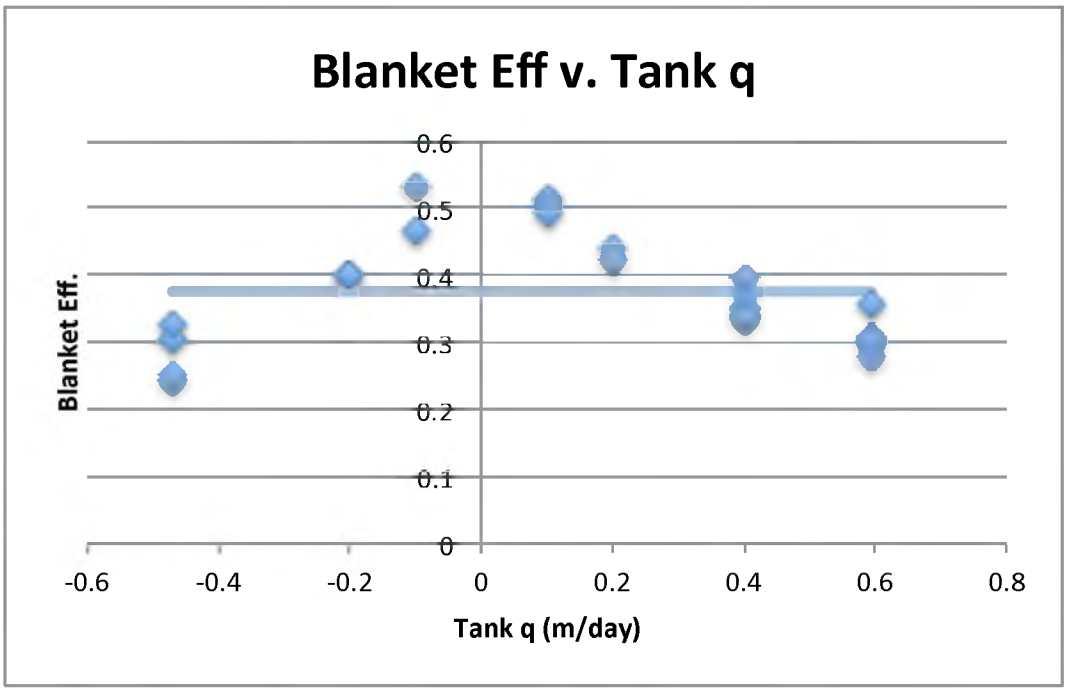

Figure F.3. Plot of tank discharge against blanket efficiency.

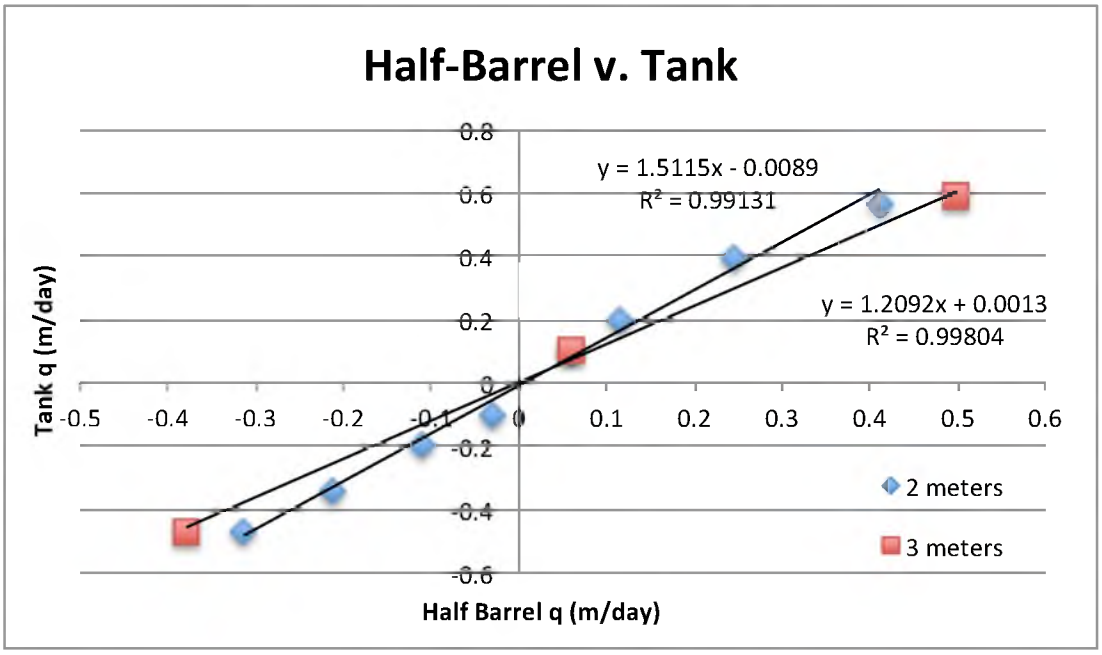

Figure F.4. Plot of tank discharge against half-barrel meter discharge.

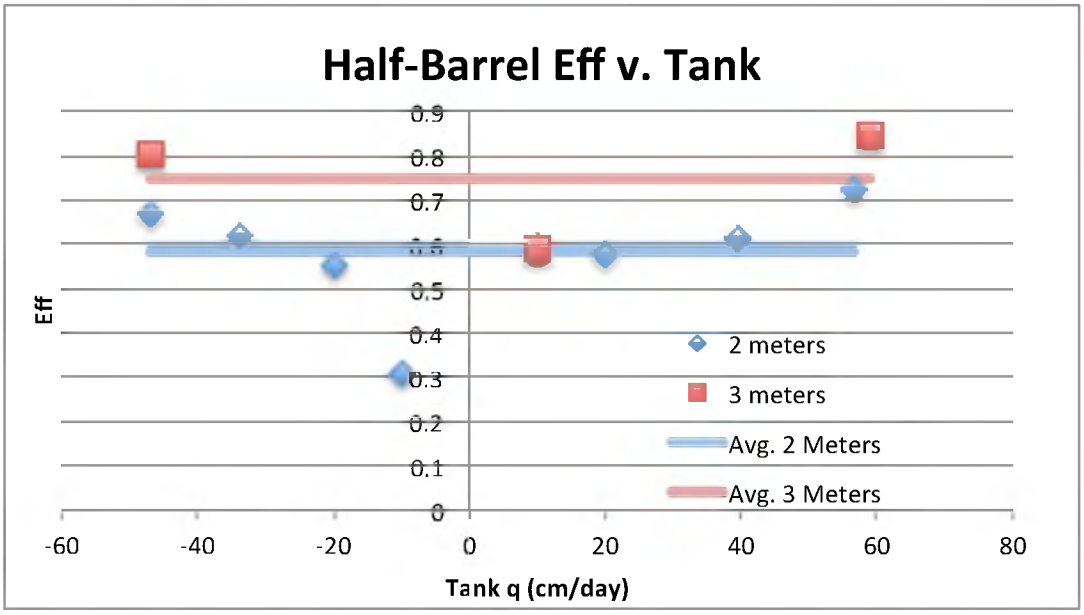

Figure F.5. Plot of tank discharge against half-barrel meter efficiency.

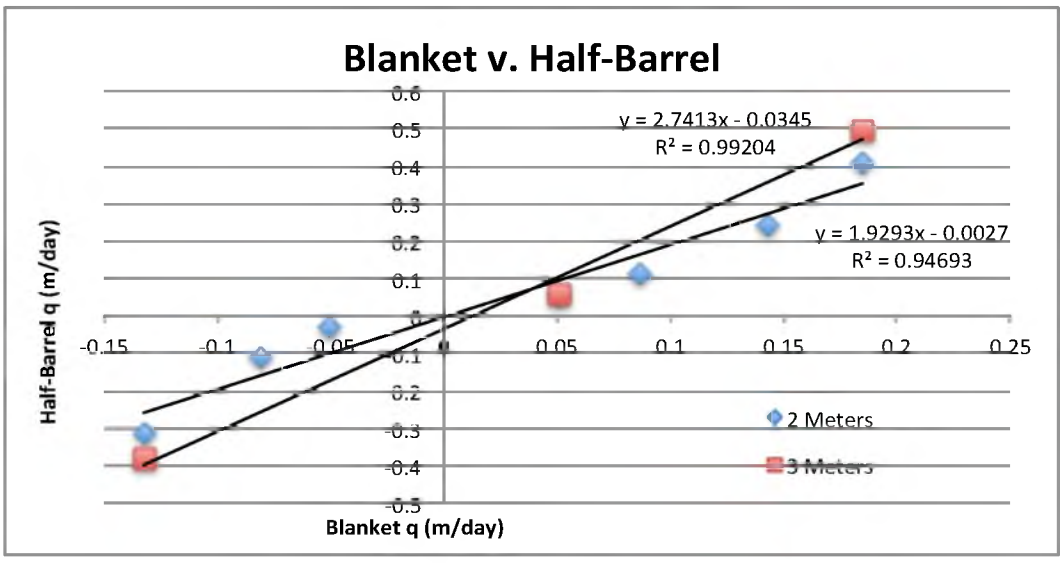

Figure F.6. Plot of half-barrel discharge against blanket discharge.

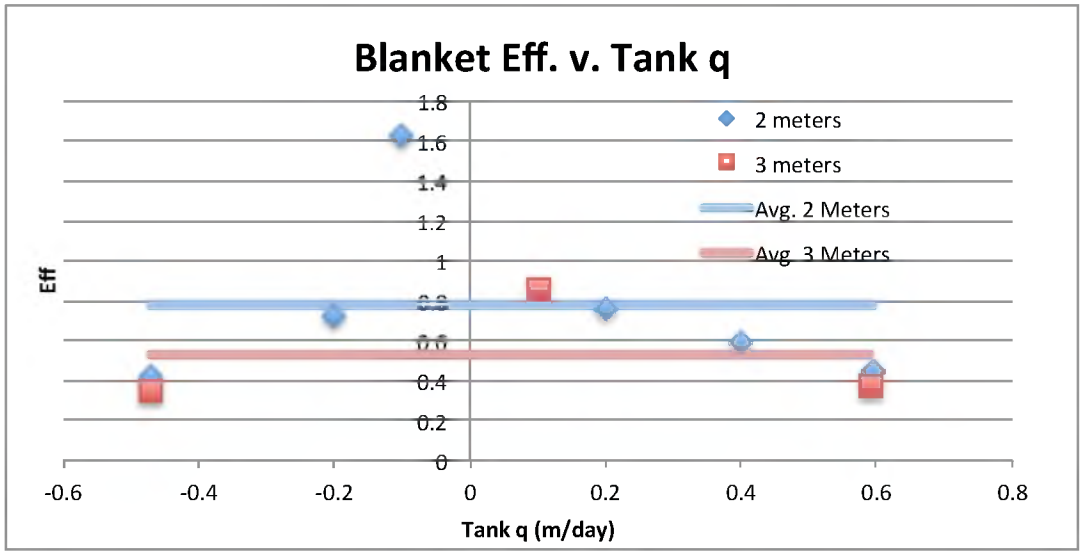

Figure F.7. Plot of half-barrel discharge against blanket efficiency as compared to half-barrel meters.

Table F.1. Tank and Blanket discharge from testing completed at the USGS Denver Federal Center. Testing completed with single blanket in tank.

Tank q ($m\ day^{-1}$)	Inv. Meas. q ($m\ day^{-1}$)	Mean q ($m\ day^{-1}$)	s.d. ($m\ day^{-1}$)	% Eff. Mean/Tank
Downward Seepage				
-0.1	-0.053 -0.047	-0.0500	0.0047	50.03
-0.2	-0.081 -0.080	-0.0802	0.0004	40.12
-0.47	-0.114 -0.119 -0.144 -0.153	-0.1324	0.0191	28.18
		Mean Efficiency		39.44
Upward Seepage				
0.1	0.052 0.051 0.049	0.0506	0.0013	50.60
0.2	0.088 0.085	0.0865	0.0022	43.24
0.4	0.135 0.150 0.159 0.139 0.142 0.134	0.1433	0.0095	35.82
0.596	0.167 0.212 0.184 0.183 0.178	0.1848	0.0169	31.01
		Mean Efficiency		40.17

Table F.2. Discharge results from the tank and half-barrel seepage meters.

Tank q ($m\ day^{-1}$)	Mean q ($m\ day^{-1}$)	% Eff. Mean/Tank
2 Meters		
Downward Seepage		
-0.1	-0.031	30.8
-0.2	-0.111	55.3
-0.34	-0.211	62.2
-0.47	-0.313	66.7
Mean Efficiency		53.8
Upward Seepage		
0.1	0.058	58.5
0.1	0.059	59.5
0.198	0.114	57.6
0.395	0.243	61.6
0.568	0.410	72.2
Mean Efficiency		61.9
3 Meters		
-0.47	-0.379	80.5
0.59	0.498	84.4
0.1	0.059	59.2
Mean Efficiency		74.7

Table F.3. Discharge results from tank, blanket, and half-barrel seepage meters.

Tank ($m\ day^{-1}$)	Blanket ($m\ day^{-1}$)	Half- Barrel ($m\ day^{-1}$)	Blanket % Eff. Blanket/H-B
2 H-B Meters			
Upward Seepage			
0.1	0.051	0.059	85.8
0.2	0.086	0.114	75.8
0.4	0.143	0.243	58.9
0.596	0.185	0.410	45.1
	Mean Efficiency		66.4
Downward Seepage			
-0.1	-0.050	-0.031	162.3
-0.2	-0.080	-0.111	72.5
-0.47	-0.132	-0.313	42.3
	Mean Efficiency		92.4
3 H-B Meters			
0.1	0.051	0.059	85.4
0.59	0.185	0.498	37.1
-0.47	-0.132	-0.379	35.0
	Mean Efficiency		52.5

APPENDIX G

REACH MASS BALANCE FOR WEST BEAR CREEK IN JULY 2012

A tracer solution of Sodium Bromide (NaBr) was injected into the stream at the site 1 km upstream of N. Beston Road Bridge, which will be referred to as the injection site. The injected solution was made by mixing 25 Kg bags of 99% pure NaBr with 50 gallons of streamwater. This was preformed four times for a total 100 Kg of NaBr dissolved in 200 gallons of water. Lab analysis of the injectate confirmed that the solution was a 3.1 M solution of NaBr. Each mixture of 50 gallons was carefully transferred to a stock tank that held the full volume of the mixture. The NaBr was injected to the stream by way of a specialized pump set up [Kimball et al., 2004; Fig. G.1, G.2, G.3] that achieved a very steady injection of the NaBr solution. At the injection site, a 3.1 molar NaBr solution was injected for 67.8 hours at an average rate of 63 milliliters per minute. An ISCO sampler at 2700 m downstream of the injection site collected samples, and two synoptic sweeps were preformed in which samples were collected every 100 m over the study reach. Measured concentration of NaBr and the interpreted discharge is shown in Fig. G.4. Using an average stream width of 7 meters, the specific discharge per 100 meters of reach was calculated as displayed in Fig. G.5.

To determine the extent of hyporheic flow and bank storage, a mass balance

calculation was performed to determine the amount of solution injected and the amount of solution "captured" at WBC 2700. The amount of solution injected was determined by taking the product of the mass flow rate (mg/s) and the total time of injection. The total mass of Br "captured" at WBC 2700 was determined by taking the product of the measured Br concentration (mg/L) and the estimated stream flow (L/s) and integrating with respect to time. The Br concentration and estimated stream discharge at WBC 2700 (Fig. G.6) was used to calculate the mass balance. An ISCO sampler collected samples for the measured Br concentrations. The stream discharge at WBC 2700 was estimated at the temporal resolution needed by correlating the stream flow at the downstream USGS stream gauge on Bear Creek at Mays Store, NC (0208925200) to Flowtracker and bromide reach mass balance measured stream discharge at WBC 2700. The mass balance analysis indicated that 81.4 +/- 1.9 kg of Br was injected into the stream and 75.1 +/- 10.4 kg was captured at WBC 2700. Given the conservation of mass between the injection site and WBC 2700, we can say that hyporheic and bank storage flow paths were completed (e.g., NaBr was returned back to the stream), and there were no unmeasured losses of streamwater along the reach.

References

Kimball, B. A., R. L. Runkel, T. E. Cleasby, and D. A. Nimick (2004), Quantification of metal loading by tracer injection and synoptic sampling, 1997–98, *U.S. Geological Survey Professional paper 1652-D6*, In *Integrated Investigations of Environmental Effects of Historical Mining in the Basin and Boulder Mining Districts, Boulder River Watershed, Jefferson County, Montana*, edited by D. A. Nimick, S. E. Church, and S. E. Finger, U. S. Geological Survey, Reston, VA.

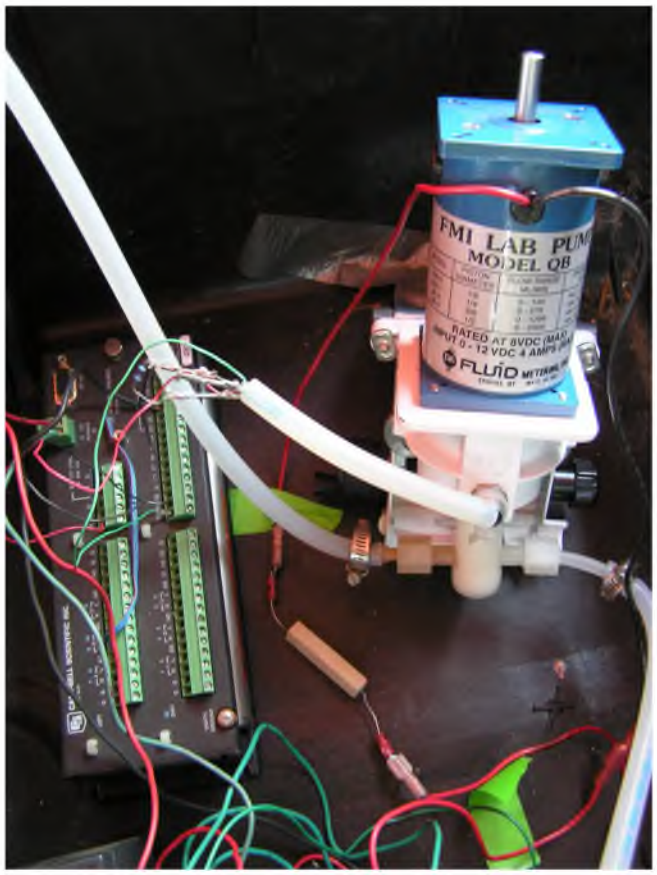

Figure G.1. Close up photo of pump and datalogger configuration for injection of bromide tracer.

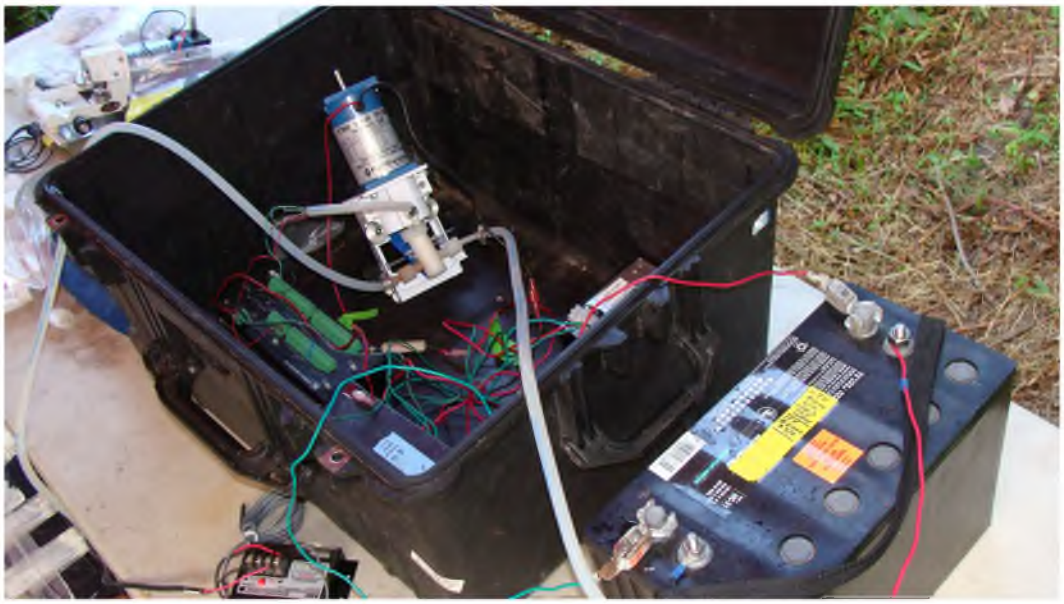

Figure G.2. Photo of pump, Datalogger, and battery configuration for injection of bromide tracer.

Figure G.3. Photo of injection site showing pump setup and stock tank holding NaBr tracer solution.

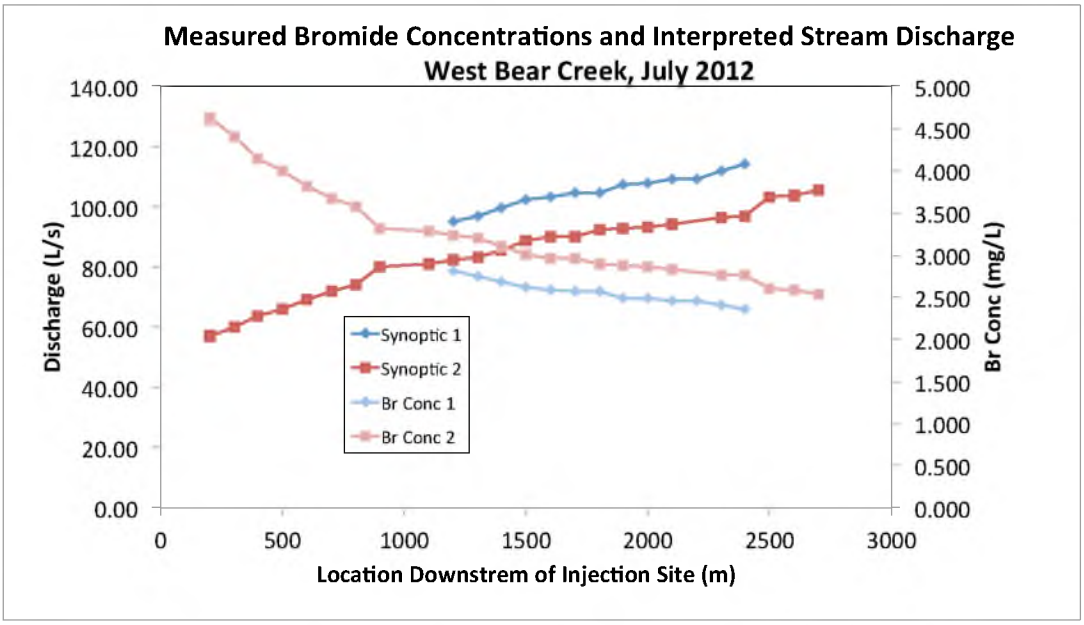

Figure G.4. Plot of measured bromide concentration and interpreted discharge along the length of the reach at West Bear Creek in July 2012.

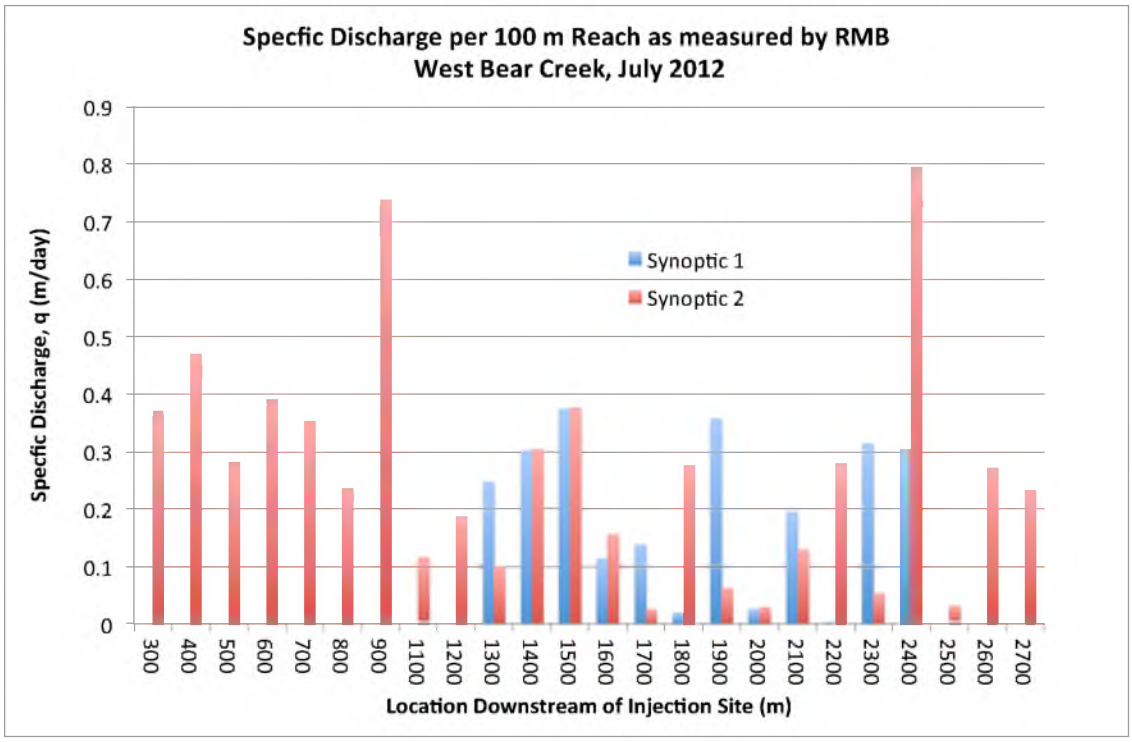

Figure G.5. Reach mass balance interpreted specific discharge per 100-meter reach of the stream given an average stream width of 7 m for West Bear Creek in July 2012.

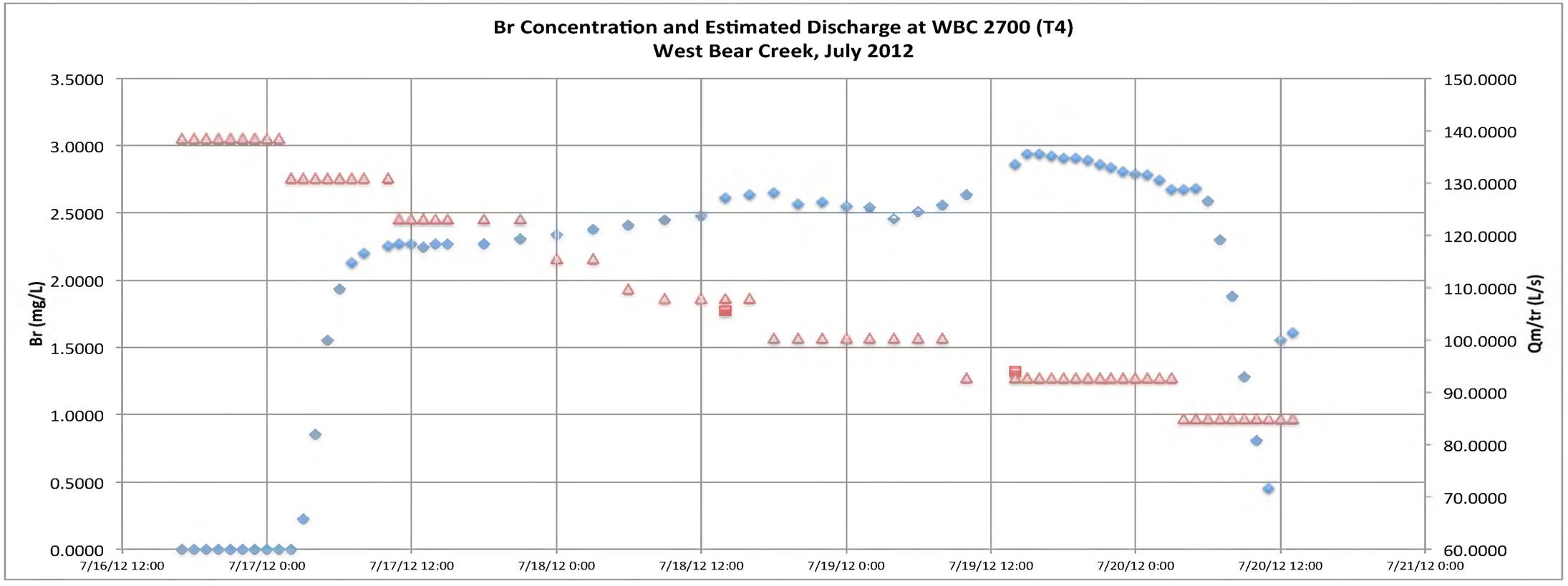

Figure G.6. Bromide concentration (blue diamond), estimated stream discharge (red triangle), and measured stream discharge (red squares) at WBC 2700 for completion of bromide mass balance on West Bear Creek, NC in July 2011.

APPENDIX H

JULY 2012 RESULTS FROM BLANKETS AND POINTS AT WEST BEAR CREEK, NC

Blanket specific discharge across a transect (Figs. H.1, H.2, H.3) shows generally higher discharge in the center of the stream. Blanket discharge as compared to points (Table H.1) suggests that the blanket method is variable which respect to the points. Overall, the blankets reported the lowest mean discharge as compared to other methods (Table H.2). This observation is in contrast to the presence of bromide (e.g. streamwater) in water sampled from the blankets (Table H.3). Given that the groundwater bromide concentration was below the analytical detection limit (0.01 mg/L) and based on the measured blanket bromide (Table H.3), the estimated stream bromide (Table H.4), and the measured blanket discharge (Table H.1), the blanket discharge can be corrected for the presence of bromide (Table H.5). The reactive dissolved gas concentrations as sampled from the blankets (Table H.6) have not been corrected for the presence of bromide given the lack of streamwater dissolved gas results. The SF_6 and CFC results presented here have been corrected for the streamwater collected by the blankets to determine the concentration of SF_6 and CFC in groundwater. This correction was done by mass balance on bromide. With a measured stream concentration of CFC and SF_6 at each transect, the blanket sample CFC and SF_6 could be corrected for presence of streamwater.

A large measured variation in CFC concentration between the stream samples (Fig. H.4) collected above and below the blanket transects created some uncertainty in the blanket CFC correction. To capture the magnitude of the uncertainty, three separate corrected blanket CFC concentrations were determined (Table H.7). The "Best Estimate" made use of a linear regression between the two measured stream CFC concentrations to estimate the stream CFC at a given transect. The "Max" and "Min" blanket CFC concentrations indicate the upper and lower bounds of the corrected blanket CFC concentrations. The corrected blanket SF_6 (Table H.8) and uncorrected blanket Noble gas results (Table H.9) are also presented here.

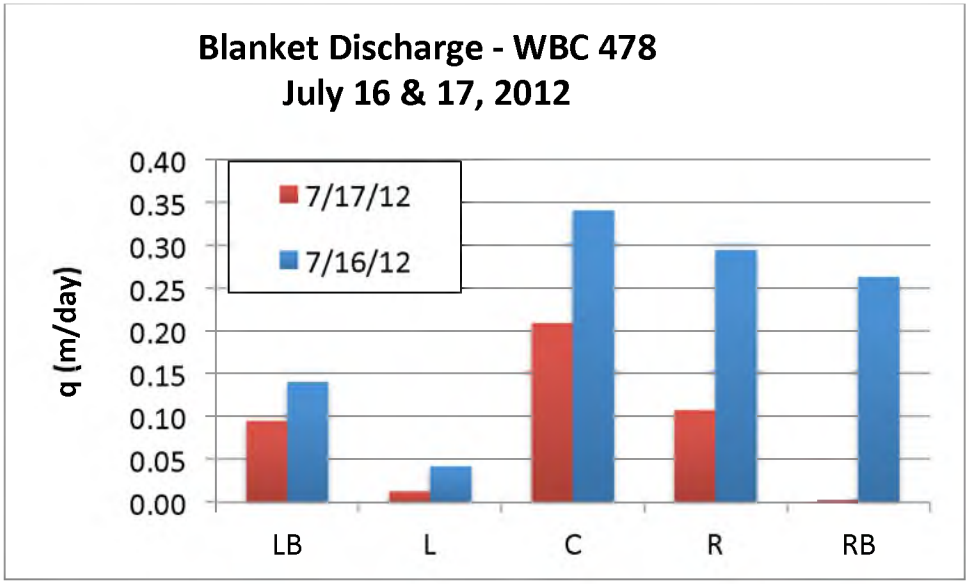

Figure H.1. Dilution flow meter measured blanket discharge from West Bear Creek, NC in July 2012. Location indicated along transect on x-axis (right bank, right, center, left, left bank) with the U indicating measurement completed by University of Utah.

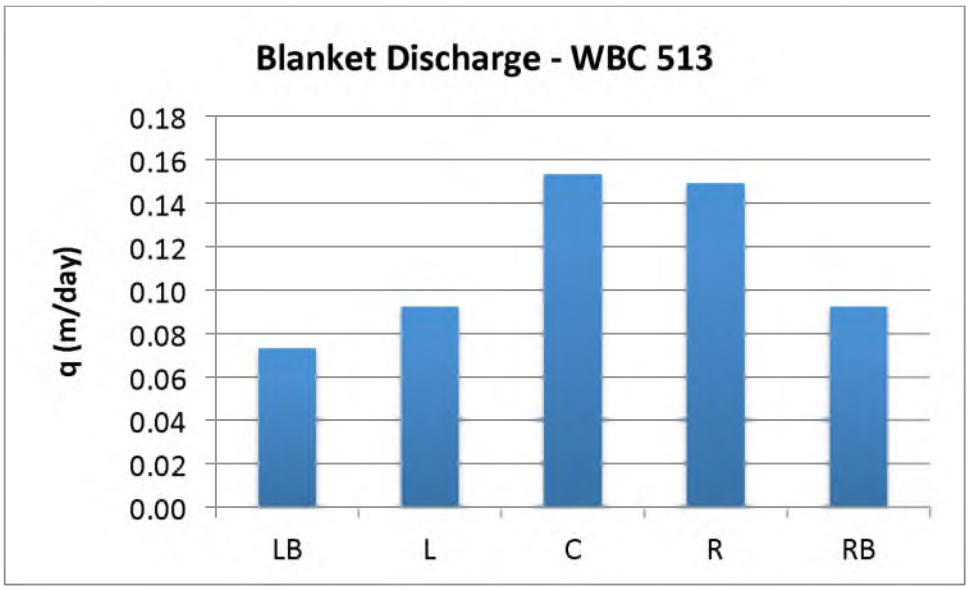

Figure H.2. Dilution flow meter measured blanket specific discharge (q) from West Bear Creek, NC in July 2012.

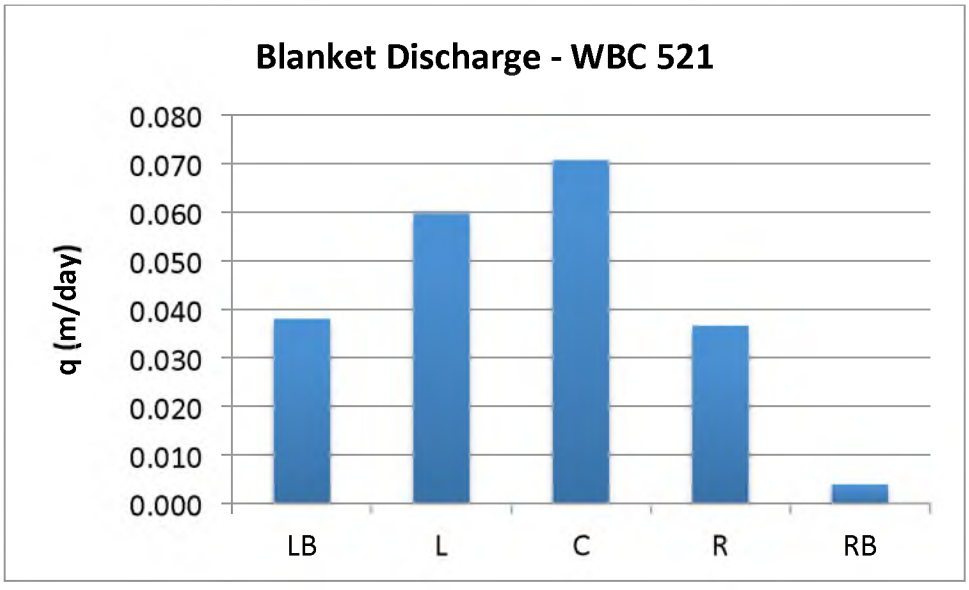

Figure H.3. Dilution flow meter measured blanket discharge from West Bear Creek, NC in July 2012. Location indicated along transect on x-axis (right bank, right, center, left, left bank).

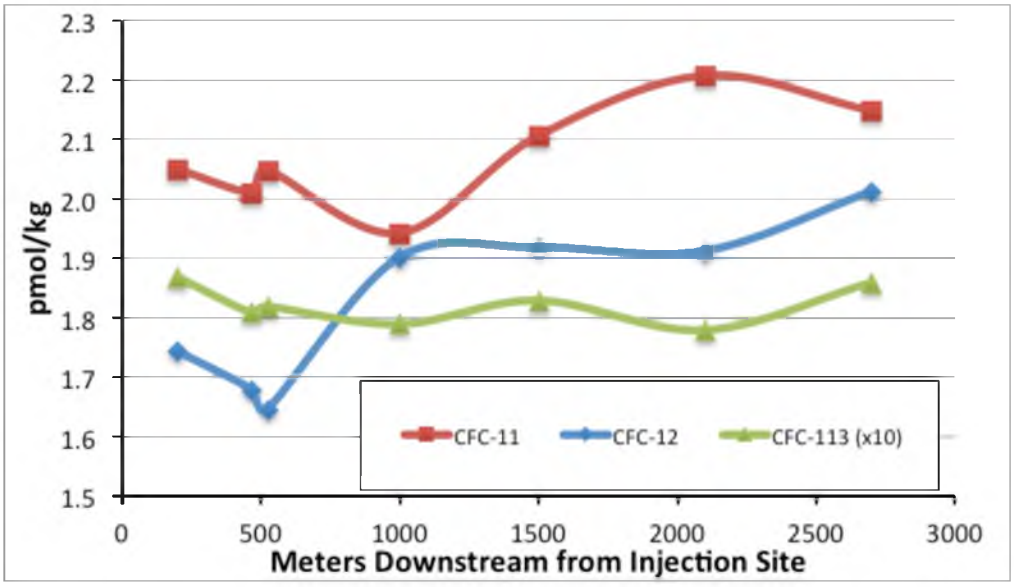

Figure H.4. Measured CFC-11, -12, and -113 concentrations in streamwater from West Bear Creek in July 2012.

Table H.1. Darcian measured specific discharge (Points) and dilution flow meter measured blanket specific discharge (Blankets) from West Bear Creek, NC in July 2012.

Transect	Location	Points		Blankets		
		q ($m\ day^{-1}$)	Mean q ($m\ day^{-1}$)	q ($m\ day^{-1}$)	Mean q ($m\ day^{-1}$)	% Capture Blanket/Point
478	LB	0.426		0.140		
	L	1.081		0.041		
	C	0.941		0.340		
	R	1.437		0.294		
	RB	0.059	0.789	0.263	0.216	0.243
513	LB	0.011		0.073		
	L	0.684		0.092		
	C	0.634		0.153		
	R	0.844		0.149		
	RB	0.066	0.448	0.092	0.112	0.523
521	LB	0.093		0.038		
	L	0.032		0.059		
	C	0.060		0.071		
	R	0.031		0.037		
	RB	0.044	0.052	0.004	0.042	0.448

Table H.2. Mean specific discharge as measured by Darcian (points), blankets, and reach mass balance (RMB) on West Bear Creek, NC for July 2012.

Location	Points (n=5)	Blankets (n=5)	RMB *
521	0.05	0.04	N.A.
513	0.45	0.11	N.A.
478	0.79	0.22	N.A.
Mean	0.43	0.12	0.38

*The RMB mean specific discharge value is the average specific discharge from WBC 400 to WBC 600 as determined by that method.

Table H.3. Blanket bromide results from West Bear Creek, NC in July 2012.

Transect	Location	Time	Br (mg L^{-1})
478	LB		0.793
	L		0.164
	C		0.906
	R		1.748
	RB		0.358
513	LB	12:00	2.081
		13:33	2.26
		14:33	2.473
	L	14:30	2.85
		16:10	3.259
	C	15:15	2.717
		16:15	2.919
		16:35	3.103
	R	12:30	0.22
		13:55	0.12
		15:05	0.98
	RB	13:07	0.169
		13:58	0.198
		15:35	0.186

* Values of 0 indicate a concentration below the analysis reporting limit.

Table H.4. Measured (C_m) and adjusted (C_{adj}) stream bromide concentrations based on measured stream bromide concentrations and least-squares linear regression for West Bear Creek, NC in July 2012.

Date	Transect	C_m (mg L^{-1})	C_{adj} (mg L^{-1})	Slope of Linear Regression
7/18/12	1200	3.228		-0.0011086
7/18/12	500	4.004		
7/17/12	1200	2.812		
7/17/12	478		3.612	
7/18/12	2700	2.647		-0.0006166
7/18/12	500	4.004		
7/19/12	2700	2.939		
7/19/12	513		4.288	

Table H.5. Corrected blanket discharge based on bromide mass balance for West Bear Creek, NC in July 2012. Total blanket discharge (Total), streamwater in blanket discharge (SW), and groundwater in blanket discharge (GW).

Transect	Location	Mean Br Conc. (mg L^{-1})	Total (L min^{-1})	SW (L min^{-1})	GW (L min^{-1})
478	LB	0.793	0.050	0.011	0.039
	L	0.164	0.006	0.000	0.006
	C	0.906	0.110	0.028	0.083
	R	1.748	0.056	0.027	0.029
	RB	0.358	0.002	0.000	0.001
513	LB	2.271	0.038	0.020	0.018
	L	3.055	0.049	0.035	0.014
	C	2.913	0.081	0.055	0.026
	R	0.146	0.078	0.003	0.076
	RB	0.184	0.049	0.002	0.046

Table H.6. Dissolved gas results collected from blankets and piezometers (points) from West Bear Creek, NC in July 2012. Analyzed at USGS Dissolved Gas Lab, Reston, VA.

Transect	Location	Concentration in mg L^{-1}				
		CO_2	N_2	O_2	Ar	CH_4*
Blankets						
	LB	42.23	14.83	1.10	0.51	0.211
478	C	48.07	17.32	0.44	0.49	0.009
	R	34.28	17.56	0.21	0.52	0.023
	LB	50.43	16.61	0.18	0.51	0.068
	L	26.73	14.58	0.70	0.50	0.023
513	C	26.17	14.65	0.84	0.49	0.023
	R	47.27	18.45	0.18	0.53	0.013
	RB	77.74	17.04	0.17	0.51	0.013
Points						
	LB	72.55	17.96	3.14	0.60	0
	L	62.40	20.07	0.31	0.54	0.003
478	C	60.39	20.40	0.19	0.50	0
	R	28.90	21.16	0.20	0.61	0.002
	RB	40.85	20.45	0.25	0.54	0
	LB	47.48	17.97	2.53	0.61	0
	L	62.16	19.45	1.03	0.58	0
513	C	55.76	19.81	0.39	0.56	0
	R	52.37	19.68	0.88	0.54	0
	RB	102.48	18.56	0.21	0.54	0.045

Table H.7. Results for CFC's collected from individual blankets (uncorrected, corrected), and piezometer (points) and flow-weighted transect mean CFC concentrations from West Bear Creek, N.C. in July 2012. Units of CFC concentration are pmol kg^{-1}.

		Uncorrected Blankets		Corrected Blankets						Points	
				Best Est.	Max	Min	Best Est.	Max	Min		
Transect	Location	CFC-11	CFC-113	CFC-11			CFC-113			CFC-11	CFC-113
478	LB	2.668	0.165	2.844	2.852	2.842	0.158	0.161	0.158	3.415	0.316
	C	1.392	0.085	1.171	1.185	1.17	0.05	0.053	0.05	0.917	0.11
	R	0.558	0.019	0.77	0.812	0.77	0	0	0	0.411	0.064
	RB	0.595	0.056	0.393	0.398	0.393	0.0005	0.002	0.005	1.108	0.096
513	LB	2.376	0.174	2.77	2.787	2.745	0.163	0.167	0.155	3.246	0.283
	L	2.108	0.165	2.314	2.349	2.256	0.12	0.129	0.104	2.23	0.184
	C	1.575	0.119	0.626	0.65	0.57	0	0	0	0.422	0.065
	R	0.774	0.045	0.73	0.73	0.729	0.041	0.041	0.04	1.584	0.17
	RB	1.961	0.136	1.959	1.959	1.958	0.134	0.134	0.134	1.575	0.165

Table H.8. Results for SF_6 collected from individual blankets (uncorrected, corrected), and piezometer (points), flow-weighted transect mean SF_6 concentrations, and apparent recharge year from West Bear Creek, N.C. in July 2012.

Transect	Location	Uncorrected Blankets		Corrected Blankets		Points	
		SF_6	Recharge Year	SF_6	Recharge Year	SF_6	Recharge Year
478	LB	4.35	1999	3.87	1996.5	3.41	1994.5
	C	2.97	1992.5	1.93	1987.5	0.92	1980.5
	R	1.71	1986.5	0	1952	0.41	1974.5
	RB	1.7	1986	1.21	1983	1.11	1982
513	LB	4.59	2000	3.06	1993	5.24	2002.5
	L	3.79	1996.5	0	1952	1.13	1982.5
	C	4.03	1997.5	3.96	1997	0.91	1980.5
	R	1	1981.5	0.82	1979.5	1.75	1986.5
	RB	2.27	1989.5	2.11	1988.5	2.82	1992

Table H.9. Nobel gas results from copper tubes collected from blankets and piezometers (points) from West Bear Creek, N.C. in July 2012. Analyzed at University of Utah Dissolved Gas Lab.

Transect	Location	Concentration in mg L^{-1}.						R/Ra	Tritium (TU)
		N_2	Ar	Ne	Kr	Xe	^4He		
Blankets									
478	RB	9.24	2.94E-01	4.58E-05	1.36E-04	1.12E-05	2.92E-05	1.5	1.9
	C	7.95	2.58E-01	6.27E-05	1.10E-04	1.58E-05	2.86E-05	1.3	1.3
	L	7.7	2.73E-01	9.31E-05	1.23E-04	4.11E-05	2.77E-05	1.5	3
	LB	6.96	3.10E-01	1.17E-04	1.84E-04	5.37E-05	4.21E-05	1.2	2.3
513	RB	6.83	2.86E-01	1.30E-04	1.53E-04	1.74E-05	3.62E-05	1	4.2
	R	7.69	2.87E-01	6.51E-05	1.24E-04	9.66E-06	2.98E-05	1.1	1.4
	C	7.51	2.89E-01	5.86E-05	1.42E-04	9.52E-06	3.49E-05	1.4	1.7
	L	7.72	2.95E-01	6.94E-05	1.44E-04	9.62E-06	3.26E-05	1.7	4.1
	LB	7.5	3.12E-01	7.01E-05	2.06E-04	9.53E-06	4.65E-05	1	3.9
Points									
478	RB	7.9	2.55E-01	5.97E-05	1.05E-04	9.25E-06	2.34E-05	1.6	3.6
	R	7.69	2.25E-01	4.86E-05	1.16E-04	7.20E-06	3.35E-05	1.4	2.9
	C	7.72	2.88E-01	6.03E-05	1.11E-04	1.05E-05	2.78E-05	1.3	1.4
	L	6.19	2.80E-01	1.12E-04	1.41E-04	1.70E-05	3.17E-05	1.3	2.5
	LB	5.67	2.73E-01	1.12E-04	1.59E-04	1.61E-05	3.75E-05	1.1	4.4
513	RB	7.86	3.50E-01	8.39E-05	1.30E-04	1.45E-05	3.00E-05	1.1	1.9
	R	7.25	2.72E-01	6.19E-05	1.15E-04	1.06E-05	3.06E-05	1.1	3.1
	C	8.82	2.63E-01	5.83E-05	1.57E-04	9.82E-06	3.86E-05	1.1	4.2
	L	8.89	2.23E-01	4.54E-05	1.49E-04	2.25E-06	3.71E-05	1.2	4.1
	LB	8.48	3.44E-01	1.78E-04	1.60E-04	1.14E-04	3.72E-05	1	3.9

APPENDIX I

MARCH 2013 RESULTS FROM BLANKETS

AT WEST BEAR CREEK, NC

Table I.1. Dilution flow meter measured blanket discharge and calculated specific discharge (q) at transect 715 (m downstream) at West Bear Creek, NC in March 2013.

		AM		PM	
Date	Location	mL min^{-1}	q ($m\ day^{-1}$)	mL min^{-1}	q ($m\ day^{-1}$)
	LB	2.9	0.01	3.2	0.01
	L	321.6	0.61	347.6	0.66
3/11	C	379.3	0.72	360.0	0.68
	R	400.2	0.76	383.1	0.73
	RB	310.1	0.59	378.3	0.72
Mean		282.8	0.5	294.4	0.6
Mean w/o Outlier		352.8	0.7	367.3	0.7
	LB			7.4	0.01
	L			305.2	0.58
3/12	C			320.3	0.61
	R			382.3	0.73
	RB			167.0	0.32
Mean				236.4	0.4
Mean w/o Outlier				293.7	0.6
	LB	6.0	0.01	4.7	0.01
	L	281.4	0.53	305.7	0.58
3/13	C	306.8	0.58	322.6	0.61
	R	282.1	0.54	267.8	0.51
	RB	429.1	0.81	334.7	0.64
Mean			261.1	0.5	247.1
Mean w/o Outlier			324.9	0.6	307.7

Table I.2. Results of samples collected during injected bromide arrival in stream and blankets at transect 715 (m downstream) from West Bear Creek, NC on March 13, 2013.

Name	Time	Concentrations in mg L^{-1}. F	Cl	Br	NO_3	SO_4
Stream	16:30	0.17	14.84	0.72	13.58	14.33
	16:50	0.19	14.79	0.71	13.39	14.27
	17:10	0.15	14.82	0.73	13.46	14.40
	17:30	0.17	14.87	0.76	13.75	14.33
	17:50	0.15	14.84	0.74	13.66	14.26
	18:10	0.15	14.82	0.79	13.62	14.37
	18:30	0.16	14.86	0.71	13.72	14.28
Average SW		0.16	14.84	0.74	13.60	14.32
SD SW		0.01	0.03	0.03	0.14	0.06
Center Blanket	16:30	0.32	14.52	0.03	29.05	17.78
	16:50	0.36	14.54	0.15	28.75	17.76
	17:10	0.33	14.29	0.19	27.68	18.67
	17:30	0.30	14.35	0.21	28.30	18.33
	17:50	0.32	14.46	0.21	29.25	18.18
	18:10	0.35	14.48	0.21	29.67	18.44
	18:30	0.33	14.43	0.21	29.72	18.36
Right Blanket	16:30	0.17	10.18	0.04	5.03	25.45
	16:50	0.16	10.36	0.03	4.58	25.66
	17:10	0.19	10.72	0.16	6.35	24.95
	17:30	0.19	10.81	0.16	6.24	24.67
	17:50	0.15	10.83	0.16	4.91	25.35
	18:10	0.15	10.79	0.20	5.02	25.02
	18:30	0.17	10.78	0.20	4.86	24.90

Table I.3. Results of samples collected during blanket sampling at transect 715 (m downstream) from West Bear Creek, NC on March 14, 2013.

Name	Time	Concentrations in mg L^{-1}.				
		F	Cl	Br	NO_3	SO_4
Left	13:34	0.24	14.55	0.49	19.61	17.32
Blanket	15:10	0.28	14.50	0.36	22.45	17.99
Center	13:40	0.21	14.80	0.62	19.60	15.84
Blanket	14:09	0.27	14.60	0.46	24.60	17.78
Right	11:20	0.15	10.62	0.26	5.66	24.15
Blanket	13:15	0.15	10.77	0.22	5.43	24.21
Right Bank	11:00	0.16	13.66	0.78	10.49	18.45
Blanket	13:16	0.15	13.21	0.67	10.23	20.41

Table I.4. Results from USGS minipoint vertical transects prior to blanket and tracer (PBT) at transect 715 (m downstream) from West Bear Creek, NC on March 10, 2013. Concentrations below the analytical detection limit are noted as (n.a.).

Name	Time	Depth (cm)	Concentrations in mg L^{-1}.				
			F	Cl	Br	NO_3	SO_4
Center PBT	14:35	3	0.16	15.11	0.07	14.87	16.52
		7	0.25	14.80	0.03	23.88	17.10
		10	0.34	14.55	0.04	38.38	18.29
		15	0.36	14.24	0.03	36.72	18.72
		20	0.35	14.27	n.a.	40.73	18.20
		25	0.34	14.30	n.a.	41.43	18.04
Left PBT	14:50	3	0.39	14.30	n.a.	26.78	20.78
		7	0.37	14.25	n.a.	26.90	21.13
		10	0.36	14.09	n.a.	28.21	20.50
		15	0.35	14.15	0.02	25.60	20.89
		20	0.39	14.20	n.a.	27.98	20.78
		25	n.a.	14.11	0.02	26.90	20.81
Right PBT	14:25	3	0.16	5.89	0.02	0.04	17.92
		7	0.14	5.67	n.a.	n.a.	15.93
		10	0.17	6.25	n.a.	n.a.	15.82
		15	0.11	6.37	0.02	n.a.	17.08
		20	0.21	7.05	0.01	n.a.	15.82
		25	0.18	5.91	0.03	n.a.	15.22

Table I.5. Results from USGS minipoint vertical transects upstream and downstream of the blankets at transect 715 (m downstream) from West Bear Creek, NC in March 2013. Concentrations below the analytical detection limit are noted as (n.a.).

Name	Time	Depth (cm)	Concentrations in mg L^{-1}. F	Cl	Br	NO_3	SO_4
Center Upstream	17:20	3	0.20	15.16	0.84	11.89	14.64
		7	0.41	15.16	0.08	30.11	20.78
		10	0.45	14.80	0.02	34.34	19.88
		15	0.36	14.53	0.02	33.41	19.54
		20	0.39	14.65	0.03	37.59	18.61
		25	0.35	14.98	0.01	41.65	17.98
Center Downstream	18:40	3	0.36	14.43	0.12	28.97	24.52
		7	0.45	14.52	0.06	32.00	24.89
		10	0.48	14.59	0.00	30.60	25.88
		15	0.46	14.36	0.07	27.01	27.37
		20	0.48	14.66	0.04	30.75	25.79
		25	0.37	14.44	0.03	34.84	21.85
Right Upstream	17:30	3	0.13	15.05	0.89	11.79	14.71
		7	0.08	9.60	0.02	10.01	36.78
		10	0.07	9.02	n.a.	8.42	34.45
		15	0.12	9.35	0.05	7.91	30.85
		20	0.07	8.14	n.a.	7.62	27.25
		25	0.10	8.78	n.a.	n.a.	24.93
Right Downstream	18:20	3	0.14	14.89	0.92	11.36	14.67
		7	0.18	15.18	0.92	12.02	15.12
		10	0.30	11.64	0.06	n.a.	31.74
		15	0.32	12.61	0.03	n.a.	36.64
		20	0.37	12.76	n.a.	0.58	38.08
		25	0.37	12.85	0.03	0.80	36.06

APPENDIX J

MEASUREMENT STATISTICS AND UNCERTAINTY FOR BLANKET DISCHARGE FIELD MEASUREMENTS

The field statistics for each blanket measurement (Tables J.1, J.2, J.3) shows the goodness of fit (e.g. R^2) for the slope calculated flow and descriptive statistics (e.g. standard deviation and coefficient of variation) of the mean instantaneous flow which display the variability of blanket discharge measurements.

The uncertainty associated with the dilution flow measurements was calculated using a Monte Carlo simulation (n = 500) that determined the average uncertainty associated with each variable and the subsequent flow calculation (Tables J.4, J.5, J.6). Each variable used in the calculation was randomly varied from +1 to -1 of the standard deviation, and the flow rate was calculated and recorded for each realization. The mean, standard deviation, and coefficient of variation were calculated for all the 500 realizations for a given flow measurement data set. The results of this simulation are presented below.

Table J.1. Statistics for field measurements of blanket discharge (Q, mL/min) by dilution flow meter from transect 478 (m downstream) on West Bear Creek, NC in July 2012. Mean Flow is flow determined by linear regression, Mean Inst. Flow is the mean value of the calculated instantaneous flows, s.d. is standard deviation, and COV is the coefficient of variation (s.d./mean) of the instantaneous flow.

Date	Location	Mean Flow (mL min^{-1})	R^2 of Linear Regress.	Mean Inst. Flow (mL min^{-1})	s.d. Inst. Flow	COV
7/16	LB	74.01	0.99986	73.99	2.44	0.03
	L	21.72	0.99913	22.82	7.39	0.32
	C	179.25	0.99975	179.92	8.02	0.04
	R	155.14	0.99960	154.41	8.47	0.05
	RB	138.38	0.99989	137.57	4.33	0.03
7/17	LB	49.97	0.99996	49.71	1.02	0.02
	L	6.47	0.99594	7.33	2.40	0.33
	C	110.18	0.98315	110.91	45.60	0.41
	R	56.38	0.98280	60.56	20.63	0.34
	RB	1.57	0.88319	1.26	0.31	0.24

Table J.2. Statistics for field measurements of blanket discharge (Q, mL/min) by dilution flow meter from West Bear Creek, NC in July 2012. Mean Flow is flow determined by linear regression, Mean Inst. Flow is the mean value of the calculated instantaneous flows, s.d. is standard deviation, and COV is the coefficient of variation (s.d./mean) of the instantaneous flow.

Transect	Location	Mean Flow (mL min^{-1})	R^2 of Linear Regress.	Mean Inst. Flow (mL min^{-1})	s.d. Inst. Flow	COV
513	LB	38.48	0.99981	38.06	2.92	0.08
	L	48.56	0.99993	48.49	1.93	0.04
	C	80.57	0.99990	79.91	2.22	0.03
	R	78.46	0.99880	76.17	4.66	0.06
	RB	48.54	0.99998	48.31	1.82	0.04
521	LB	19.97	0.99678	19.70	5.08	0.26
	L	31.54	0.99908	30.61	4.25	0.14
	C	37.24	0.99956	36.82	7.44	0.20
	R	19.21	0.99603	19.43	4.02	0.21
	RB	2.00	0.99863	2.04	0.36	0.18

Table J.3. Statistics for field measurements of blanket discharge (Q, mL/min) by dilution flow meter from transect 715 (m downstream) on West Bear Creek, NC in March 2013. Mean Flow is flow determined by linear regression, Mean Inst. Flow is the mean value of the calculated instantaneous flows, s.d. is standard deviation, and COV is the coefficient of variation (s.d./mean) of the instantaneous flow.

Date and Time	Location	Mean Flow (mL min^{-1})	R^2 of Linear Regress.	Mean Inst. Flow (mL min^{-1})	s.d. Inst. Flow	COV
3/11 AM	LB	2.91	0.99895	2.95	0.39	0.13
	L	321.64	0.99972	319.62	18.21	0.06
	C	379.31	0.99933	379.04	44.98	0.12
	R	400.20	0.99894	398.76	58.84	0.15
	RB	310.12	0.99772	310.32	65.20	0.21
3/11 PM	LB	3.24	0.99941	3.22	0.42	0.13
	L	347.58	0.99908	347.18	64.22	0.18
	C	360.02	0.99992	360.61	18.38	0.05
	R	383.09	0.99971	377.33	47.60	0.13
	RB	378.31	0.99819	382.07	74.66	0.20
3/12 PM	LB	7.41	0.99938	7.44	0.54	0.07
	L	305.20	0.99834	308.99	85.51	0.28
	C	320.25	0.99806	314.61	70.68	0.22
	R	382.29	0.99969	377.85	20.49	0.05
	RB	166.99	0.99964	166.89	12.73	0.08
3/13 AM	LB	5.97	0.99955	5.83	0.57	0.10
	L	281.44	0.99700	287.84	73.80	0.26
	C	306.79	0.99938	296.18	74.73	0.25
	R	282.11	0.99937	276.89	32.78	0.12
	RB	429.10	0.99900	426.16	71.01	0.17
3/13 PM	LB	4.68	0.99912	4.65	0.27	0.06
	L	305.70	0.99955	310.15	41.04	0.13
	C	322.61	0.99990	318.94	18.05	0.06
	R	267.75	0.99912	273.13	33.47	0.12
	RB	334.72	0.99674	328.35	121.39	0.37

Table J.4. Statistics for field measurements of blanket discharge (Q, mL/min) by dilution flow meter and Monte Carlo results from transect 478 (m downstream) on West Bear Creek, NC in July 2012. Mean Inst. Flow is the mean value of the calculated instantaneous flows, Mean Flow is mean value of the 500 realizations, s.d. is standard deviation, and COV is the coefficient of variation (s.d./mean).

Date	Location	Dilution Flow Meter Calculated			Monte Carlo Results		
		Mean Inst. Flow (mL min^{-1})	s.d.	COV	Mean Flow (mL min^{-1})	s.d.	COV
7/16	LB	73.99	2.44	0.03	74.25	10.26	0.14
	L	22.82	7.39	0.32	22.94	9.27	0.40
	C	179.92	8.78	0.05	179.84	12.12	0.07
	R	154.41	4.85	0.03	154.35	11.42	0.07
	RB	137.57	4.33	0.03	137.62	10.86	0.08
7/17	LB	49.71	1.02	0.02	49.83	9.59	0.19
	L	7.33	2.40	0.33	7.28	9.12	1.25
	C	110.91	45.60	0.41	110.90	11.02	0.10
	R	60.56	21.22	0.35	60.72	10.26	0.17
	RB	1.88	2.51	1.33	1.91	8.25	4.31

Table J.5. Statistics for field measurements of blanket discharge (Q, mL/min) by dilution flow meter and Monte Carlo results from West Bear Creek, NC in July 2012. Mean Inst. Flow is the mean value of the calculated instantaneous flows, Mean Flow is mean value of the 500 realizations, s.d. is standard deviation, and COV is the coefficient of variation (s.d./mean).

Transect	Location	Dilution Flow Meter Calculated Mean Inst. Flow (mL min^{-1})	s.d.	COV	Monte Carlo Results Mean Flow (mL min^{-1})	s.d	COV
513	LB	38.06	2.92	0.08	38.20	7.46	0.20
	L	48.49	1.93	0.04	48.49	7.97	0.16
	C	79.91	6.20	0.08	79.75	7.86	0.10
	R	76.17	4.66	0.06	76.27	8.57	0.11
	RB	48.31	2.07	0.04	48.25	8.45	0.18
521	LB	19.70	5.54	0.28	19.67	8.04	0.41
	L	30.61	4.25	0.14	30.64	8.90	0.29
	C	36.82	5.50	0.15	36.80	8.65	0.23
	R	19.43	4.02	0.21	18.95	8.66	0.46
	RB	2.04	0.36	0.18	1.94	7.58	3.90

Table J.6. Statistics for field measurements of blanket discharge (Q, mL/min) by dilution flow meter and Monte Carlo results from transect 715 (m downstream) on West Bear Creek, NC in March 2013. Mean Inst. Flow is the mean value of the calculated instantaneous flows, Mean Flow is mean value of the 500 realizations, s.d. is standard deviation, and COV is the coefficient of variation (s.d./mean).

Date and Time	Location	Dilution Flow Meter Calculated Mean Inst. Flow (mL min^{-1})	s.d.	COV	Monte Carlo Results Mean Flow (mL min^{-1})	s.d.	COV
3/11 AM	LB	2.95	0.39	0.13	2.93	3.59	1.23
	L	319.62	18.21	0.06	319.86	24.75	0.08
	C	379.04	44.98	0.12	380.23	27.32	0.07
	R	398.76	43.42	0.11	398.66	26.22	0.07
	RB	310.32	65.20	0.21	310.45	24.29	0.08
3/11 PM	LB	3.22	0.42	0.13	3.15	4.27	1.35
	L	347.18	64.22	0.18	346.92	25.93	0.07
	C	360.61	13.44	0.04	360.68	27.43	0.08
	R	377.33	47.60	0.13	377.46	27.06	0.07
	RB	382.07	74.66	0.20	381.88	27.15	0.07
3/12 PM	LB	7.44	0.54	0.07	7.44	2.92	0.39
	L	308.99	85.51	0.28	309.00	25.71	0.08
	C	314.61	70.68	0.22	314.51	25.89	0.08
	R	377.85	20.49	0.05	378.16	28.46	0.08
	RB	166.89	13.24	0.08	167.02	18.57	0.11
3/13 AM	LB	5.83	0.58	0.10	5.78	1.47	0.25
	L	287.84	73.80	0.26	287.93	24.27	0.08

Table J.6. Continued

3/13 AM	L*	199.49	53.38	0.27	199.61	20.86	0.11
	C	296.18	74.73	0.25	296.75	24.34	0.08
	R	276.89	32.78	0.12	277.30	23.23	0.08
	RB	426.16	71.01	0.17	426.35	33.69	0.08
3/13 PM	LB	4.65	0.27	0.06	4.73	1.72	0.36
	L	310.19	41.04	0.13	310.69	25.69	0.08
	C	318.94	18.06	0.06	319.30	25.73	0.08
	R	273.13	33.47	0.12	273.04	22.98	0.08
	RB	328.35	121.09	0.37	328.67	25.52	0.08

* repeat measurement was made at the left location.